Physical systems include the ocean, lakes, rivers, glaciers, and snowpack that are part of the water cycle. Globally, warming temperatures have altered the water cycle, resulting in the decrease in Northern Hemisphere spring snow cover, a global retreat of glaciers, warming oceans, sea level rise, and reduced oxygen levels in ocean waters (IPCC, 2021).

In California, every aspect of the water cycle has been changing. With less precipitation falling as snow, less water is stored in the Sierra Nevada snowpack. Runoff from melting snow has historically accounted for approximately one-third of the state's yearly water supply. A greater fraction of this runoff has been flowing earlier in the spring, diminishing the amount of water available from snowpack during the warmer summer months. These changes have tremendous implications for California's water, for freshwater habitats, and for forest ecosystems—including increasing the risk of wildfires. Reduced stream flows and warmer air temperatures lead to warmer water temperatures. The Salmon River, Lake Tahoe and other rivers, streams and lakes in the state are warming.

Among the most visible indicators of climate change, California glaciers continue to shrink. Water from melting mountain glaciers and ice sheets is the main source of global sea level rise today (IPCC, 2019; Slater et al., 2020). Heat-driven expansion of ocean waters has also been a major contributor (IPCC, 2019). Consistent with global observations, sea levels are rising along most of California's coast, threatening coastal infrastructure and communities – where flooding hazards pose disproportionate impacts on low-income households – and ecosystems (CCC, 2015; LAO, 2020).

The oceans have absorbed over 90 percent of the increased heat energy on the Earth over the past 50 years (Jewett and Romanou, 2017; NOAA, 2021; Rhein et al., 2013). Along California, coastal waters have warmed over the past century, particularly off Southern California. An unprecedented marine heatwave off the California coast from 2014 to 2016 led to a wide range of effects on marine life and significant economic loss. Along with warmer ocean temperatures, the associated reduction in dissolved oxygen levels and ocean acidification present serious threats to global marine ecosystems.

INDICATORS: IMPACTS ON PHYSICAL SYSTEMS

Snow-water content *(updated)*
Snowmelt runoff *(updated)*
Glacier change *(updated)*
Lake water temperature (*updated*)
Salmon River water temperature *(new)*
Coastal ocean temperature *(updated)*
Sea level rise *(updated)*
Dissolved oxygen in coastal waters *(updated)*

References:

CCC (2015). *California Coastal Commission Sea Level Rise Policy Guidance: Interpretive Guidelines for Addressing Sea Level Rise in Local Coastal Programs and Coastal Development Permits*. California Coastal Commission. San Francisco, CA.

IPCC (2019). *Special Report on the Ocean and Cryosphere in a Changing Climate.* Pörtner HO, Roberts DC, Masson-Delmotte V, Zhai P, Tignor M, et al. (Eds.). Intergovernmental Panel on Climate Change. Geneva, Switzerland.

IPCC (2021). *AR6 Climate Change 2021: The Physical Science Basis. Contribution of Working Group I to the Sixth Assessment Report of the Intergovernmental Panel on Climate Change.* Masson-Delmotte V, Zhai P, Pirani A, Connors SL, Péan C, Berger S, et al. (Eds.). Geneva, Switzerland: Intergovernmental Panel on Climate Change.

Jewett L and Romanou A (2017). Ocean acidification and other ocean changes. In: *Climate Science Special Report: Fourth National Climate Assessment, Volume I.* Wuebbles DJ, Fahey DF, Hibbard KA, Dokken DJ, Stewart BC and Maycock TK (Eds). U.S. Global Change Research Program, Washington, DC. pp. 364-392.

LAO (2020). *What Threat Does Sea Level Rise Pose to California?* California Legistlative Analyst's Office.

NOAA (2021).National Centers for Environmental Information, State of the Climate: Global Climate Report for Annual 2020, published online January 2021. Retrieved on May 20, 2021.

Rhein M, Rintoul SR, Aoki S, Campos E, Chambers D, et al. (2013). Observations: Ocean. *In: Climate Change 2013: The Physical Science Basis. Contribution of Working Group I to the Fifth Assessment Report of the Intergovernmental Panel on Climate Change*. Stocker TF, Qin D, Plattner G-K, Tignor M, Allen SK, et al. (Eds.). Cambridge University Press. Cambridge, United Kingdom and New York, NY, USA.

Slater T, Hogg AE and Mottram R (2020). Ice-sheet losses track high-end sea-level rise projections. *Nature Climate Change* **10**(10):879-881.

SNOW-WATER CONTENT

The amount of water stored in the state's snowpack varies greatly from year to year, reflecting the variability in the amount and form of precipitation over California's mountain areas. Average statewide snow-water content—a measure of the amount of liquid water contained in the snowpack—is about 28 inches. It has ranged from a high of about 240 percent of average in 1952 to a record low of 5 percent in 2015. In 2022, snow-water content was 35 percent of average.

Figure 1. Statewide April 1 snow-water content based on snow courses* (Percent of average)

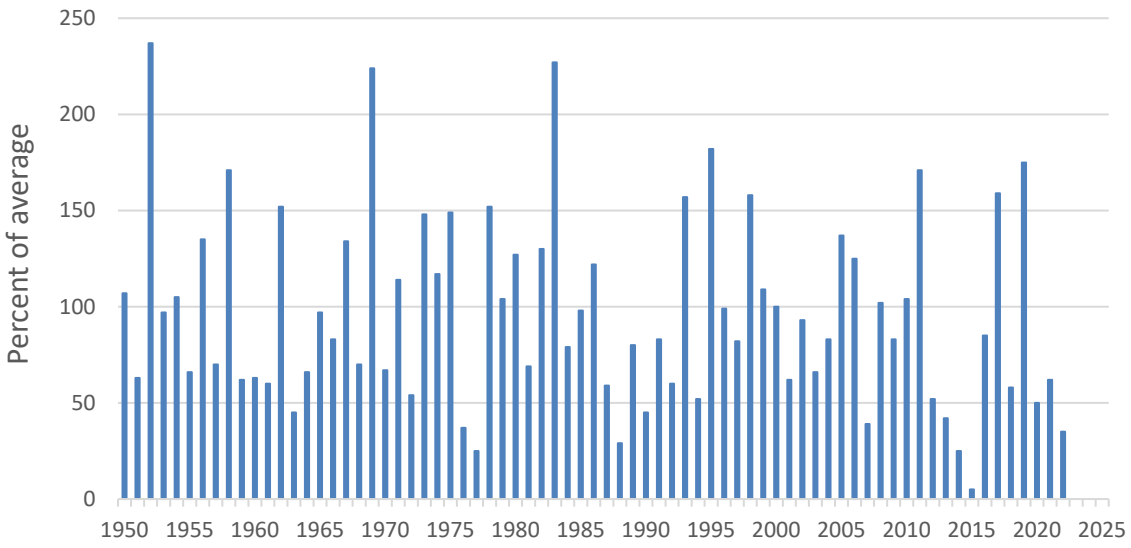

Source: DWR, 2022a

*Snow courses are permanent locations where snow-water content is measured by weighing cores of snow pulled from the entire depth of the snowpack at a given location. The measurements represent snowpack conditions at a given elevation in a given area.

What does the indicator show?

Since 1950, statewide snow-water content has been highly variable, ranging from more than 200 percent of average in 1952, 1969 and 1983, to 5 percent in 2015 during the multi-year drought (2012 to 2016) (Figure 1). The past decade included years that were among the lowest (2013, 2014, 2015 and 2022) and the highest (2011, 2017, 2019) on record. In 2022, snow-water content was 35 percent of average. The historical average snow-water content on April 1, based on the water years 1991-2020, is about 28 inches.

Snow-water content – also referred to as snow water equivalent – is the amount of water contained in snowpack. It represents the depth of water that would cover the ground if the snow cover was in a liquid state (NWS, 2018). It is traditionally measured by weighing the mass of a core of snow — from snow surface to soil — collected by an observer (snow gauger) in the field. The weight of snow is a measure of how much

liquid water would be obtained by melting the snow over a given area. Manual measurements are taken near the first of the month starting about January 1 and ending in May. The most important one is taken around April 1, near the time when the snowpack has historically been deepest on a monthly scale. The statewide values are based on measurements taken at about 260 snow course stations from the Trinity Alps and Mount Shasta in northern California, and throughout the Sierra Nevada down to the Kern River basin in the south (see map in *Technical Considerations*).

Why is this indicator important?

This indicator tracks how much water is locked up in the state's snowpack, which accumulates from October through March in the Sierra Nevada and southern Cascade Mountains. Although some of this water will be lost to direct evaporation and transpiration, most will be available to percolate into soils or run off into streams and rivers as temperatures rise. Sierra Nevada snowpack provides the primary source of streamflow in the Central Valley. The snowpack supplies water to meet human needs such as domestic and agricultural uses and hydroelectric production. It also supports ecosystems, for example by providing suitable aquatic habitat and moisture for forest vegetation. Snowpack is also vital for winter recreation and tourism (Hatchett and Eisen, 2018).

Historically, California's snowpacks contained the most water (about 15 million acre-feet) between mid-March and mid-April of each year, and the Sierra Nevada snowpack added about 35 percent to the reservoir capacity available in the state. While the date of maximum snow-water content may vary from year to year and place to place, measurements taken on April 1 have been used to estimate how much water stored in the state's snowpacks will be released as snowmelt later in the year.

Monitoring snowpack is key to managing both the state's water supplies and flood risks. California's water managers have developed a strategy of maintaining empty space in major reservoirs during winter, so that flows can be captured or at least reduced during large storms to prevent floods. By about April 1, flood risks generally decline considerably as large winter storms stop impacting California. At this time, reservoir managers change strategies and instead capture and store as much streamflow as possible in reservoirs for the summer when water demands are highest. This strategy works primarily because, during winter, the state's snowpacks are holding copious amounts of the winter's precipitation in the mountain watersheds, only releasing most of it as runoff after about April 1. In big snowpack years like 2017 and 2019, some of the early portion of the snowmelt is released in March and April prior to the normal peak snowmelt. The gradual release of snowmelt during the spring precludes the need for overly high-volume reservoir releases later in the runoff season. Forecasts of runoff volume and timing based on snow-water content data are a critical tool to guide reservoir operations. (Forecasts are published by the Department of Water Resources in Bulletin 120)

The series of maps in Figure 2 showing early March snowpack clearly illustrate the variability over the last six years in the Sierra Nevada: record low snowpack in 2015, an average year in 2016, two of the highest snowpack years in 2017 and 2019, and two years at about 60 and 50 percent of average – 2018 and 2020, respectively.

Figure 2. Snow-water equivalents across the Sierra Nevada in early March, 2015 to 2020

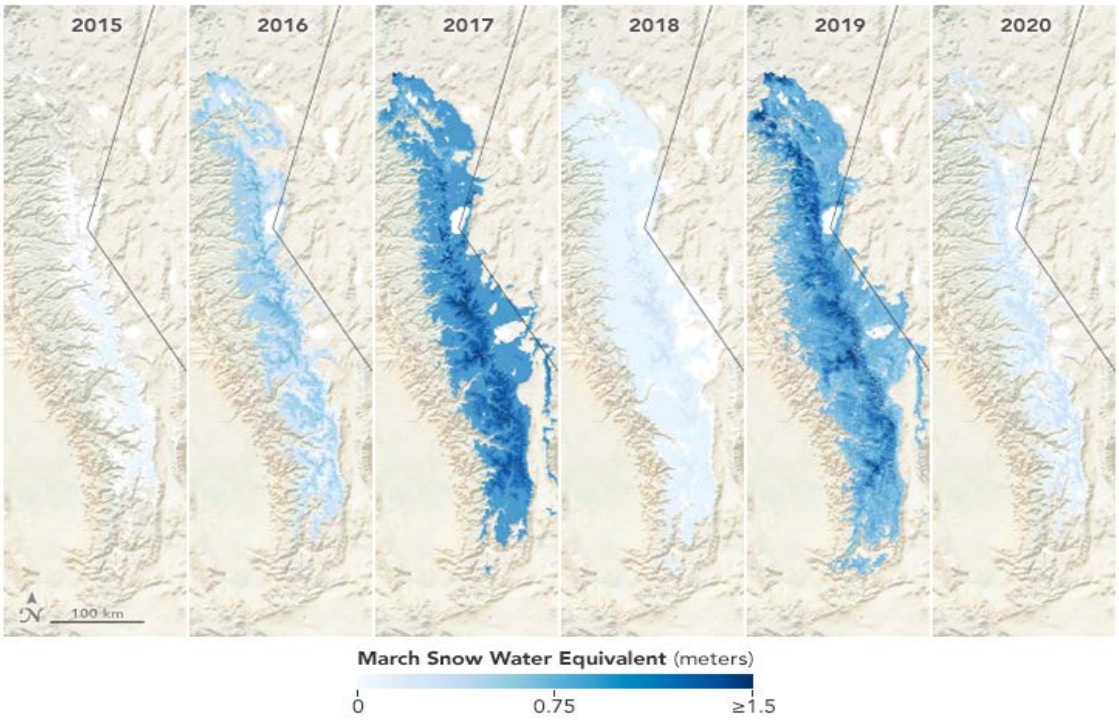

Source: NASA 2020

Maps developed by the University of Colorado's Center for Water, Earth Science, and Technology. Data are derived from ground-based data, computer models, and satellite imagery. They incorporate a data set from the Jet Propulsion Laboratory called the MODIS Snow Covered Area and Grain-size (MODSCAG), which uses data from NASA's Terra satellite to determine properties of the snow—things like the area covered, grain size, and albedo—that are useful for deriving accurate estimates of snow-water equivalent.

Adaptive strategies employing advanced observations, forecasts, and system management perspective are needed to maintain the functionality of the existing water management infrastructure in the face of climate change. Current management practices for water supply and flood management in California will need to be revised for a changing climate (Siirila-Woodburn et al., 2021). This is in part because such practices were designed for historical climatic conditions, which will continue to change as the climate warms. Adapting to a warming climate will bring numerous challenges to both supply and demand sides (Sterle et al., 2019), however planning for a future characterized by less water availability is prudent based on the state of climate science.

What factors influence this indicator?

Factors that affect snow-water content include winter and spring precipitation, air temperature, and elevation. Colder air temperatures at higher elevations generally mean higher snow accumulations compared to lower elevations. The influence of elevation is evident in an analysis of snowpack trends in the Sacramento River, San Joaquin River, and Tulare Lake Basins (see Figure 3; Riddlebarger et al., 2021).

Figure 3. 60-year trends in April 1 snow water equivalent at Sierra Nevada and Cascade Mountain snow courses, by elevation

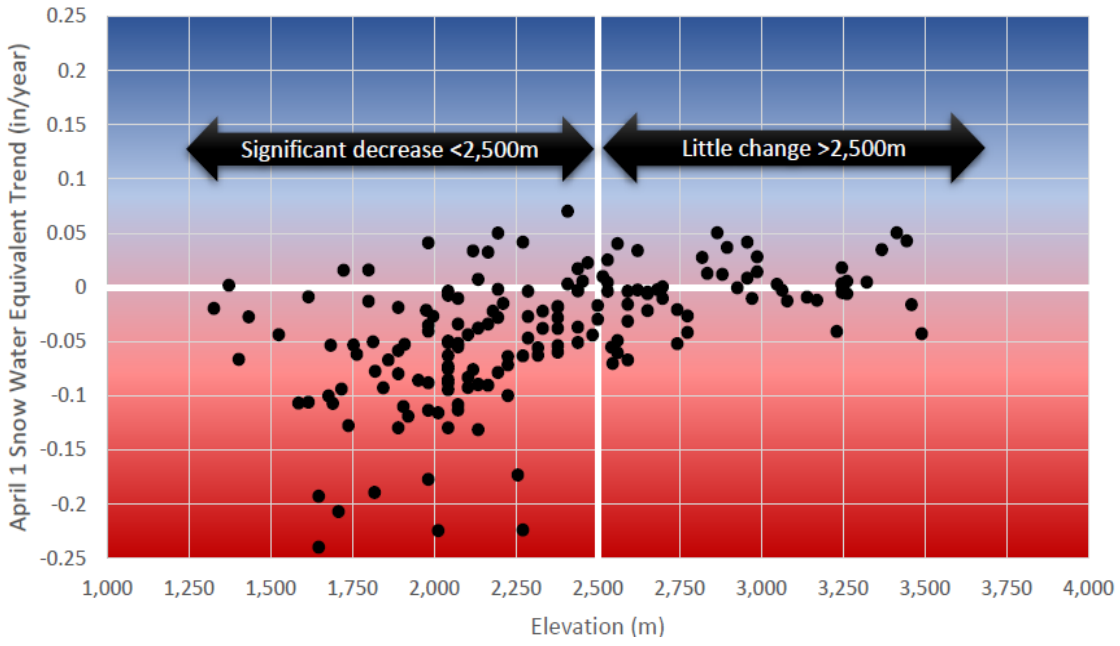

Source: Riddlebarger et al., 2021

The 60-year trend at each snow course is represented by each dot. Over this period, snowpack has declined at 78 percent (129 of 166) of the snow courses: snow courses at elevations below 2,500 meters showed negative trends at an overall average of --0.07 inch/year; at higher elevations, the trends clustered between -0.05 and +0.05 inch/year.

The snow courses that make up the northern Sierra group in Figure 2 are at lower elevations (average 6,900 feet) compared to the southern group (average 8,900 feet). In the past 70 years, the proportion of precipitation as snow has decreased at the rate of 4 percent per decade over lower and middle elevation regions of the northern Sierra Nevada, while the highest elevations of the southern Sierra Nevada, where temperatures remain at or below 0°C during winter and spring, showed no declines (Lynn et al., 2020). In an analysis of data on April snow-water content and temperature from 1985 to 2016, the northern Sierra Nevada was found to be more vulnerable to warming than the southern region (Huning and AghaKouchak, 2018). Over the past decade, the average snow level (the altitude where precipitation changes from snowfall to rain) along the western slope of the northern Sierra Nevada has risen over 1,200 feet (Hatchett et al., 2017).

A study of trends in the Sierra Nevada snowpack found warm daily maximum temperatures in March and April to be associated with a shift toward earlier timing of peak snow mass by 0.6 day per decade since 1930; this earlier trend is associated with snow melting earlier, which also results in trends toward lower snow-water equivalent (Kapnick and Hall, 2010). Under climate change, warming is likely to lead to less snowpack if precipitation does not increase too markedly (Knowles and Cayan, 2004). If precipitation increases, snow-water content could increase in those areas above the retreating snowlines that are still cold enough to receive snowfall; if precipitation decreases, snow-water content may be expected to decline even faster than due to warming alone.

The term “snow drought” refers to anomalously low snow-water content (Cooper et al. 2016). Snow drought occurs under conditions that reflect either a lack of winter precipitation (“dry” snow drought) or near-normal winter precipitation when temperatures prevent accumulation of snowpack (“warm” snow drought) (Harpold et al., 2017). During water years 1951 to 2017 in the northern Sierra Nevada, snow droughts have originated and evolved in various ways, including from extreme early season precipitation, frequent rain-on-snow events, low precipitation years, lower fractions of precipitation falling as snow, and midwinter peak runoff events (Hatchett and McEvoy, 2018). Consecutive snow drought years, which currently occur in the western United States at about 7 percent of the time, are projected to become more frequent in the mid-21st century, occurring at about 42 percent of the time under a high greenhouse gas emissions scenario (Marshall et al., 2019).

The record low snowpack in 2015 was accompanied by the warmest winter temperatures as well as the fifth lowest precipitation volume since 1950 (see *Air Temperature* and *Precipitation* indicators). In addition to enhancing the likelihood of rain instead of snow, warm temperatures increase the frequency of melt events, leading to a reduction of snow-water content. Across western North America, early snowmelt has increased at over one-third of the long-term snow stations studied; at these locations, snowmelt occurred before peak snow accumulation (Musselman et al., 2021). The same study found decreased snow-water content at about 11 percent of snow stations. Snowmelt trends were found to be highly sensitive to temperature, while trends in snow water equivalent were more sensitive to variability in precipitation.

Across the western United States, a broad pattern of declining snowpack has been reported (e.g., Siirila-Woodburn et al. 2021; Musselman et al., 2021; Mote et al., 2018; Mote, 2003; Barnett et al., 2008). Declining trends have been observed across all months, states, and climates, but are largest in spring, in the Pacific states, and in locations with mild winter climate (Mote et al., 2018). By removing the influence of natural variability, investigators showed a robust anthropogenic decline in western U.S. snowpack since the 1980s, particularly during the early months of the accumulation season (October–November) (Siler et al., 2019).

To a lesser extent, snow-water content may be influenced by the amount of solar radiation that falls on the snowpack in each season, which, in turn, depends on cloudiness and timing of the beginning of the snowmelt season (Lundquist and Flint, 2006). Cloudiness decreases solar radiation on the snowfields, and would tend to result in less wintertime snowmelt and thus more snow-water content left by April 1 (the opposite would occur if cloudiness declines in the future).

A potential confounding factor in the variation and trends in snowpack is the effect of dust and air pollutants (including black carbon, a component of soot) on both the initial formation of mountain snowpack and on snowmelt timing. Field measurements and modeling have shown that the presence of dust in the atmosphere, including dust from Asia and the Sahara carried to California by high-altitude winds, may increase snowfall over the Sierra Nevada by serving as ice nuclei, which in turn could contribute to increased snowpack (Ault et al., 2011; Cremean et al., 2013). Recent studies in the Colorado River Basin have helped to quantify important influences on snowmelt timing and, ultimately, amounts that are due to springtime snow albedo (reflectivity) changes associated with dust (mostly from within the region) falling onto snow surfaces across the Western US (e.g., Painter et al., 2010). Black carbon, which in burned forests is deposited onto the snow surface, has been measured in the Sierra Nevada snowpack at concentrations sufficient to increase surface temperatures and increase snowmelt (Hadley et al., 2010). These factors likely play roles in past and future variations of April 1 snowpack amounts, but the long-term past and future trends in these additional factors in California remain largely unknown at present.

Technical Considerations

Data characteristics

Statewide snow-water content is based on observations from permanent snow courses. At these locations, snow-water content is measured by weighing cores of snow pulled from the whole depth of the snowpack at a given location. Since the 1930s, within a few days of the beginning of each winter and spring month, measurements have been taken along snow course locations that represent snowpack conditions at a given elevation in a given area.

Measurements are taken by skiing or flying to remote locations and extracting 10 or more cores of snow along ¼ mile-long pre-marked “snow course” lines on the ground. The depth of snow and the weight of snow in the cores are measured. The weights are converted to a depth of liquid water that would be released by melting that weight of snow, and the results from all the measurements at the snow course are averaged to arrive at estimates of the snow-water content at that site (Osterhuber, 2014). More than 50 state, federal and private entities pool their efforts in collecting snow data from over 250 snow courses in California (see Figure 4 for locations).

Figure 4. Location of snow courses

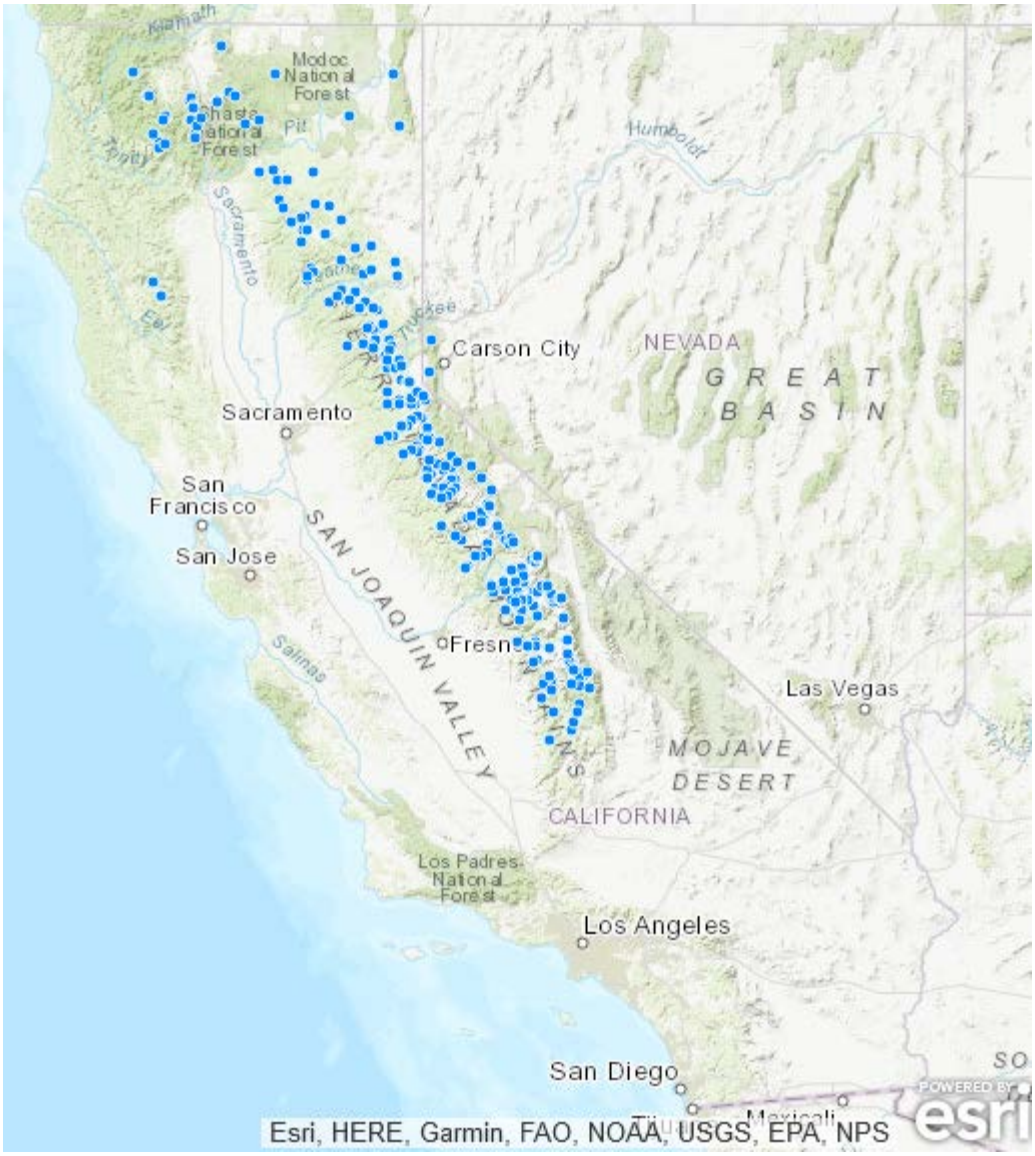

Source: DWR, 2022b

The map shows permanent snow courses where snow-water content is measured during regular snow surveys (more details in text).

Data from monthly snow surveys are supplemented by daily information from an automatic snow sensor network (often called snow pillows), developed and deployed over the last 30 years. They serve as a valuable check on the representativeness and accuracy of the snow-course measurements. The snow sensors measure the accumulation and melting cycles in the snowpack, providing data on the effect of individual storms or hot spells. In addition to tracking changes during the snow accumulation season, snow sensor data help greatly in forecasting water volumes involved in the late-season filling of reservoirs. There are approximately 130 snow

sensor sites from the Trinity Alps to the Kern River, with 36 sites included from the Trinity area south to the Feather and Truckee basins, 57 sites from the Yuba and Tahoe basins to the Merced and Walker basins, and 36 sites from the San Joaquin and Mono basins south to the Kern basin.

Snow-water content data for snow courses and snow sensors can be downloaded from the Department of Water Resources' California Data Exchange Center.

Strengths and limitations of the data

The measurements are relatively simple, and the methods have not changed since monitoring started. Averaging of the 10 or more measurements at each course yields relatively accurate and representative results for each survey.

OEHHA acknowledges the expert contribution of the following to this report:

Sean de Guzman, P.E.
California Department of Water Resources
sean.deguzman@water.ca.gov

Michael L. Anderson, Ph.D., P.E.
Michael.L.Anderson@water.ca.gov

Elissa Lynn
elissa.lynn@water.ca.gov

Peter Coombe
peter.coombe@water.ca.gov

Benjamin Hatchett, Ph.D.
Western Regional Climate Center
Benjamin.Hatchett@dri.edu

References:

Ault AP, Williams CR, White AB, Neiman PJ, Creamean JM, et al. (2011). Detection of Asian dust in California orographic precipitation. *Journal Geophysical Research* **116**(D16).

Barnett TP, Pierce DW, Hidalgo HG, Bonfils C, Santer BD, et al. (2008). Human-Induced Changes in the Hydrology of the Western United States. *Science* **319**(5866): 1080-1083.

Cayan DR and Webb R (1992). El Niño/Southern Oscillation and streamflow in the western United States. In: *El Niño: Historical and Paleoclimatic Aspects of the Southern Oscillation*. Diaz HF and Markgraf V (Eds.). New York: Cambridge University Press, 29-68.

Cooper MG, Nolin AW and Safeeq M (2016). Testing the recent snow drought as an analog for climate warming sensitivity of Cascades snowpacks. *Environmental Research Letters* **11**: 084009.

Creamean J, Suski K, Rosenfeld D, Cazorla A, DeMott P, et al. (2013). Dust and biological aerosols from the Sahara and Asia influence precipitation in the Western U.S. Science **339**: 1572–1578.

DWR (2022a). California Department of Water Resources. Snow Course Data provided by Peter Coombe and Sean de Guzman, also California Statewide April 1 Snow Water Equivalent. Retrieved January 9, 2022. Individual snow course data available from California Data Exchange Center.

DWR (2022b). California Department of Water Resources. Snow Courses in California. California Data Exchange Center: CDEC Station Locator. Retrieved January 9, 2022.

Hadley OL, Corrigan CE, Kirchstetter TW, Cliff SS and Ramanathan V (2010). Measured black carbon deposition on the Sierra Nevada snow pack and implication for snow pack retreat. *Atmospheric Chemistry and Physics* **10**: 7505-7513.

Hatchett BJ, Daudert B, Garner CB, Oakley NS, Putnam AE et al. (2017). Winter Snow Level Rise in the Northern Sierra Nevada from 2008 to 2017. *Water* **9**(11): 899.

Kapnick S and Hall A (2010). Observed Climate–Snowpack Relationships in California and their Implications for the Future. *Journal of Climate* **23**: 3446–3456.

Knowles N and Cayan DR (2004). Elevational dependence of projected hydrologic changes in the San Francisco estuary and watershed. *Climatic Change* **62**(1-3): 319-336.

Knowles N, Dettinger MD and Cayan DR (2006). Trends in Snowfall versus Rainfall in the Western United States. *Journal of Climate* **19**: 4545–4559.

Lundquist JD and Flint AL (2006). Onset of snowmelt and streamflow in 2004 in the western United States: How shading may affect spring streamflow timing in a warmer world. *Journal of Hydrometeorology* **7**(6): 1199-1217.

McCabe GJ and Dettinger MD (2002). Primary modes and predictability of year-to-year snowpack variations in the western United States from teleconnections with Pacific Ocean climate. *Journal of Hydrometeorology* **3**(1): 13-25.

Mote PW (2003). Trends in snow water equivalent in the Pacific Northwest and their climatic causes. *Geophysical Research Letters* **30**(12): 1601.

Mote, PW, Hamlet AF, Clark MP and Lettenmaier DP (2005). Declining mountain snowpack in western North America. *American Meteorological Society* **86**(1): 39–49.

NASA (2021). National Aeronautics and Space Administration: Thin Snow Cover in the Sierra Nevada Snowpack in the Sierra Nevada. Retrieved July 29, 2021.

NRCS (2018). Natural Resources Conservation Service. Snow Surveys and Water Supply Forecasting. Retrieved February 21, 2018.

NWS (2018). National Weather Service. Snow water equivalent and depth information. Retrieved February 21, 2018.

Osterhuber R (2014). Snow Survey Procedure Manual. Prepared for the California Department of Water Resources, California Cooperative Snow Surveys.

Painter TH, Deems JS, Belnap J, Hamlet AF, Landry CC et al. (2010). Response of Colorado River runoff to dust radiative forcing in snow. *Proceedings of the National Academy of Sciences* **107**(40): 17125-17130.

Riddlebarger M, Curtis DC and Cunha L (2021). *Sierra Nevada Mountain Snowpack Trends*. White Paper. WEST Consultants, Inc. April 8, 2021.

Roos M (2000). Possible Effects of Global Warming on California Water or More Worries for the Water Engineer. *W.E.F. Water Law and Policy Briefing*. San Diego, CA, Department of Water Resources.

Roos M and Fabbiani-Leon A (2017). Recent Changes in the Sierra Snowpack in California. Presented at the 2017 Western Snow Conference.

Roos M and Sahota S (2012). Contrasting Snowpack Trends in the Sierra Nevada of California. Presented at the 2012 Western Snow Conference.

Siirila-Woodburn ER, Rhoades AM, Hatchett BJ. Huning LS, Szinai J, et al. (2021). A low-to-no snow future and its impacts on water resources in the western United States. *Nature Reviews Earth Environment* **2**: 800–819.

Sterle K, Hatchett BJ, Singletary L and Pohll G (2019). Hydroclimate variability in snow-fed river systems: Local water managers' perspectives on adapting to the new normal. *Bulletin of the American Metrological Society* **100**(6): 1031-1048.

USEPA (2016). US Environmental Protection Agency. Climate Change Indicators: Snowpack. Retrieved December 1, 2017.

SNOWMELT RUNOFF

The fraction of snowmelt runoff from the Sierra Nevada into the Sacramento River and the San Joaquin River hydrologic regions between April and July relative to total year-round water runoff, while highly variable, has declined over the past century.

Figure 1. Sacramento River spring runoff
(April-July runoff as a percentage of total water year runoff)

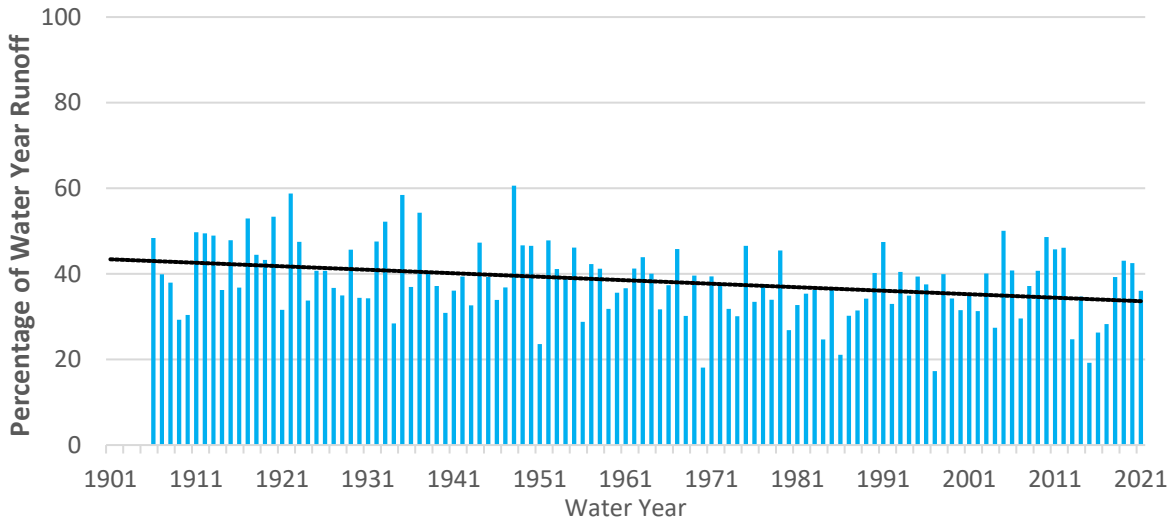

Source: DWR, 2022

Figure 2. San Joaquin River spring runoff
(April-July runoff as a percentage of total water year runoff

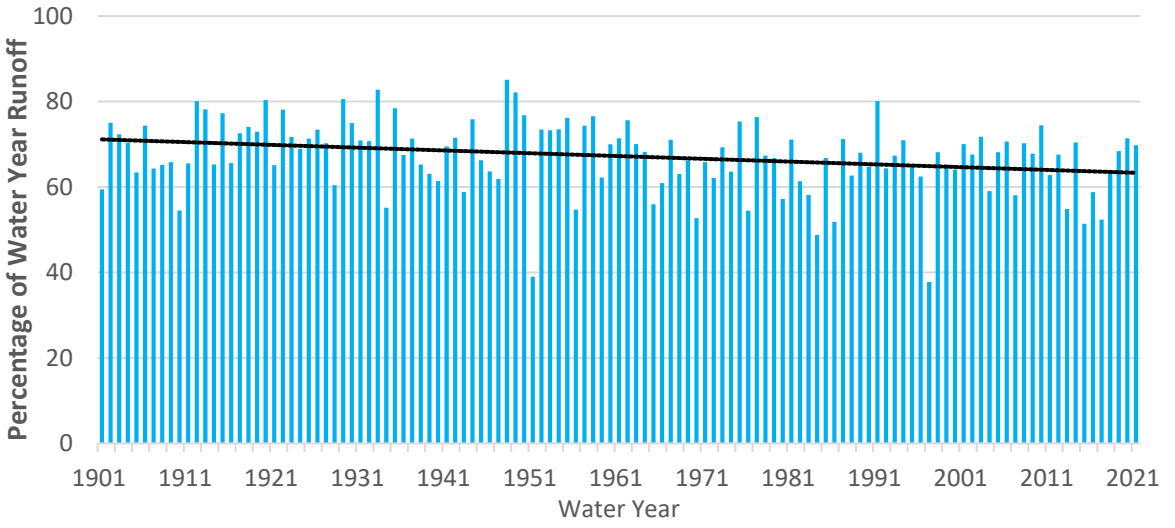

Source: DWR 2022

What does the indicator show?

The fraction of annual unimpaired snowmelt runoff that flows into the Sacramento River and the San Joaquin River between April and July ("spring") has decreased by about eight and seven percent per century, respectively, while showing large year-to-year

variability. Figures 1 and 2 show this spring fraction as a percentage of total runoff for the entire water year, the period from October through the following September. In the Sacramento River, three of the last ten years ranked among the ten lowest in the percentage of total water year runoff occurring in the spring: 2015, 2013 and 2016 were third, seventh and eighth lowest, respectively. In the San Joaquin River, two of the last ten years had among the lowest in percentage of total runoff in the spring (2015 and 2017 were ranked fourth and sixth lowest, respectively); notably, 2015 recorded the lowest, and 2017 the fifth highest, spring runoff volumes. The 2015 water year also saw the lowest snowpack on record. There is no significant trend in total water year runoff into either river, just a change in the timing: i.e., an increasingly larger proportion of runoff occurring earlier in the spring.

Average values for the percentage of runoff in the spring are higher for the "snow-dominated" San Joaquin River, compared to the "rain-dominated" Sacramento River – about two-thirds and one-third of the total water year runoff, respectively (DWR 2021). This difference is explained further in *What factors influence this indicator?*

Why is this indicator important?

The Sacramento River and the San Joaquin River, the two largest river systems in California, serve as the major sources of water for the state. Snowmelt runoff into streams and rivers supplies water to meet human needs and to support ecosystems. In the Sierra Nevada and southern Cascade Mountains, snow accumulates from October through March (see *Snow-water content* indicator), preserving much of California's water supply in cold storage. As temperatures warm in the spring and there is more daylight and solar radiation, the snowpack melts, releasing runoff, typically from April through July.

Spring runoff averages around 14.1 million acre feet (18 billion cubic meters) water, which is about 35 percent of the usable annual supply for agriculture and urban needs (Roos and Anderson, 2006; DWR, 2021). Spring runoff data, along with related snowpack information, are used for water supply and flood forecasting. (Forecasts of seasonal runoff are published weekly by the Department of Water Resources in Bulletin 120.

Much of the state's flood protection and water supply infrastructure was designed to capture high volumes during winter storms to prevent flooding. In the spring, as much streamflow as possible is captured and stored in reservoirs to be delivered for multiple uses during the drier summer and fall months. This infrastructure was designed and optimized for historical conditions. Changing patterns of spring runoff, such as in the timing of peak monthly runoff, can strain the current water management system, requiring adjustments in water storage and flood strategies. In the last 30 years, peak runoff has shifted earlier by a month on the Sacramento River (March instead of April), compared to earlier years in the record (1931-1960); no such shift occurred in the San Joaquin River (see Figure 3).

Figure 3. Monthly average runoff: historical (1931-1960) vs. current (1991-2020)

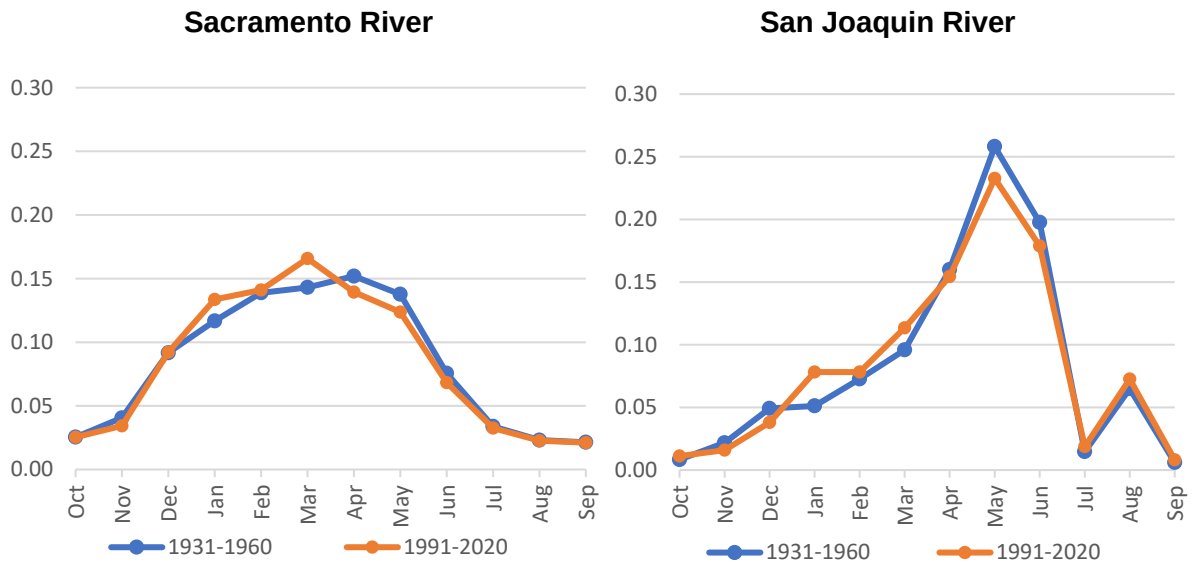

Source: DWR, 2022

A comparison between historical and current 30-year averages of the fraction of total water year runoff that occurs each month shows peak runoff occurring earlier in recent years in the Sacramento River, while the San Joaquin River is largely unchanged.

The earlier onset of spring runoff generally results in less available water in warmer months for domestic and agricultural uses, hydroelectric power production, recreation and other uses. This results in lower soil moisture, which could stress vegetation, lead to tree deaths (see *Forest tree mortality* indicator), and increase wildfire risk (see *Wildfires* indicator). Changes in the amount and the timing of snowmelt runoff can alter streamflow and impair cold water habitats, particularly for salmonid fishes (Roos, 2000; Halofsky, 2021). Runoff during rain-on-snow events – when rain falls on existing snowpack – has been associated with mass erosion of slopes, damage to riparian zones, and downstream flooding (Li et al., 2019). Past warming has been shown to increase early season runoff in the Sierras by about 30 percent, thus increasing runoff-driven flood risk (Huang et al., 2018).

What factors influence this indicator?

Lower water volumes of spring snowmelt runoff compared to the rest of the water year indicate warmer winter temperatures or early onset of warm springtime temperatures. With warmer winter temperatures, a greater proportion of precipitation occurs as rain, and snow falls and accumulates at higher elevations than in the past. Higher elevations of the snow line mean reduced snowpack and runoff in the spring.

Increased winter snowmelt was found to be highly sensitive to temperature in 34 percent of snow monitoring stations across western North America (Musselman et

al., 2021). In the Sierra Nevada, the peak snow mass and snowmelt shifted earlier over the past 30 years, as daily maximum temperatures increased in March and April (Kapnick and Hall, 2010). Years of "snow drought" – defined as anomalously low snow-water content (Cooper et al., 2016) –between 1951 and 2017 originated and evolved in various ways in the northern Sierra Nevada (Hatchett and McEvoy, 2018), including from extreme early season precipitation, frequent rain-on-snow events, lower fractions of precipitation falling as snow, and midwinter peak runoff events. These conditions are generally associated with earlier snowmelt runoff.

The characteristics of a watershed affect changes in runoff. Because they are located at lower elevations, the Sacramento River watersheds are more vulnerable to reduced snowpack than the San Joaquin River watersheds. A study of projected changes in runoff in the 21st century found that the rain-dominated Sacramento watersheds will experience earlier and increased amounts of peak runoff; in contrast, in the snow-dominated San Joaquin watersheds, runoff peak timing and amounts are projected to remain relatively unchanged (He et al., 2019; He et al., 2020).

Technical Considerations

Data characteristics

Runoff for the Sacramento River system is the sum of the estimated unimpaired runoff of the Sacramento River and its major tributaries, the Feather, Yuba, and American Rivers. "Unimpaired" runoff refers to the amounts of water produced in a stream unaltered by upstream diversions, storage, or by export or import of water to or from other basins. The California Cooperative Snow Surveys Program of the California Department of Water Resources (DWR) collects the data. Runoff forecasts are made systematically, based on historical relationships between the volume of April through July runoff and the measured snow water content, precipitation, and runoff in the preceding months (Roos, 1992).

Related snowpack information is used to predict how much spring runoff to expect for water supply purposes. Each spring, about 50 agencies, including the United States Departments of Agriculture and Interior, pool their efforts in collecting snow data at about 260 snow courses throughout California. A snow course is a transect along which snow depth and water equivalent observations are made, usually at ten points. The snow courses are located throughout the state from the Kern River in the south to Surprise Valley in the north. Courses range in elevation from 4,350 feet in the Mokelumne River Basin to 11,450 feet in the San Joaquin River Basin.

Since the relationships of runoff to precipitation, snow, and other hydrologic variables are natural, it is preferable to work with unimpaired runoff. To get unimpaired runoff, measured flow amounts have to be adjusted to remove the effect of infrastructure or water management operations such as reservoirs, diversions, or imports (Roos, 1992). The water supply forecasting procedures are based on multiple linear regression

equations, which relate snow, precipitation, and previous runoff terms to April-July unimpaired runoff.

Major rivers in the forecasting program include the Trinity, Pit, McCloud, Sacramento, Feather, Yuba, American, Cosumnes, Mokelumne, Stanislaus, Tuolumne, Merced, San Joaquin, Kings, Kaweah, Tule, Kern, Truckee, East and West Carson, East and West Walker, and Owens.

Strengths and limitations of the data

River runoff data have been collected for over a century for many monitoring sites. Stream flow data exist for most of the major Sierra Nevada watersheds because of California's dependence on their spring runoff for water resources and the need for flood forecasting. The April to July unimpaired flow information represents spring rainfall, snowmelt, as adjusted for upstream reservoir storage calculated depletions, and diversions into or out from the river basin. Raw data are collected through water flow monitoring procedures and used along with the other variables in a model to calculate the unimpaired runoff of each watershed.

Over the years, instrumentation has changed and generally improved; some monitoring sites have been moved short distances to different locations. The physical shape of the streambed can affect accuracy of flow measurements at monitoring sites, but most foothill sites are quite stable.

OEHHA acknowledges the expert contribution of the following to this report:

Sean de Guzman, P.E.
California Department of Water Resources
sean.deguzman@water.ca.gov

Michael L. Anderson, Ph.D., P.E.
Michael.L.Anderson@water.ca.gov

Elissa Lynn
elissa.lynn@water.ca.gov

Peter Coombe
peter.coombe@water.ca.gov

Benjamin Hatchett, Ph.D.
Western Regional Climate Center
Benjamin.Hatchett@dri.edu

References:

DWR (2021). California Department of Water Resources:Hydroclimate Report, Water Year 2020. Office of the State Climatologist. August 2021.

DWR (2022). Chronological Reconstructed Sacramento and San Joaquin Valley Water Year Hydrologic Classification Indices. Data provided by Peter Coombe and Sean de Guzman, California Department of Water Resources.

Halofsky JE (2021). Chapter 2: Climate Change Effects in the Sierra Nevada. In: *Climate change vulnerability and adaptation for infrastructure and recreation in the Sierra Nevada*. Halofsky JE, Peterson DL, Buluc LY, Ko JM (Eds). General Technical Reports PSW-GTR-2xx. U.S. Department of Agriculture, Forest Service, Pacific Southwest Research Station. Albany, CA.

He M, Anderson M, Schwarz A, Das T, Lynn E, et al. (2019). Potential Changes in Runoff of California's Major Water Supply Watersheds in the 21st Century. *Water* **11**(8): 1651.

Huang X, Hall AD and Berg N ((2018). Anthropogenic warming impacts on today's Sierra Nevada snowpack and flood risk. *Geophysical Research Letters* **45**: 6215–6222.

Kang S, Zhang Y, Qian Y and Wang H (2020). A review of black carbon in snow and ice and its impact on the cryosphere. Earth-Science Reviews **210**: 103346.

Kapnick S and Hall A (2010). Observed Climate–Snowpack Relationships in California and their Implications for the Future. *Journal of Climate* **23**: 3446–3456.

Li D, Lettenmaier DP, Margulis SA and Andreadis K (2019). The role of rain-on-snow in flooding over the conterminous United States. *Water Resources Research* **55**: 8492–8513.

Mantua NJ and Hare SR (2002). The pacific decadal oscillation. *Journal of Oceanography* **58**(1): 35-44.

Mote PW, Li S, Lettenmaier DP. et al. (2018). Dramatic declines in snowpack in the western US. *npj Climate and Atmospheric Science* **1**: 2.

Musselman KN, Addor N, Vano JA and Molotch NP (2021). Winter melt trends portend widespread declines in snow water resources. *Nature Climate Change* **11**: 418–424.

NPS (2017). National Park Service: Hydrology, Yosemite National Park. Retrieved August 2017.

Roos M (1992). Water Supply Forecasting Technical Workshop. California Department of Water Resources.

Roos M (2000). *Possible Effects of Global Warming on California Water or More Worries for the Water Engineer*. W. E. F. Water Law and Policy Briefing. Department of Water Resources. San Diego, CA.

Roos M and Anderson M (2006). Monitoring monthly hydrologic data to detect climate change in California. *Third Annual Climate Change Research Conference*. Sacramento, CA.

Waliser D, Kim J, Xue Y, Chao Y, Elderling A, et al. (2011). Simulating cold season snowpack: Impacts of snow albedo and multi-layer snow physics. *Climatic Change* **109**: 95–117.

GLACIER CHANGE

California's glaciers have melted dramatically over the past century. From the beginning of the twentieth century to 2021, some of largest glaciers in the Sierra Nevada have lost an average of about 75 percent of their area. Of the two glaciers in the Trinity Alps, one has recently disappeared and the other has lost more than 98 percent of its area.

Figure 1. Change in area, selected Sierra Nevada glaciers (as fraction 1903 area)

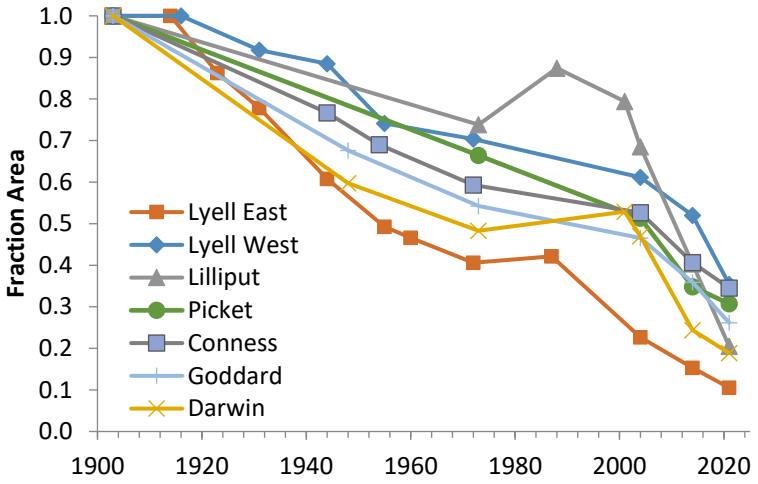

Source: Basagic and Fountain, 2011
(updated 2021 H. Basagic, unpublished data)

Figure 2. Change in area, Trinity Alps glaciers and snowfields (as fraction of 1994 area)

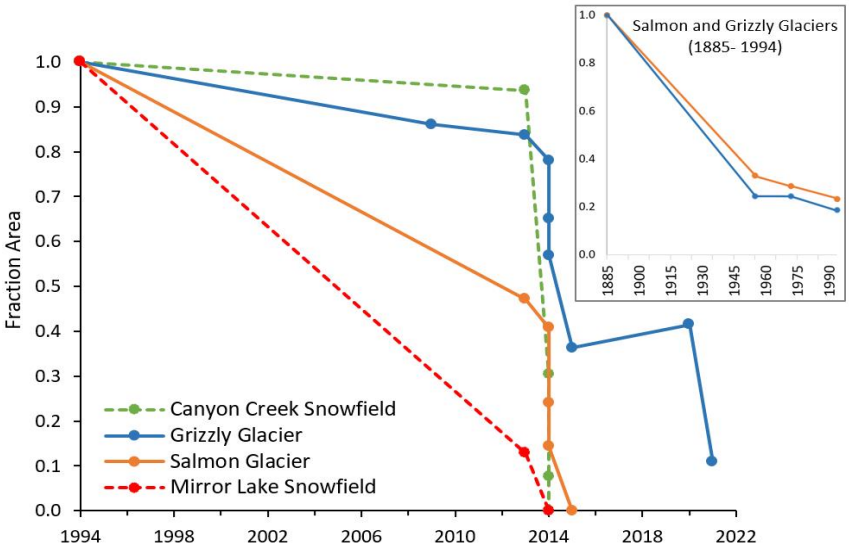

Source: Garwood et al., 2020
(updated 2021, J. Garwood, unpublished data)

Note: inset shows change in glacier areas relative to about 1885.

What does the indicator show?

Dramatic reductions in the area of selected glaciers and snowfields have occurred in California (see Figure 3 for locations). A "glacier," by definition, is a mass of perennial snow or ice that moves (Cogely et al., 2011). Figure 1 shows large declines in the area of seven Sierra Nevada glaciers relative to 1903. Figure 2 shows substantial losses in the size of glaciers and snowfields in the Trinity Alps since 1994. Historical and contemporary photographs allow for a visual comparison of the changes (see Appendix A).

Figure 3. Glaciers and perennial snow regions in California

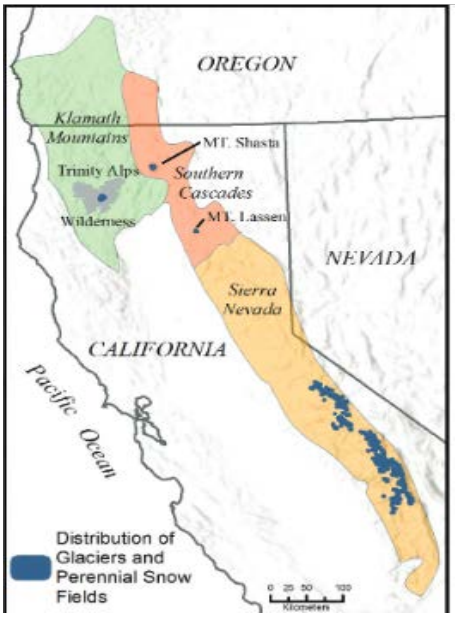

Source: Garwood et al., 2020

As shown in Figure 1, by 2021, the Sierra Nevada glaciers lost 65 to 89 percent (an average of about 75 percent) of their 1903 area, after having lost about half of their area since the 1970s (Basagic and Fountain, 2011, updated to 2021). These findings are consistent with those from a separate study of 769 glaciers and perennial snowfields that were identified within the Sierra Nevada in the 1970s and 1980s based on the US Geological Survey's 1:24,000-scale, topographic maps (Fountain et al., 2017). The largest 39 glaciers, free of rock debris mantling the surface, covered an area of 2.74 ± 0.12 square kilometers (km^2) in the 1970s and 1980s. By 2014, overall, they lost about 50 percent of their area.

The main graph in Figure 2 shows the percentage glacier area remaining relative to 1994 for two glaciers and two perennial snowfields in the Trinity Alps between 1994 and 2015 (Garwood et al., 2020) and subsequent measurements of Grizzly Glacier recorded through 2021 (Garwood, unpublished data). The inset shows changes in the area of Grizzly and Salmon Glaciers relative to their estimated areas around 1885; data prior to 1994 are not available for the Canyon Creek and Mirror Lake Snowfields. Both glaciers had lost 70 to 75 percent of their area between 1885 and 1955; by 1994, only about 20 percent of their 1885 area remained. Between 1994 and 2013, Salmon Glacier experienced far greater loss than Grizzly Glacier: 53 and 16 percent, respectively, of their areas in 1994. The extended drought, which occurred from 2012 to 2016, resulted in the catastrophic loss of both glaciers. In 2015, Salmon Glacier disappeared entirely and the lower half of Grizzly Glacier broke apart into large ice blocks, leaving only the upper portion of the glacier intact (see historical and contemporary photographs in Appendix A).

Measurements of Grizzly Glacier taken between the fall of 2020 and the fall of 2021 revealed more catastrophic decline with a 76 percent further reduction in area. Given this substantial reduction, it is uncertain whether what remains in the fall of 2021 is still

considered a glacier, or whether it is now a perennial icefield. Appendix B shows the outlines of the glaciers for selected years between approximately 1885 to 2015 for Salmon Glacier and 1885 to 2021 for Grizzly Glacier; estimated areas from 1955 to 2021 are presented in an accompanying table.

Two prominent snowfields that were still present in 1994 completely melted during the extended drought. Mirror Lake Snowfield diminished precipitously and disappeared by 2014; Canyon Creek Snowfield melted gradually between 1994 and 2013, shrank in area by almost 70 percent from late 2013 to mid 2014, and disappeared in late 2014. Both snowfields have yet to persist more than a year through 2021 due to low winter precipitation and high summer temperatures (Garwood et al., 2020, updated to 2021).

Figure 4. Regional cumulative mass change of global reference glaciers*

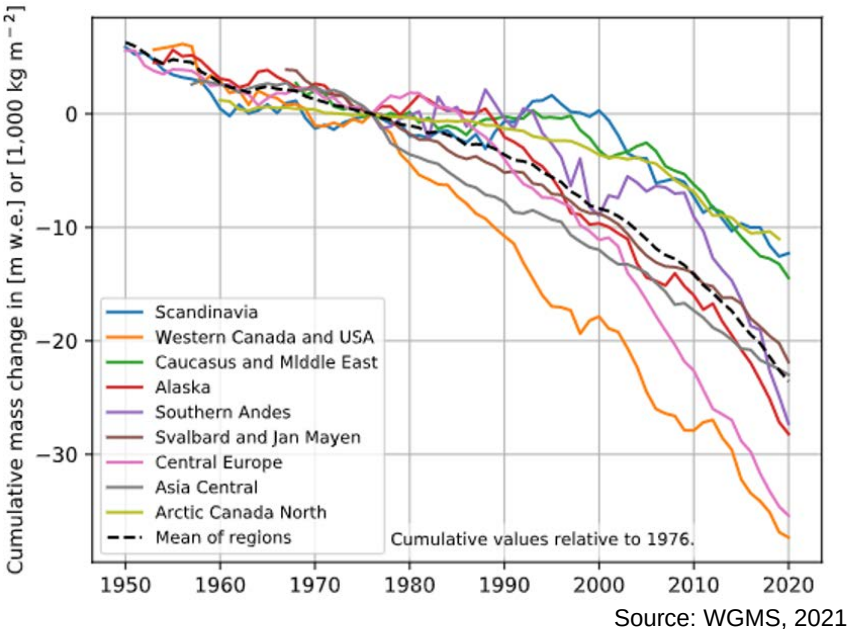

Source: WGMS, 2021

*"**Cumulative mass change**" is reported in meters of water equivalent (m w.e.) or 1,000 kilogram per square meter (kg m^{-2}). Cumulative values are relative to 1976 and calculated using a single value (averaged) for each mountain range. **Regional values** are calculated as arithmetic averages. **Global values** are calculated using one single value (averaged) for each region with glaciers to avoid a bias to well-observed regions.*

Over the 20th century, with few exceptions, alpine glaciers have been receding throughout the world in response to a warming climate. Figure 4 presents trends since 1950, although global measurements date back to 1917 or earlier. The graph is based on standardized observations of a set of glaciers collected by the World Glacier Monitoring Service (WGMS, 2021) in more than 40 countries worldwide. Regional mass changes are shown relative to 1976 global mean values (dotted line). Glacier mass change is reported as "cumulative mass change in meters of water equivalent (m w.e.)"; this unit is the equivalent of a mass loss of 1,000 kilograms per square meter of ice

cover or an annual glacier-wide ice thickness loss of about 1.1 meter per year. As shown in the graph, glaciers in the Western United States and Canada (two in Alaska and seven in the Cascade and Pacific Coast Ranges of Washington State and Canada) are experiencing greater glacier loss than other regions of the world.

Why is this indicator important?

Glaciers are important indicators of climate change. Because glaciers are sensitive to fluctuations in temperature, they provide visual evidence of warming. Glacier loss can lead to cascading effects on hydrology, alter aquatic habitats, contribute to sea level rise, and impact recreation and tourism (USGS, 2021a).

Glaciers are important to alpine hydrology by acting as frozen reservoirs of snow. They begin to melt most rapidly in late summer after the bright, reflective seasonal snow disappears, revealing the darker ice beneath. This often causes peak glacial runoff to occur in late summer when less water is available and demand is high. Glacier shrinkage reduces this effect, resulting in earlier peak runoff and drier summer conditions. These changes are likely to have ecological consequences for flora and fauna in the area that depend on available water resources. For example, many aquatic species in alpine and subalpine environments require cold water temperatures to survive. Some aquatic insects – fundamental components of the food web – are especially sensitive to stream temperature and require glacial meltwater for survival. Finally, glacier shrinkage worldwide is an important contribution to global sea level rise (IPCC, 2019).

The Trinity Alps is a glaciated subrange of the Klamath Mountains in northwest California (see Figure 3 map). This region has experienced much greater fractional losses of glacier area than the Sierra Nevada and other glaciated regions of the western US. Around 1885, at least six glaciers existed in the Trinity Alps (Garwood et al., 2020). Grizzly and Salmon glaciers are the only two that persisted into the 21st century. In addition, all snowfields throughout the Trinity Alps and greater Klamath Mountains of southern Oregon and northern California had fully disappeared by 2014.

The Trinity Alps and entire Klamath Range ecoregion are globally recognized for their rich biodiversity (DellaSala et al., 1999; Olson et al., 2012). Glacial ice and persistent snow influence local species composition and their distributions by extending perennial wetlands into high elevations that normally lack surface waters. The freshwater habitats of the region support exceptionally high levels of endemic species. Most mollusk populations have declined dramatically throughout the region, and over 10 fish taxa have a special status designation due to habitat degradation and changes in hydrology and water quality. A beetle species (*Nebria praedicta*) endemic to the Grizzly Glacier basin depends on perennial snow and ice to maintain the cool microclimate needed to survive (Kavanaugh and Schoville, 2009). The coastal tailed frog (*Ascaphus truei*), a California Species of Special Concern (see Figure 5), is adapted to cold-water streams.

Its highest known population across its range was discovered in 2009 directly below the Canyon Creek snowfield, which disappeared in 2014 (Garwood et al., 2020).

Figure 5. Coastal Tailed Frog

Photo credit: Thompson *et al.*, 2016

The Coastal tailed frog (Ascaphus truei) ranges from British Columbia to northern California, from near sea level in Humboldt County up to elevations of 2150 meters in the Trinity Alps (CDFW, 2016).

Three watersheds in this region contribute glacial and/or snowmelt cold-water streamflow directly to fish-bearing streams containing small populations of spring Chinook salmon (*Oncorhynchus tshawytscha*) and summer steelhead (*Oncorhynchus mykiss*). The Klamath-Trinity River spring Chinook salmon were listed as threatened by the State of California in June 2021 (CDFW, 2021) and are currently being considered for listing as endangered under the Federal Endangered Species Act (Federal Register 2018, 2019). These species migrate from the Pacific Ocean to these streams and stage in deep cold-water pools throughout the summer months before spawning in the fall. The dramatic local declines of glacial ice and annual snowpack in the Klamath Range foretell how climate change threatens the unique distributions and resiliency of fish adapted to local glacier and snow dependent environments (Garwood et al, 2020).

What factors influence this indicator?

A glacier is a product of regional climate, responding to the combination of winter snow and spring/summer temperatures. Typically, glaciers exist in areas with significant accumulations of snow, temperatures during the year that do not result in the complete loss of the winter snow accumulation, and average annual temperatures near freezing, (USGS, 2021b). Winter snowfall nourishes the glaciers; winter temperature determines whether precipitation falls as rain or snow, thus affecting snow accumulation and glacier mass gain. The greater the winter snowfall, the healthier the glacier. Spring and summer air temperature affects the rate of snow and ice melt.

In the early 20th century, glaciers retreated (decreased in size) rapidly throughout the western US in response to the end of the Little Ice Age and warming air temperatures (Basagic and Fountain, 2011). In recent years, increasing winter and spring temperatures across North America have led to less snowpack in spring and early summer (Mote *et al.*, 2018). Based on their assessment of studies of glaciers in various parts of the world, the Intergovernmental Panel on Climate Change concluded that human-induced warming likely contributed substantially to widespread glacier retreat during the 20th century (IPCC, 2021).

Alpine glaciers gain or lose mass primarily through climatic processes controlling energy and mass exchange with the atmosphere, then respond by either growing (advancing) or shrinking (retreating). The area changes observed in the Sierra Nevada study glaciers were triggered by a changing climate and modified by the dynamics of ice flow. Hence, glacier change is a somewhat modified indicator of climate change, with local variations in topography and climate either enhancing or reducing the magnitude of change so that each glacier's response is somewhat unique. Because glaciers persist across decades and centuries, they can serve as indicators of long-term climatic change.

Sierra Nevada

The glacier retreat in the Sierra Nevada occurred during extended periods of above average spring and summer temperatures; winter snowfall appears to be a less important factor (Basagic and Fountain, 2011). Following a cool and wet period in the early part of the 20th century, during which glacier area was constant, the Sierra Nevada glaciers began to retreat rapidly with warmer and drier conditions in the 1920s. The glaciers ceased retreating, while some glaciers increased in size (or "advanced") during the wet and cool period between the 1960s and early 1980s with below average temperatures. By the late 1980s, with increasing spring and summer temperatures, glacier retreat resumed, accelerating by 2001. Hence, the timing of the changes in glacier size appears to coincide with changes in air temperatures. In fact, glacier area changes at East Lyell and West Lyell glaciers were found to be significantly correlated with spring and summer air temperatures. In the past century, average annual temperatures in the Sierra Climate Region have warmed by almost 2 degrees Fahrenheit (°F), with summer and fall having warmed the most (2.6 and 2.5°F, respectively) (WRCC, 2021).

As can be seen from Figure 1, the seven glaciers studied have all decreased in area. However, the magnitude and rates of change are variable, suggesting that factors other than regional climate influenced these changes. One of these factors is glacier geometry. A thin glacier on a flat slope will lose more area compared to a thick glacier in a bowl-shaped depression, even if the rate of melting is the same. In addition, local topographic features, such as headwall cliffs, influence glacier response through shading solar radiation, and enhancing snow accumulation on the glacier through avalanching from the cliffs.

Trinity Alps

Grizzly and Salmon Glaciers and Canyon Creek and Mirror Lake Snowfields in the Trinity Alps occur at 2,460 meters, an elevation far lower than other glaciated areas in California. The high latitude region has a particularly wet climate during the winter months due to its proximity to the Pacific Ocean (Garwood et al., 2020). Although a marginal climate for glaciers, these glaciers have persisted into the 21st century due to topographic features where tall headwalls increase shading and enhance localized snow accumulation through avalanching and wind transport.

Although large data gaps exist, clearly the largest amount of ice loss in the Trinity Alps occurred during the first half of the 20th century with a combined area loss of 72 percent for Grizzly and Salmon glaciers (inset, Figure 2) (Garwood et al., 2020; also see Appendix B). Since then, the glaciers receded at a much slower but steady rate and persisted even while winter precipitation in the Trinity Alps was below the long-term average (using 1895 to 2015 as baseline) in 9 of the 20 years from 1996 to 2015, and summer temperatures exceeded the long-term average in 18 years of the same period. Scientists attribute the recent glacial retreat in the Trinity Alps (see Appendix, Figures A-2 and A-3) largely to unprecedented and consistently high summer temperatures coincident with record-low winter precipitation in the region during the 2012 to 2016 drought (Garwood et al., 2020) and thereafter in 2020 and 2021 (Garwood, unpublished data).

California's recent drought differed from earlier periods of persistent low precipitation by coinciding with a period of consistently record-high summer temperatures (see *Drought* indicator). During the severe drought, snowpack was at an all-time low – no other year since 1950 reported an April 1st snowpack of less than 34 percent in the Klamath Mountains (Garwood et al., 2020). As shown in Figure 2, it was this time period where Salmon Glacier melted completely and Grizzly Glacier partially broke apart and declined greatly in size.

Technical considerations

Data characteristics

Sierra Nevada

To quantify the change in glacier extent, seven glaciers in the Sierra Nevada were selected based on the availability of past data and location: Conness, East Lyell, West Lyell, Darwin, Goddard, Lilliput, and Picket glaciers. Glacier extents were reconstructed using historical photographs and field measurements. Aerial photographs were scanned and imported into a geographic information system (GIS). Only late summer photographs, largely snow free, were used in the interpretation of the ice boundary. The historic glacier extents were interpreted from aerial photographs by tracing the ice boundary. Early 1900 extents were based on ground-based images and evidence from moraines. To obtain recent glacier areas, the extent of each glacier was recorded using a global positioning system (GPS) in 2004. The GPS data were processed (2 to 3 meter accuracy), and imported into the GIS database. Glacier area was calculated within the GIS database. The 2014 outlines were derived from aerial photographs acquired by the US Department of Agriculture National Agricultural Imagery Program, 1-meter ground resolution. The 2021 imagery were acquired from DigitalGlobe WorldView © 2021 Maxar, 0.5-meter ground resolution. For both years, the imagery was loaded into ArcGIS and the glacier outlines digitized at a scale of about 1:500.

Trinity Alps

Long-term changes in glaciers and perennial snowfields were quantified using clearly defined moraines (loose sediment and rock debris deposited by glacier ice); vertical aerial orthophotos (photographs geometrically corrected such that the scale is uniform); high-resolution satellite images; and GPS mapping (Garwood et al., 2020; Garwood, unpublished data). The 1885 outlines were generated by mapping the ridgelines of prominent Holocene moraines coupled with mapping the near vertical bedrock headwalls at the upper extent of the glaciers. Eleven aerial and satellite images were acquired from 1955 to 2021. All aerial photographs had spatial resolutions of 1 meter; satellite imagery resolutions ranged from 0.33 to 0.5 meter. In addition, glacier perimeters were mapped using a GPS with an accuracy ± 2.6 meters. Ground-based photograph monitoring stations were established at each of the two glaciers to document qualitative changes in glacier geometry and morphology during field visits between the years of 2009 and 2018.

To examine the response of glaciers and perennial snowfields in the Trinity Alps to variations in climate, changes in glacier area were compared to winter precipitation and summer air temperature from the PRISM re-analysis data (Daly et al. 2008, PRISM Climate Group 2018), employing a similar analysis as Sitts et al. (2010), using data for the 4 km × 4 km PRISM grid cell centered on Thompson Peak for the period of January 1895 to September 2015.

Strengths and limitations of the data

The observation of tangible changes over time demonstrates the effects of climate change in an intuitive manner. This indicator relies on data on glacier change based on photographic records, which are limited by the availability and quality of historical photographs. The use of both aerial photographs and satellite images provides high quality visual data for measuring changes in glacier area. Detailed information about uncertainties associated with mapping the area of glaciers can be found in the methods section of Garwood et al. (2020). A limitation in relying on satellite and photographic images is that change in glacial volume cannot be assessed.

Increasing the number of studied glaciers and the number of intervals between observations would provide a more robust data set for analyzing statistical relationships between glacier change and climatological and topographic parameters. Additionally, volume measurements would provide valuable information and quantify changes that area measurements alone may fail to reveal.

OEHHA acknowledges the expert contribution of the following to this report:

Andrew G. Fountain, Ph.D. and Hassan J. Basagic
Department of Geology
Portland State University
andrew@pdx.edu
(503) 725-3386
www.glaciers.us

Justin Garwood
California Department of Fish and Wildlife
Northern Region
Justin.Garwood@wildlife.ca.gov

Reviewer:

Whitney Albright, CDFW

References:

Basagic HJ and Fountain AG (2011, updated by Basagic H, 2021). Quantifying 20th century glacier change in the Sierra Nevada, California. *Arctic, Antarctic, and Alpine Research* **43**(3): 317-330.

CDFW (2016). *Coastal Tailed Frog.* In: California Amphibian and Reptile Species of Special Concern, by Thompson RC, Wright AN, and Shaffer HB. California Department of Fish and Wildlife, University of California Press. pages 51-58.

CDFW (2021). *State and Federally Listed Endangered and Threatened Animals of California.* California Department fo Fish And Wildlife. October 2021.

Cogley JG, Hock R, Rasmussen LA, Arendt AA, Bauder A, *et al.* (2011). *Glossary of Glacier Mass Balance and Related Terms, IHP-VII Technical Documents in Hydrology No. 86, IACS Contribution No. 2, UNESCO-IHP*.

Daly CM, Halbleib J, Smith W, Gibson M, Doggett G, et al. (2008). Physio-graphically-sensitive mapping of temperature and precipitation across the conterminous United States. *International Journal of Climatology* **28**:2031-2064.

DellaSala DA, Reid SB, Frest TJ, Strittholt JR and Olson DM (1999). A global perspective on the biodiversity of the Klamath-Siskiyou ecoregion. *Natural Areas Journal* **19**:300-319.

Federal Register (2018). Endangered and threatened wild-life; 90-day finding on a petition to list Chinook salmon in the upper Klamath-Trinity Rivers Basin as threatened or endangered under the Endangered Species Act. Federal Register **83**:8410-8414, Washington, DC.

Federal Register (2019). Endangered and threatened wild-life; 90-day finding on a petition to list summer-run steelhead in northern California as threatened or endangered under the Endangered Species Act. Federal Register **84**:16632-16636, Washington, DC.

Fountain AG, Glenn B and Basagic HJ (2017). The geography of glaciers and perennial snowfields in the American West. *Arctic, Antarctic, and Alpine Research* **49**(3): 391-410.

Garwood JM, Fountain AG, Lindke KT, van Hattem MG and Basagic HJ (2020). 20th century retreat and recent drought accelerated extinction of mountain glaciers and perennial snowfields in the Trinity Alps, California: *Northwest Science* **94**(1): 44-61. Published By: Northwest Scientific Association:

IPCC (2019). *Special Report on the Ocean and Cryosphere in a Changing Climate*. Pörtner HO, Roberts DC, Masson-Delmotte V, Zhai P, Tignor M, *et al.* Geneva, Switzerland: Intergovernmental Panel on Climate Change.

IPCC (2021). *Climate Change 2021: The Physical Science Basis. Contribution of Working Group I to the Sixth Assessment Report of the Intergovernmental Panel on Climate Change* [Masson-Delmotte V, Zhai P, Pirani A, Connors SL, Péan C, et al. (eds.)]. Cambridge University Press. In Press.

Kavanaugh D and Schoville S (2009). A new and endemic species of Nebria latreille (Insecta: Coleoptera: Carabidae: Nebriini), threatened by climate change in the Trinity Alps of northern California. *Proceedings of the California Academy of Sciences* Series 4, **60**: 73-84.

Olson D, DellaSala DA, Noss RF, Strittholt JR, Kass J, *et al.* (2012). Climate change refugia for biodiversity in the Klamath-Siskiyou ecoregion. *Natural Areas Journal* **32**: 65-74.

PRISM Climate Group (2018). Spatial climate dataset. Oregon State University, Corvallis. Retrieved 06 November 2018.

PSU (2021). Portland State University: Glaciers of the American West. Retrieved December 21, 2021.

Sitts DJ, Fountain AG and Hoffman MJ (2010). Twentieth century glacier change on Mount Adams, Washington, USA. *Northwest Science* **84**: 378-385.

USGS (2021a). Glaciers – Understanding Climate Divers. US Geological Survey, Northern Rocky Mountain Science Center. Retrieved December 21, 2021.

USGS (2021b). What is a Glacier? US Geological Survey. Retrieved December 21, 2021.

WGMS (2021). World Glacier Monitoring Service: Latest Glacier Mass Balance Data. Retrieved March 2, 2021.

WRCC (2021). Sierra (California Climate Region) Mean temperatures for spring, summer, fall, winter and annual average. California Climate Tracker, Western Regional Climate Center. Retrieved December 15, 2021.

APPENDIX A. Historical and Contemporary Glacier Photographs

Historical glacier responses preserved in photographs are important records of past climates in high alpine areas where few other climate records exist. Repeat photographs – paired historical and contemporary images – for selected glaciers are presented below. Additional photographs of the Sierra Nevada, Trinity Alps and other western glaciers can be viewed at the "Glaciers of the American West" web site (PSU, 2017).

Figure A-1. Historical and contemporary late summer photographs of two Sierra Nevada glaciers

Dana Glacier

Credit: U.S. Geological Service, photo station ric046: I.C. Russell, 1883 (left); R. Hallnan (right)

Conness Glacier

Credit: National Park Service, photo station Conness 5555 (left); H. Basagic (right)

Figure A-2. Salmon Glacier, repeat photographs

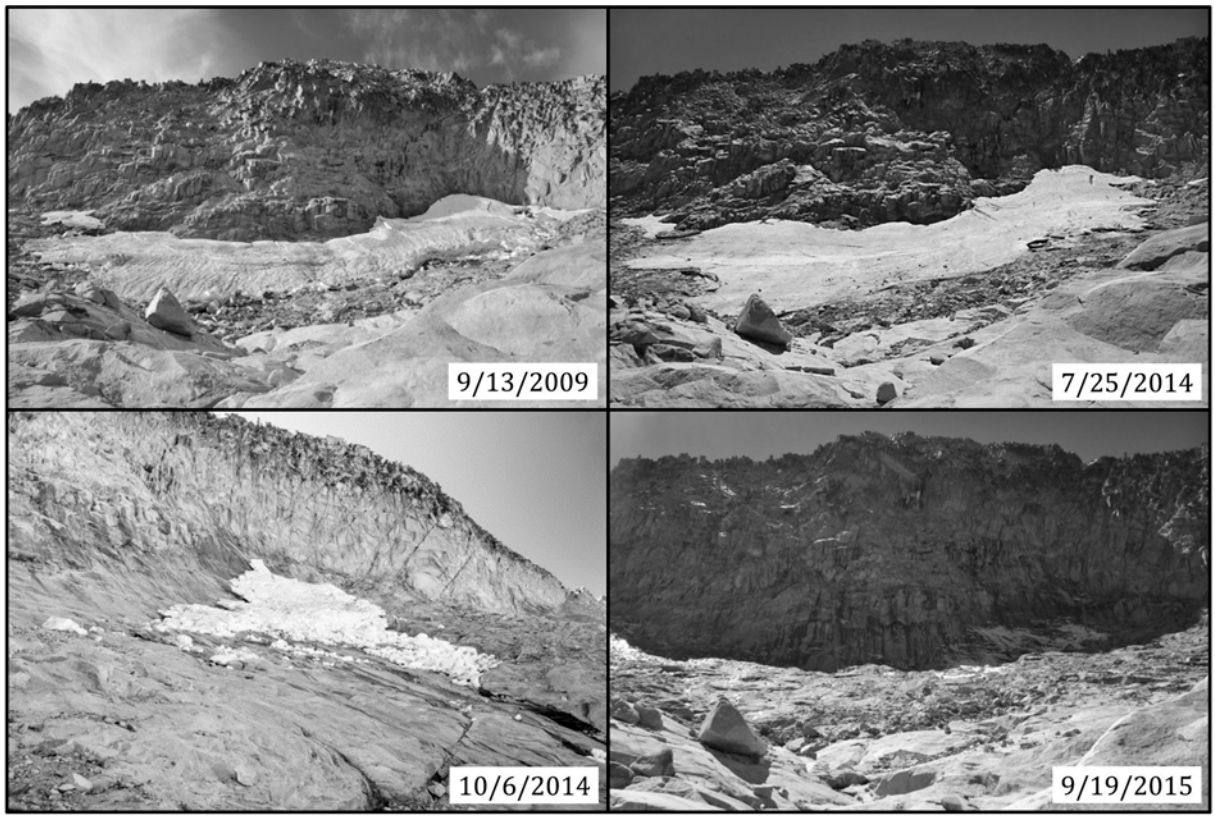

Credit: Photos taken by J. Garwood (September 2009 and 2015), R. Bourque (July 2014) and J. Barnes (October 2014)

Repeat photographs of Salmon Glacier were taken between September 2009 and September 2015. The October 2014 image was taken northeast of the feature facing southwest whereas the others were taken north of the feature facing due south. The glacier broke apart in 2014 and completely melted away by the fall of 2015. The patchy snow observed in shadows of the 2015 image accumulated during a small storm that occurred two days prior to the image date (Garwood et al., *2020).*

Figure A-3. Grizzly Glacier, repeat photographs

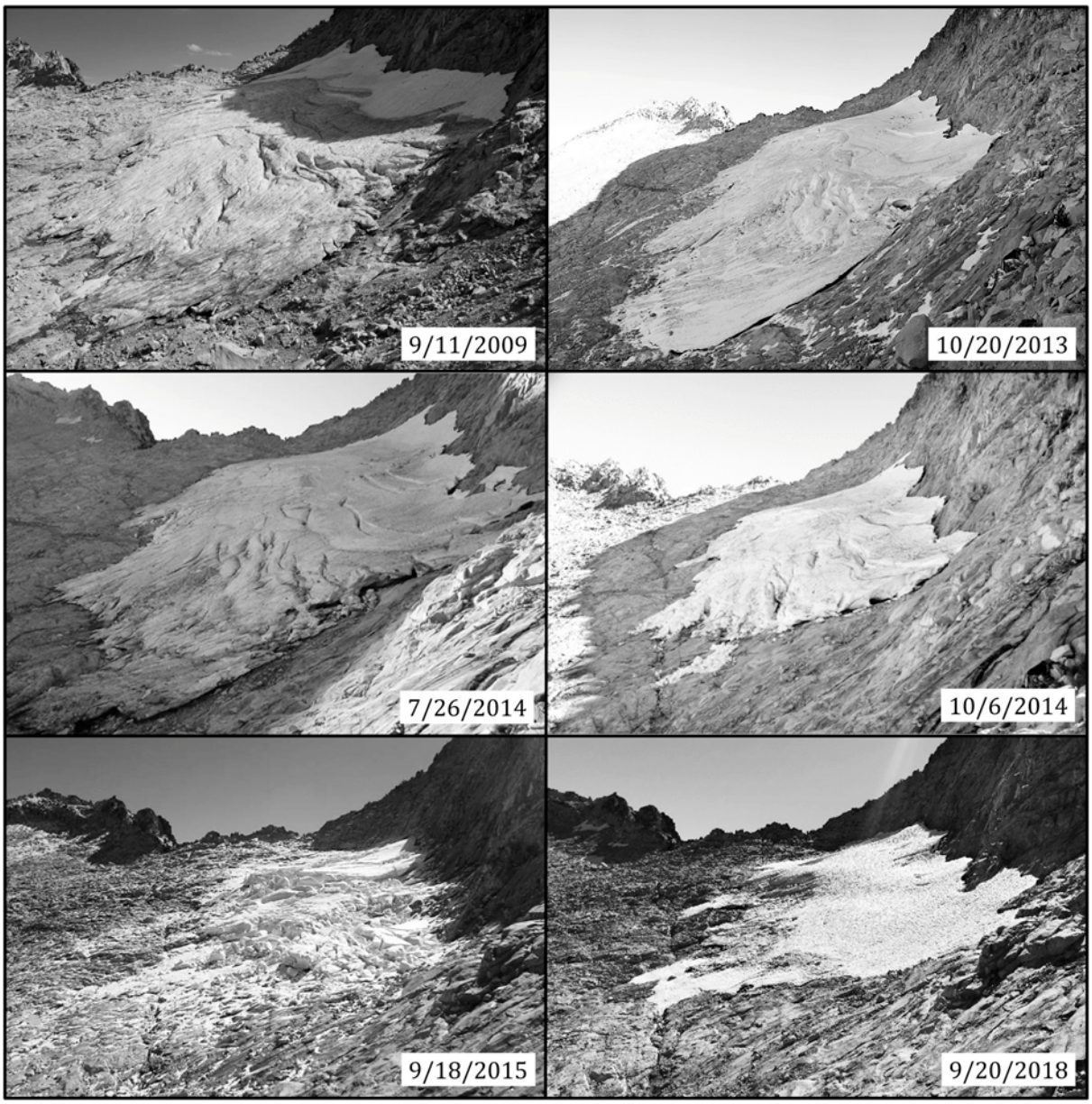

Credit: All photographs taken by J. Garwood with exception of October 2013 by K. Lindke and October 2014 by J. Barnes

Repeat photographs of Grizzly Glacier were taken between September 2009 and September 2018. The lower half of the glacier broke apart in the fall of 2015. A thin layer of fresh snow visible in the September 2015 image accumulated during a brief storm that occurred two days prior to the image date. This snow cover visually exaggerates the actual glacier size beyond the visible pile of scattered ice debris visible in the photo; a result of extreme calving in the lower half of the feature during the summer of 2015 (Garwood et al., 2020).

APPENDIX B. Glacier area loss for in the Trinity Alps, California

Digitized outlines of Grizzly Glacier (B-1) and Salmon Glacier (B-2) from approximately 1885 to 2021. Salmon Glacier disappeared completely by the fall of 2015 while Grizzly Glacier maintained a similar area between 2015 and 2020 before losing 76 percent of its 2020 area during the summer and early fall of 2021. The 1885 outlines were generated by mapping the ridgelines of prominent Holocene moraines coupled with mapping the near vertical bedrock headwalls at the upper extent of the glaciers. The 1885 outlines represent the most recent Little Ice Age glacial advance. Due to extensive residual snow cover on Salmon Glacier in 1955 and 1972, outlines include a minimum estimated area (solid colors) and additional maximum estimated area dotted lines. Satellite base image date is from 26 July 2014. Approximate surface elevations are noted at four locations at each glacier.

Figure B-1. Grizzly Glacier, digitized outlines

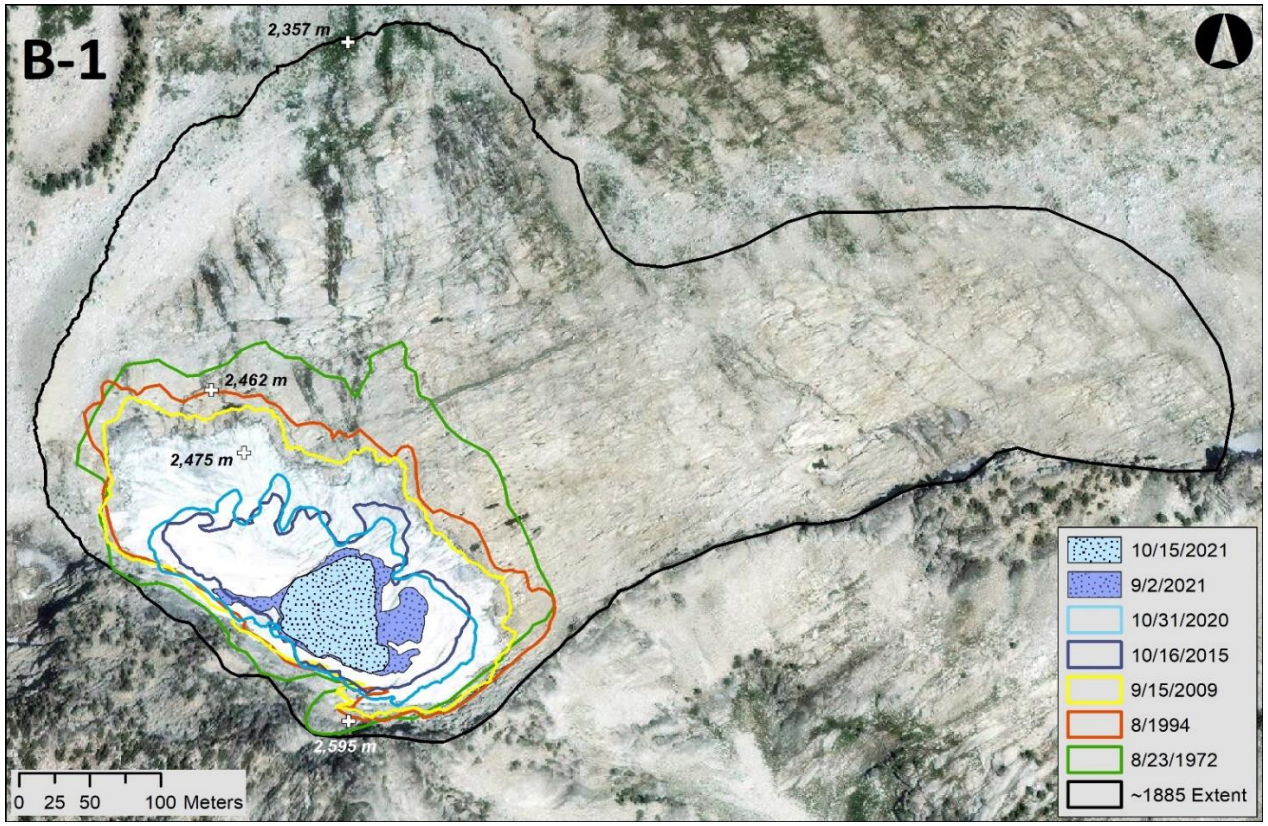

Source: Garwood et al., 2020 (updated 2021; J. Garwood, unpublished data)

Figure B-2. Salmon Glacier, digitized outlines

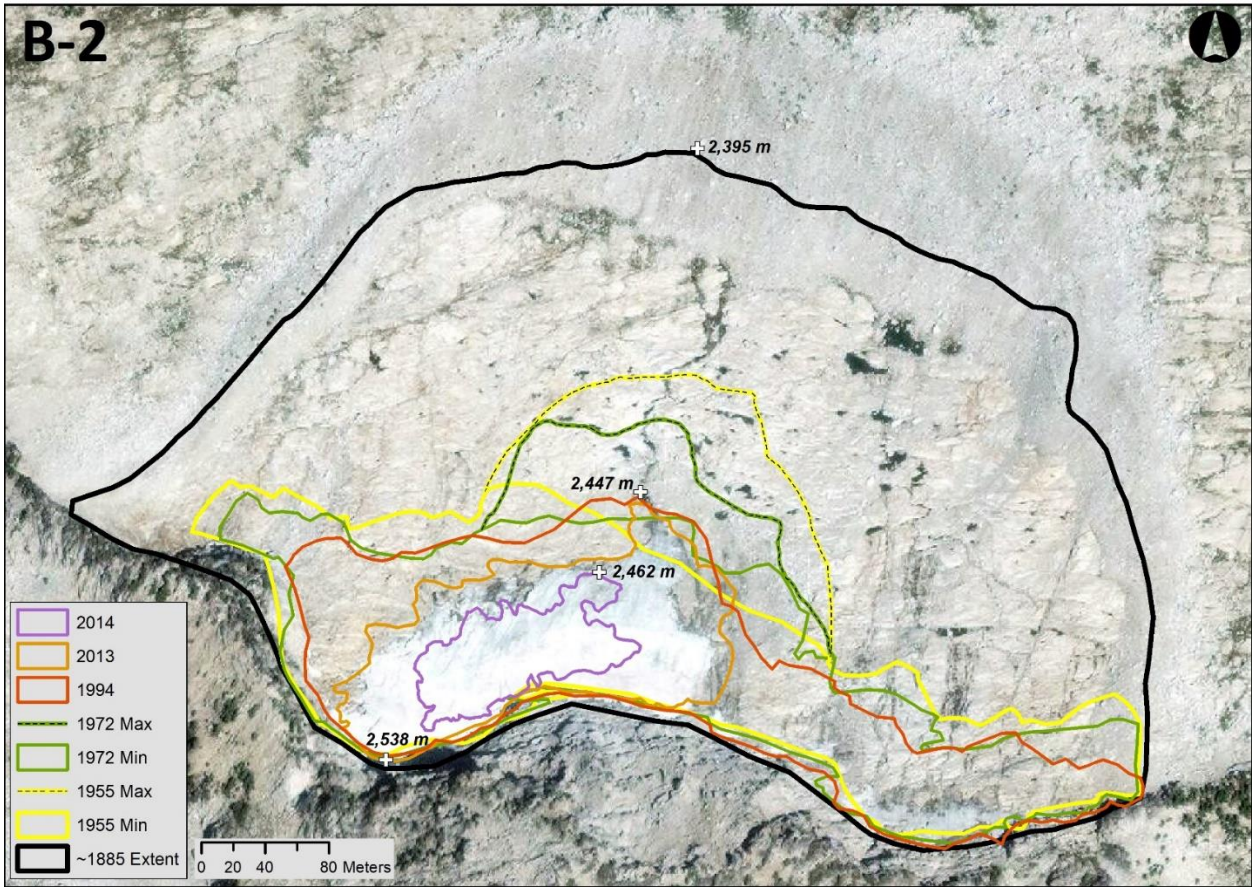

Source: Garwood et al., 2020

Table 1. Estimated areas* in hectares of glaciers in the Trinity Alps, from ca. 1885 to 2021

Year	Grizzly Glacier	Salmon Glacier
ca. 1885	24.44	19.40
1955	6.01*	6.45
1972 (Aug)	6.00*	5.58
1994 (Aug)	4.60	4.54
2009 (Sept)	3.96	not measured
2013 (Oct)	3.85	2.14
2014 (July)	3.59	1.85
2014 (Sept)	2.99	1.09
2014 (Oct)	2.62	0.65
2015 (Oct)	1.67	extinct
2020 (Oct)	1.91	extinct
2021 (Oct)	0.45	extinct

Source: Garwood et al., 2020 (updated 2021; J. Garwood, unpublished data)

* Average areas shown are estimated due to residual snow cover partially obscuring lower glacier margin;
1 hectare = 10,000 square meters or 2.5 acres

LAKE WATER TEMPERATURE

Lake Tahoe waters are warming in response to changing climate conditions in the Sierra Nevada.

Figure 1. Annual average water temperatures at Lake Tahoe

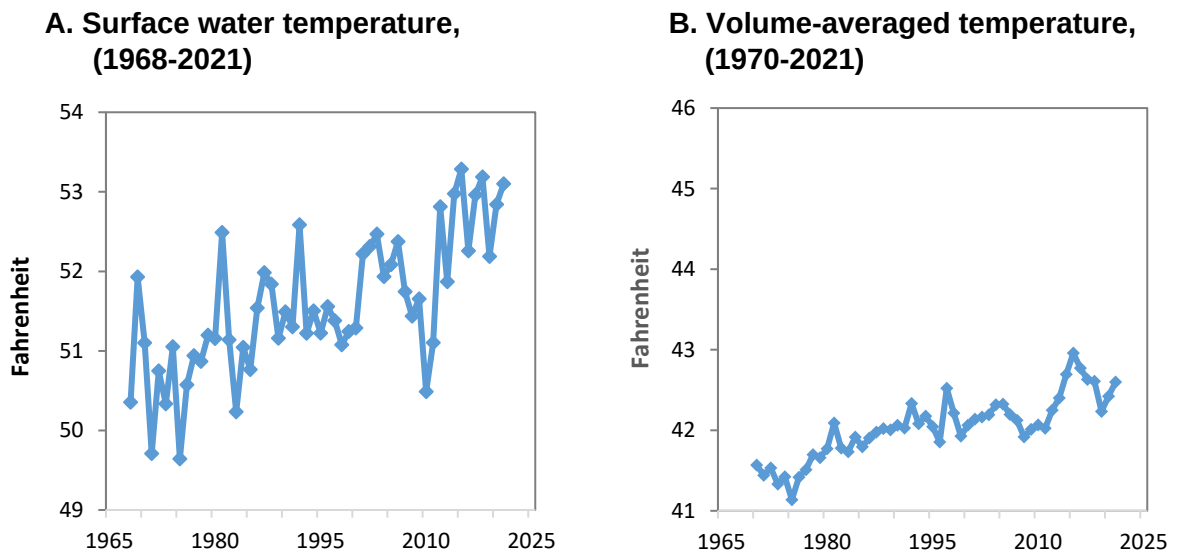

Source: UC Davis, 2022

What does the indicator show?

Annual average surface water temperatures at Lake Tahoe, which varied greatly from year to year, have increased by 1.97 degrees Fahrenheit (°F) since 1968, at a rate of 0.39°F per decade (Figure 1A). The highest average surface temperatures were recorded in seven of the last 10 years, with 2015 reporting the warmest on record (53.29°F).

Figure 1B shows annual average lake water temperatures across multiple depths (”volume-averaged”). Volume-averaged temperatures have warmed overall in the past fifty years by approximately 1.1°F, at a rate of 0.22°F per decade: a smaller increase compared to surface water temperatures (Figure 1A). After peaking in 2015, volume-averaged temperatures trended down until 2019, but showed an uptick in 2020 and 2021.

While Lake Tahoe is unique, the physical, chemical and biological forces and processes that shape it reflect those acting in most natural ecosystems. Thus, Lake Tahoe can serve as an indicator for other systems both in California and worldwide (UC Davis, 2022).

Warming has also been reported in other lakes in the western United States. Temperature data derived from satellite observations show increasing summertime surface water temperatures in a 16-year study of four lakes in Northern California

(including Lake Tahoe) and two in Nevada (Schneider et al., 2009). From 1992 to 2008, these six lakes showed a significant warming trend for summer (July through September) nighttime surface temperatures, ranging from 0.05 degrees Celsius (°C) per year at Clear Lake to 0.15°C per year at Lake Almanor and Mono Lake. The lakes exhibited a fairly similar rate of change, with the mean warming rate of 0.11°C per year (± 0.03°C per year).

Why is this indicator important?

Climate change is among the greatest threats to lakes (O'Reilly et al., 2015). Lakes are sensitive to climate, respond rapidly to change, and integrate changes in the land areas that drain into them (catchment). Thus, they also serve as good sentinels for climate change. Lakes in mountain regions may be particularly sensitive to ongoing changes in climate in part because high-elevation ecosystems are warming at among the fastest rates found globally. Aquatic habitats most vulnerable to climate effects, especially rising temperatures, are alpine lakes like Lake Tahoe that sit at high altitude.

Even small changes in water temperature are known to affect physical and biological processes and the functioning of ecosystems in mountain lakes (Sadro et al., 2019). In the Sierra, interrelated factors such as the amount of snowpack, the timing and magnitude of snowmelt, and water temperature have important implications for growth of benthic algae and phytoplankton, primary productivity and food web dynamics. Elevated water temperatures can increase metabolic rates of organisms, from plankton to fish (UC Davis, 2022).

Rising lake water temperatures reduce water quality by increasing thermal stability (stratification) and altering lake mixing patterns (O'Reilly et al., 2015). During the summer, Lake Tahoe water forms horizontal layers with less mixing due to differing water temperatures. In the late fall and winter, surface waters cool and sink to the bottom, and upwelling brings nutrients to the surface. The magnitude of cooling during winter helps to determine how deep the lake mixes vertically. This mixing plays a critical role in providing nutrients to the food web and distributing oxygen throughout the lake. Without this circulation, oxygen-rich surface water does not make it to the lake bottom, depriving fish and other aquatic life of oxygen.

When winter temperatures are warm, mixing tends to occur at more shallow depths, resulting in warmer lake temperatures. In 2020 and 2021, relatively shallow mixing likely contributed to warmer surface temperatures, while in 2019, top to bottom mixing of lake waters led to cooler water temperatures (UC Davis, 2022). Resistance to lake mixing increases markedly even at temperature increases of only a few degrees (Sahoo et al., 2015). Since 1968, the amount of time Lake Tahoe has been in its stratified, 'summer'-state has increased by a month (UC Davis, 2022). Scientists are predicting that in a warming climate, mixing in Lake Tahoe will become less frequent — a change that will disrupt fundamental processes that support a healthy ecosystem. For example, suppressed mixing may create new thermal niches that introduced species can take

advantage of, potentially disadvantaging native species that have evolved under clear, cold water conditions.

The lack of seasonal lake mixing can cause shifts in Lake Tahoe's algal species and their distribution (UC Davis, 2022). When mixing is suppressed, larger algae sink and leave the smallest algae suspended at the surface where they scatter light and decrease the lake's clarity. As clarity decreases, greater warming of the surface water takes place, increasing stratification and the likelihood of more small algal species. This vicious cycle presents an additional climate-induced challenge. Reduced mixing may also prolong periods of reduced lake clarity that occur following years of heavy stream runoff, by causing fine particles to be retained in the upper layer of the lake (Coats et al., 2006).

Water clarity measurements have been taken continuously at Lake Tahoe since 1968 using an instrument called a Secchi disk (UC Davis, 2022). This allows for a better understanding of how factors such as temperature, precipitation, and nutrient and sediment inputs into the lake are changing physical, chemical, and biological processes that affect the lake's clarity. While the average clarity of the lake has been relatively stable over the past 20 years, there is a long-term trend of reduced summer clarity. Because water clarity impacts the amount of light penetration, it has important implications for the diversity and productivity of aquatic life that a system can support. In addition, clear waters are valued for aesthetic and recreational purposes.

Photo credit: UC Davis/Getty

Lake Tahoe is a crystal-clear high altitude mountain lake, considered one of the jewels of the Sierra. It is known around the world for its water clarity and cobalt blue color. The lake is 22 miles long, has a surface area of 190 square miles, and a total volume of 130 million acre feet. Its maximum depth of 1,644 feet makes it the third deepest lake in North America, and the eleventh deepest lake in the world. The UC Davis Tahoe Environmental Research Center documents changes in physical and biological parameters to inform management strategies for the lake and its surrounding area (UC Davis, 2021b).

A recent study describes a widespread decline in dissolved oxygen levels among 393 temperate lakes across the US from 1941 to 2017 (Jane et al, 2021). The decline in surface waters was primarily associated with reduced oxygen solubility under warmer water temperatures. By contrast, the decline in dissolved oxygen in deep waters was associated with stronger thermal stratification and loss of water clarity. The authors concluded that despite a wide range of lake and catchment characteristics, the overall trend of lake deoxygenation is clear. Reduced dissolved oxygen in deep water lake habitats may lead to future losses of cold-water and oxygen-sensitive species, the

formation of harmful algal blooms, and potentially increased storage and subsequent outgassing of methane.

A decline in the water clarity and ecosystem health of the lake could jeopardize future tourism. The scenic beauty of Lake Tahoe offers cultural and recreational opportunities, such as hiking, skiing, camping and boating. The annual visitor population of about 15 million (California Tahoe Conservancy, 2021) makes it a region of national economic significance, with estimated annual revenues of 4.7 billion dollars (Mooney and Zavaleta, 2016).

What factors influence this indicator?

Lake temperature responses to climate change can vary and in part from the multiple ways in which climate interacts with lake 'heat budgets' (Sadro et al., 2019; Sharma et al., 2017; Woolway et al., 2020). Climate affects lake temperature by increasing heat gains or reducing heat losses. Key drivers controlling lake water temperature are solar radiation, air temperature (influenced by greenhouse gas concentrations), ice cover, cloud cover, humidity, and wind. In addition, suppressed lake mixing (discussed above) can enhance warming of surface waters. Landscape characteristics such as latitude, elevation, and catchment features or land cover can modulate climate effects on individual lakes (Schmid et al., 2014). The climate signal might be further modified by a lake's morphometric attributes, such as lake size and shape, or through differences in the source and magnitude of water inputs (Rose et al. 2016).

A study of lakes around the world found summer air temperature to be the single most consistent predictor of lake summer surface water temperature (LSSWT) (O'Reilly et al., 2015) largely because so many of the factors that control lake temperature are correlated with air temperature. The study reported that LSSWT is warming significantly, with a mean trend of 0.34°C per decade across 235 globally distributed lakes between 1985 and 2009. This warming water surface rate is consistent with the annual average increase in air temperatures and ocean surface temperatures over a similar time period (1979–2012).

Lake Tahoe warming trends reflect overall air temperature trends in the region (UC Davis, 2022). Since 1912, the average daily *maximum* temperature has risen by 2.25°F (1.2°C) and the average daily *minimum* temperature has increased by 4.5°F (2.5°C). Although year-to-year variability is high, the number of days when air temperatures averaged below-freezing has declined by almost 30 days since 1911. Snow has declined as a fraction of total precipitation, from an average of 52 percent in 1910 to 33 percent in 2020. A warming climate is affecting other physical changes at Lake Tahoe -- including a shift in snowmelt timing to earlier dates—that may have significant impacts on lake ecology and water quality. For more information about meteorological trends in the Lake Tahoe area, refer to: *Tahoe: State of the Lake 2022* (UC Davis, 2022).

In California lakes that experience ice cover, the amount of snowpack, timing of snowmelt runoff, and ice formation and ice-off (date of ice thawing and breakup)

influence lake water temperatures (Melack et al., 2020; Sadro et al., 2019; Smits et al., 2020). For example, Emerald Lake is a high elevation lake in the southern Sierra Nevada that is covered with ice six to nine months of the year. Despite a strong warming trend in regional air temperature over the past three decades, researchers found warming water temperatures occurred only during drought years, when snowpack was reduced (Sadro et al., 2019). Snowpack and lake temperature are strongly correlated in mountain systems likely due to tight coupling between snowpack and ice cover in lakes (Smits et al., 2020). Years with low snowpack at Emerald Lake were accompanied by a reduction in the duration of ice-cover, which acts to buffer lake water from exposure to solar radiation and warming. As snowpack declines in the Sierra Nevada and other mountain ranges (see *Snow-water content* indicator), lake temperature will become increasingly sensitive to warming with reduced ice cover.

Technical Considerations

Data characteristics

The University of California, Davis and its research collaborators collect the measurements used for monitoring Lake Tahoe. They have recorded water temperature measurements at two locations in Lake Tahoe since 1968:

(1) at the Index Station (about 0.6 kilometers off the California side west shore) at depth increments of 2 to 15 meters starting at the surface to a depth of about 100 meters, on an approximately weekly basis (and since 1996 at 20-centimeter increments to a depth of 125 meters biweekly);
(2) at the Midlake Station, the exact location of which has varied slightly over time, at nominal depths of 0, 50, 100, 200, 300 and 400 meters, on an at least monthly basis through 1996, and since then monthly at 20-centimeter intervals to a depth of 450 meters.

Strengths and limitations of the data

A variety of thermometers and digital thermographs have been used at the Index Station over the years. Although the sensitivity, accuracy, and calibrations of these instruments have varied over time, these data are adequate for characterizing the thermal structure of the epilimnion and thermocline. Temperatures at the Midlake Station were originally measured at 13 depths with mercury-reversing thermometers, as follows: a protected thermometer, unaffected by pressure, records the temperature at reversal depth; readings from this thermometer are corrected for glass expansion and, along with a second, unprotected thermometer affected by pressure in deep water, provide measure of the actual depth of the temperature reading (Coats et al., 2006). These instruments were accurate to 0.01^{o}C. More recently temperature is measured using a high precision thermistor that is part of a suite of instruments on a Seabird SBE-25plus profiler. Accuracy of the thermistor is 0.001^{o}C. The Seabird measures at a rate of 8 times per second as it falls through the water at a velocity of 60 centimeters/sec.

Lake surface temperature data derived from thermal infrared satellite imagery (ATSR and MODIS), when validated against corresponding *in situ* data for Lake Tahoe, were found to agree very well over the entire range of temperatures. This, along with an additional assessment of inter-sensor bias between all ATSR sensors, indicates that accurate and stable time series of lake surface temperature can be retrieved from ATSR and MODIS satellite data.

OEHHA acknowledges the expert contribution of the following to this report:

S. Geoffrey Schladow
Professor of Water Resources and
Environmental Engineering
Director, Tahoe Environmental Research Center
University of California Davis
(530) 752-3942
http://edl.engr.ucdavis.edu

Reviewer:

Steven Sadro, Ph.D.
University of California Davis
Department of Environmental Science and Policy
ssadro@ucdavis.edu

Additional input from:

Sudeep Chandra
University of Nevada, Reno

References:

Bachmann RW, Canfield DE, Sharma S and Lecours V (2020). Warming of near-surface summer water temperatures in lakes of the conterminous United States. *Water* **12**: 3381.

California Tahoe Conservancy (2021). Tahoe Climate Adaptation Action Portfolio.

Coats R, Perez-Losada J, Schladow G, Richards R and Goldman C (2006). The warming of Lake Tahoe. *Climatic Change* **76**(1): 121-148.

Jane SF, Hansen GJA, Kraemer BM, Leavitt PR, Mincer JL, et al. (2021). Widespread deoxygenation of temperate lakes. *Nature* **594**: 66-70.

Melack JM, Sadro S, Sickman JO, and Dozier J (2021). Lakes and Watersheds in the Sierra Nevada of California: Responses to Environmental Change. *University of California Press*. First Edition

Mooney H and Zavaleta E (Eds.) (2016). *Ecosystems of California*. Oakland, California: University of California Press.

O'Reilly CM, Sharma S, Gray DK, Hampton SE, Read JS, et al. (2015). Rapid and highly variable warming of lake surface waters around the globe. *Geophysical Research Letters* **42**(24): 10,773-10,781.

Rose KC, Winslow LA, Read JS and Hansen GJA (2016). Climate-induced warming of lakes can be either amplified or suppressed by trends in water clarity: Clarity-climate warming of lakes. *Limnology and Oceanography Letters* **1**: 44–53.

Sadro S, Melack JM, Sickman JO and Skeen K (2019). Climate warming response of mountain lakes affected by variations in snow. *Limnology and Oceanography* **4**(1): 9-17.

Sahoo GB, Forrest AL, Schladow SG, Reuter JE, Coats R and Dettinger M (2015). Climate change impacts on lake thermodynamics and ecosystem vulnerabilities. *Limnology and Oceanography* **61**(2): 496-507.

Schmid M, Hunzike S and Wüest A (2014). Lake surface temperatures in a changing climate: A global sensitivity analysis. *Climatic Change* **124**: 301–315.

Schneider P, Hook SJ, Radocinski RG, Corlett GK, Hulley GC, et al. (2009). Satellite observations indicate rapid warming trend for lakes in California and Nevada. *Geophysical Research Letters* **36**(22): L22402.

Sharma S, Gray D, Read JS, O'Reilly CM, Schneider P, *et al.* (2015). A global database of lake surface temperatures collected by *in situ* and satellite methods from 1985–2009. *Scientific Data* **2**: 150008.

Smits AP, MacIntyre S and Sadro S (2020). Snowpack determines relative importance of climate factors driving summer lake warming. *Limnology and Oceanography* **5**(3): 271-279.

UC Davis (2021). 2020 Lake Tahoe Clarity Report. UC Davis news and media relations/Tahoe Regional Planning Agency. Retrieved July 08, 2021.

UC Davis (2022). *Tahoe: State of the Lake Report 2022*. University of California, Davis. Davis, CA: Tahoe Environmental Research Center.

Woolway RI, Kraemer BM, Lenters JD, Merchant CJ, O'Reilly C, et al. (2020) Global lake responses to climate change. *Nature Reviews Earth and Environment* **1**: 388–403.

SALMON RIVER WATER TEMPERATURE

Water temperatures in the Salmon River and its tributaries have been warming, coincident with warming air temperatures and decreasing snowpack. The Salmon River watershed's relatively modest human influences make it an excellent location for tracking the effect of climate change.

Figure 1. Salmon River Water Temperatures* (1992-2020)

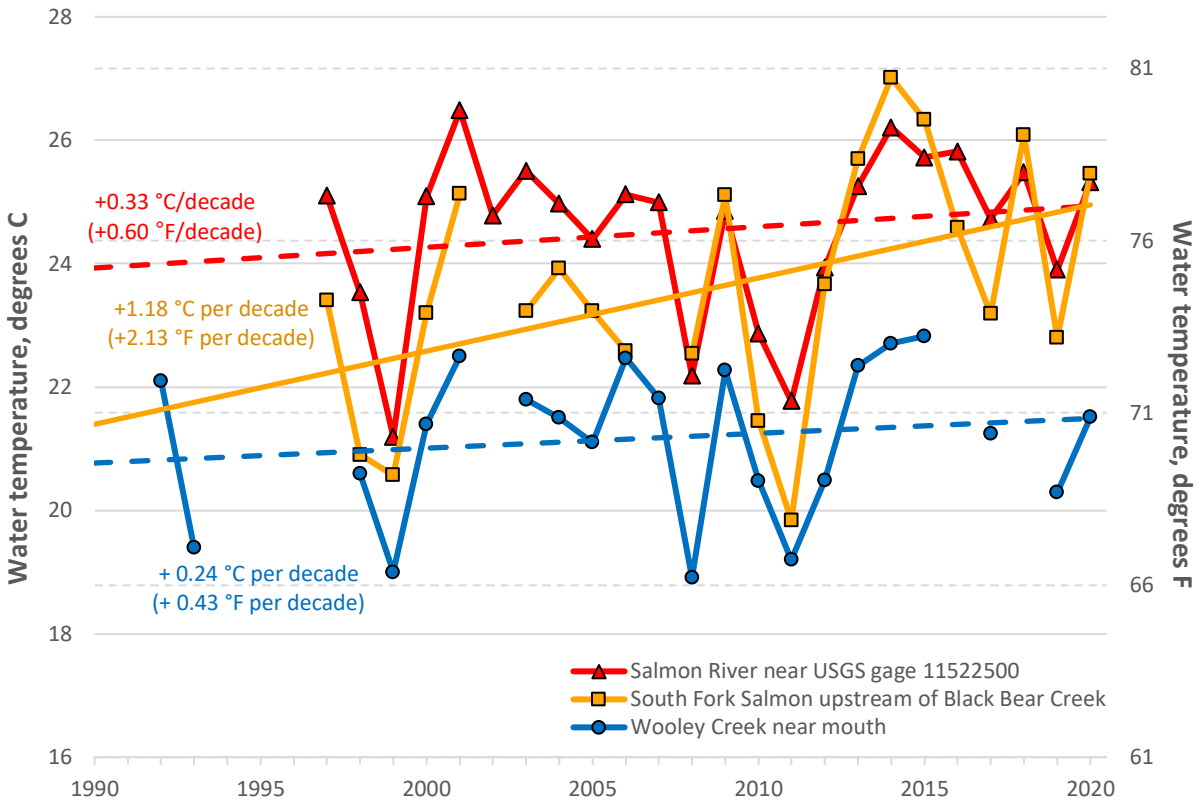

Source: Karuk Tribe, SRCC, and USFS 2021

The value for each year is the **annual maximum temperature -- i.e., the highest instantaneous maximum temperature--during the summer. Solid line denotes statistically significant trend ($p<0.05$).*

What does the indicator show?

From 1992 to 2020, water temperatures, measured as annual maximum temperature (AMT) at three sites in the Salmon River watershed (Figure 1) have been variable but trending higher. The Salmon River watershed is a 750-square mile sparsely populated area in Siskiyou County surrounded by subranges of the Klamath Mountains. Temperatures at the South Fork Salmon River site upstream from Black Bear Creek are increasing the fastest, with a rate of 2.13 degrees Fahrenheit (°F) per decade. Water temperatures at the Wooley Creek and Salmon River at US Geological Survey (USGS)

gage stations are increasing more slowly, with rates of 0.60°F and 0.43°F per decade, respectively.

The three monitoring sites (shown in Figure 2) are a subset of many sites throughout the Salmon River and its tributaries where water temperatures are monitored. A previous analysis combined 27 long-term sites in the watershed to assess collective trends for the month of August during the period 1995-2017, finding that daily maximum temperatures warmed by 0.70°F per decade and daily mean temperatures warmed at a rate of 0.38°F per decade (Asarian et al. 2019). Years showing higher water temperatures generally coincided with low stream and river flows and high air temperatures; years reporting the lowest stream temperatures coincided with high flows and cool air temperatures (Asarian et al., 2019).

Figure 2. Location of three temperature monitoring sites in the Salmon River watershed

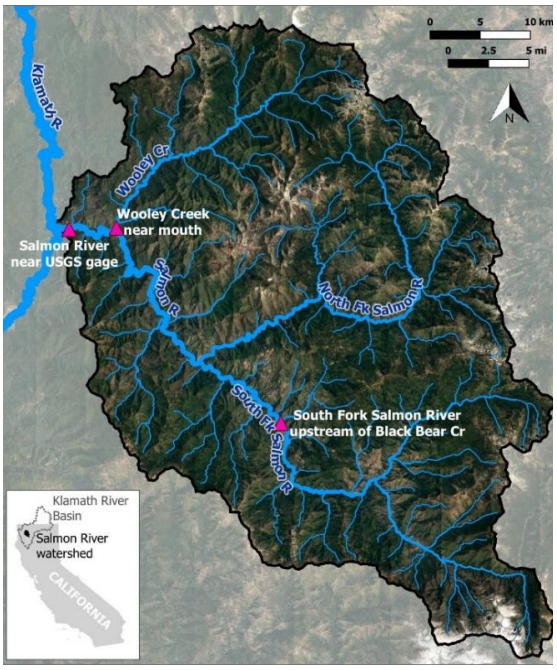

Source: Riverbend Sciences

Why is this indicator important?

Water temperature is a fundamental regulator of river ecosystems. It influences species' metabolism, growth rates, reproduction and distributions (David et al., 2018). The Salmon River watershed provides cold water habitat for anadromous fish, notably steelhead and Coho and Chinook salmon. Identified as a Key Watershed by the US Forest Service, it serves as refugia for at-risk salmon and steelhead stocks in the Pacific Northwest (Elder et al., 2002). This river system still retains wild runs of salmonid species that have disappeared from much of their historic range within California (SRRC, 2020).

Although the Salmon River (pictured in Figure 3) is still affected by the legacy of historic mining that began in the mid-19th century during the California Gold Rush, and some of the watershed's forests have been logged, today's relatively modest human influences make it an excellent location for tracking the effect of climate change on water temperatures (Asarian et al., 2019). The river has no dams and much less water is diverted for human uses in the Salmon River watershed than in other areas of California due to the area's low population density.

Warming summer water temperatures threaten the production and health of culturally and economically important fish in the Salmon River watershed (Asarian et al., 2019). Higher temperatures can increase metabolic demands, susceptibility to disease and pose a threat to fish populations, especially to spring-run Chinook salmon. Fish live in

these habitats through the entire summer, and under current conditions peak summer temperatures in portions of the river and its tributaries are likely at or exceeding thermal suitability for this species. The year 2020 marks the second lowest number of returning spring Chinook since surveys began in 1990 and the sixth consecutive year that numbers have been below average (SRRC, 2020). The survival of the dwindling population of spring Chinook salmon, as well as Coho salmon, hangs in the balance. These fish are critical to the food security, cultural survival and well-being of the Karuk Tribe and other indigenous peoples in the Klamath Basin (Karuk Tribe, 2016).

The Karuk Tribe's Ancestral Territory occupies 60 percent of the Salmon River watershed, a sub-basin of the larger Klamath River Basin (Elder et al., 2002). The Karuk consider the Salmon River sub-basin as one of the most culturally significant watersheds within the Klamath National Forest. There is a strong commitment for cooperative stewardship of the watershed among local residents, the Salmon River Restoration Council (SRRC), the Karuk Tribe, the US Forest Service (USFS), and the California Department of Fish and Wildlife (CDFW) (Elder et al., 2002).

In 1994, the North Coast California Regional Water Quality Control Board and the US Environmental Protection Agency determined that beneficial uses in the Salmon River, including cold water salmonid fisheries, are impaired due to elevated water temperatures (NCRWQCB, 2005). Regulations intended to address those impairments were adopted in 2005. Coho salmon in the basin are state and federally listed as threatened (NCRWQCB, 2005). Spring Chinook salmon were listed as endangered by the State of California in June 2021 (Karuk Tribe, 2021) and are currently being considered for listing by the federal government (NMFS, 2021).

Figure 3. Salmon River

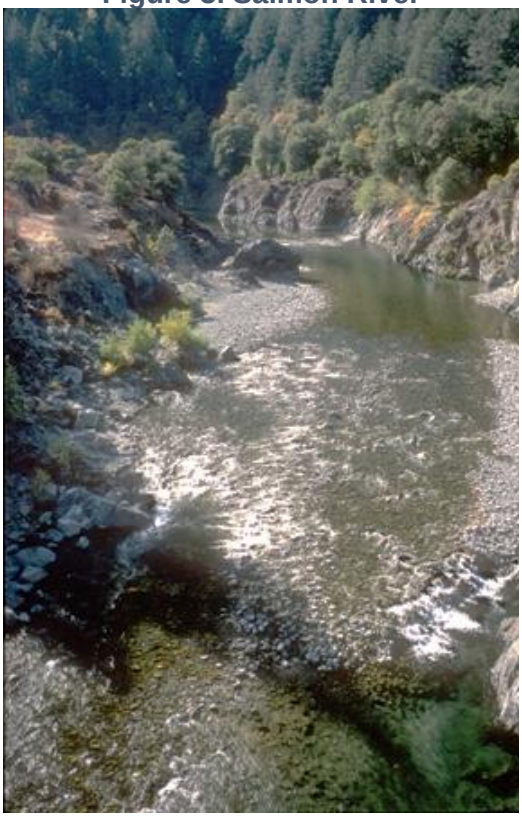

Photo Credit: USDA Forest Service

The Salmon River flows from the high peaks of the Salmon Mountains, a sub-range of the Klamath Mountains, in far Northern California. It is the second largest tributary to the Klamath River and joins the Klamath at Somes Bar, California, about 106 km (66 miles) upstream from the Pacific Ocean.

What factors influence this indicator?

Summer stream temperatures in the Salmon River and its tributaries are trending warmer due to warming air temperatures, decreased snowpack, earlier snowmelt and spring runoff, and decreases in water flow (Asarian et al., 2019). Years of low snowpack and snow water runoff tend to yield decreases in stream and river flow in watersheds

(Asarian, 2020). Since the 1940s, April 1 snowpack has been decreasing in the Salmon River watershed (CDEC, 2021; Van Kirk and Naman, 2008). Since summer river flow is strongly influenced by snowpack, temperatures at the South Fork Salmon River site are particularly sensitive to climate change and have warmed relatively rapidly since monitoring began in 1997. Water temperature has been increasing at the highest rate at this location (Figure 1).

Streamflow is an important determinant of water temperature. River and stream temperatures are cooler when flows are high and warmer during years with diminished flows. Figure 4 shows the relationship between stream flow rates during the month of August at the Salmon River monitoring station and maximum temperatures at the three stations shown in Figure 1. Low August flow rates coincided with warmer stream temperatures in 2001, 2014, and 2015. Conversely, higher flow rates in 1999, 2010, and 2011 corresponded with much cooler stream temperatures during those years.

Figure 4. River water temperatures and August stream flow (1992-2020)

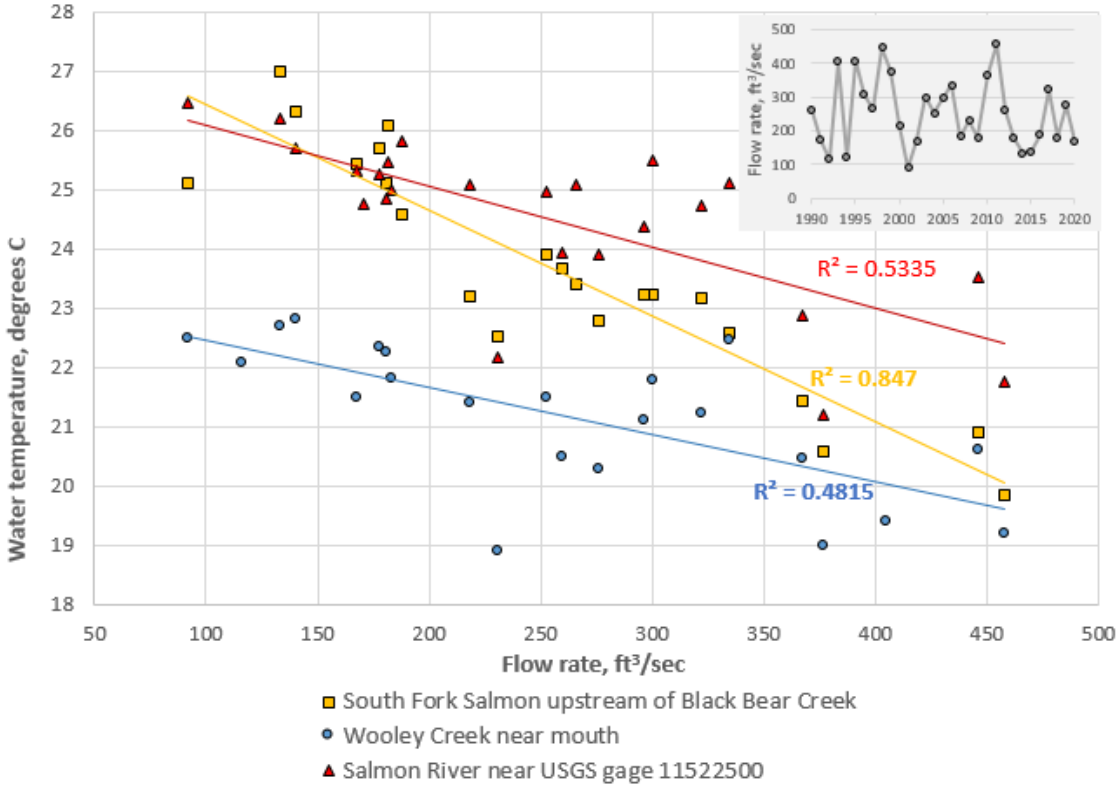

Source: Karuk Tribe, SRCC, and USFS 2021 (water temperatures); USGS 2021 (streamflow)

Annual maximum water temperatures at the three monitoring sites are plotted against average August streamflow measured at the Salmon River monitoring station (at Somes Bar, USGS Gage 11522500). (R^2 values indicate the strength of the correlation; a value of 1 indicates a perfect correlation between the variables.) The inset graph presents annual average August streamflow over the past 30 years.

A symptom of warmer temperatures and less snow is the complete melting of the Salmon Glacier in the Trinity Alps at the headwaters of the Salmon River's South Fork in 2015 following a multi-year drought and many decades of ice loss (Garwood et al., 2020; also see *Glacier change* indicator). The nearby Grizzly Glacier which drains to the Trinity River has declined by 97 percent since 1885. When these glaciers were larger in previous decades, they fed cold water to streams during the summer.

A number of other physical factors influence water temperatures in streams and rivers, including solar radiation, heat radiated from objects (e.g., clouds and vegetation), evaporation, convection of heat from air to water, conduction of heat between the water and stream bed, and mixing of water from different sources (Dugdale et al., 2017). During the summer, water temperatures in streams and rivers with wider channels that are more exposed to solar radiation tend to be warmer than water upstream in small well-shaded streams. Water temperatures fluctuate over time in response to atmospheric conditions (air temperatures, clouds, and smoke), hydrologic conditions (snowmelt, rain, stream flow, and groundwater), and growth or loss of vegetation. Factors affecting spatial patterns in water temperature include elevation (cooler air temperatures at higher elevations), topography (mountainous terrain reduces solar exposure), and near-stream vegetation (cooler temperatures where trees provide shade). Wooley Creek flows through steep, mountainous terrain, which partially protects it from solar radiation and keeps its waters relatively cool for its size. As shown in Figure 1, temperatures are increasing at a slower rate at Wooley Creek due to these characteristic features.

Shade provided by near-stream vegetation has the effect of cooling water temperatures. Fire plays an integral role in regulating vegetation in the Salmon River watershed. Prior to fire suppression that became effective in the early/mid-20th century, fires burned more frequently and typically in smaller patches compared to what is occurring today (Skinner et al., 2018). Approximately a century of fire suppression has dramatically altered forest structure and fuel continuity. As a result, when fires now occur and escape containment, the probability of high fire severity is increased, which can reduce stream shade and increase water temperature (Karuk Tribe, 2016).

Researchers have been studying the effects of wildfire smoke and its potential to cool water temperatures. David et al. (2018) analyzed ground-based measurements of air and water temperatures from 12 stations throughout the lower Klamath River Basin in correlation with atmospheric smoke data derived from satellite imagery during six years with widespread wildfires. The analysis indicated that wildfire smoke had a cooling effect on both air and water temperatures at all study locations. This smoke-induced cooling has the potential to benefit cold-water adapted species, particularly because wildfires are more likely to occur during the warmest and driest years and seasons. A follow-up analysis of a larger number of stations showed the cooling effects of smoke were greater in August than in other months and were stronger in larger waterbodies

than smaller waterbodies (Asarian et al., 2020). Wildfire smoke has limited increases in August water temperatures, but has not affected annual maximum water temperatures because in most years fires do not start until after the year's hottest water temperatures have already occurred. The Karuk Tribe has used fire to manage the mid-Klamath landscape since time immemorial, and has proposed using prescribed fire smoke as an emergency measure to cool potentially lethal stream temperatures in fish habitat areas (Karuk Tribe, 2019).

Researchers conducted an analysis of both climate and non-climate factors and their comparative influence on August stream temperatures using statistical models (Asarian et al., 2019). The climate parameters evaluated were streamflow, air temperature, snowpack, and smoke; the non-climate parameters included landscape features such as riparian vegetation and river channel morphology. The results of the analysis indicated that the warming stream temperatures observed across the Salmon River watershed are largely attributed to climate conditions. The greatest amount of warming occurred at sites whose temperatures are highly sensitive to river flow, including the South Fork of the Salmon River.

Technical considerations

Data characteristics

The Salmon River Restoration Council (SRRC); the Karuk Tribe; and US Forest Service (USFS) [Klamath National Forest (KNF) and Six Rivers National Forest (SRNF)] have been monitoring water temperatures in the Salmon River Watershed since 1990 using automated probes that record measurements every 15–60 minutes. Probes are placed in well-mixed flowing water and are intended to represent overall conditions (i.e., "stream temperature"), not isolated pockets of cold or warm water. At most sites, probes are deployed in late spring or early summer, remain through the summer, and are retrieved in the fall for data download (KNF, 2011). A few sites are monitored year-round.

Sampling and equipment and monitoring techniques have changed since monitoring began in 1992. Prior to 2010, the KNF, SRNF, and SRRC used a combination of Pro v2 u22-001, Optic StowAway, and other ONSET temperature logger models (Onset Computer Corporation, 1999). Ryan TempMentors data loggers were used only by KNF in 1992–1993 at Wooley Creek (TFWTWG, 1990). At the Salmon River gage, the Karuk Tribe used a Hydrolab 4a for 2005–2006 and a YSI 6600 V2 datasonde for 2007 to present (Karuk Tribe 2006, 2007, 2018). Since 2010, KNF, SRNF, and SRRC have used ONSET Pro v2 data logger u22-001 for all temperature monitoring (KNF, 2011).

Although many sites are monitored, a subset of three sites that have long, relatively complete records were selected for this indicator:

1) Salmon River at USGS gage 11522500, approximately 1 mile upstream from its confluence with the Klamath River. In addition to the seasonal temperature probes placed by the USFS at this site, the Karuk Tribe also operates a

permanent monitoring station here that provides year-round multi-parameter water quality data available online in real-time at: https://waterquality.karuk.us/Data/Location/Summary/Location/11522500

2) Wooley Creek, approximately 0.3 miles upstream from its confluence with the Salmon River. Wooley Creek is one the Salmon River's largest tributaries and its watershed is entirely protected within the Marble Mountain Wilderness, so human impacts are slight.

3) South Fork Salmon River upstream of Black Bear Creek. Long-term data analyses (Asarian et al., 2020) show that water temperatures at this site are highly sensitive to river flow, with temperatures being cool in high-flow years and warm in low-flow drought years.

Strengths and limitations of the data

There are many ways to summarize stream temperature data, and previous Salmon River analyses (Asarian et al., 2019, 2020) evaluated trends for multiple metrics of summer stream temperature. For this indicator, annual maximum temperature is the highest instantaneous maximum temperature recorded during the summer. This metric was chosen because it is simple to calculate, easy to understand, and biologically meaningful. This metric was calculated only for sites and years when there were enough data to be representative (i.e., complete measurements available during the hottest period of the summer) (Asarian et al., 2020). Equipment and techniques for monitoring these sites have improved over time.

Figure 1 shows data gaps for certain years at the Wooley Creek and South Fork monitoring sites. Reasons for data gaps include logistical constraints preventing site access (e.g., fires or staffing shortages), probes malfunctioning, loss of probes due to vandalism, or low water levels exposing probes to air.

OEHHA acknowledges the expert contribution of the following to this report:

Eli Asarian
Riverbend Sciences
(707) 832-4206
eli@riverbendsci.com

Bonnie Bennett
Lyra Cressey
Salmon River Restoration Council
(530) 462-4665
bonnie@srrc.org;
lyra@srrc.org

Grant Johnson
Karuk Tribe
gjohnson@karuk.us

LeRoy Cyr
Six Rivers National Forest
(530) 627-3262
leroy.cyr@usda.gov

Jon Grunbaum
Klamath National Forest
(530) 493-1719
jon.grunbaum@usda.gov

The Klamath Tribal Water Quality Consortium (Karuk Tribe, Yurok Tribe, Hoopa Valley Tribe, Quartz Valley Indian Reservation, and Resighini Rancheria) funded the development of this indicator using resources provided by US EPA Region 9.

OEHHA respects the right of tribal nations to govern the collection, ownership, and application of their data. The Karuk Tribe has given OEHHA permission to use the water temperature data and related information presented in this indicator.

References:

Asarian JE, Cressey L, Bennett B, Grunbaum J, Cyr L, et al. (2019). *Evidence of Climate-Driven Increases in Salmon River Water Temperatures*. Prepared for the Salmon River Restoration Council by Riverbend Sciences with assistance from the Salmon River Restoration Council, Klamath National Forest, Six Rivers National Forest, and Karuk Tribe Department of Natural Resources. 53 p.+ appendices.

Asarian JE, Cressey L, Bennett B, Grunbaum J, Cyr L, et al. (2020). *Influence of Snowpack, Streamflow, Air Temperature, and Wildfire Smoke on Klamath Basin Stream Temperatures, 1995-2017*. Prepared for the Klamath Tribal Water Quality Consortium by Riverbend Sciences with assistance from the Salmon River Restoration Council, Klamath National Forest, Six Rivers National Forest, Karuk Tribe Department of Natural Resources, and Quartz Valley Indian Reservation. 44p. + appendices.

CDEC (2021). California Data Exchange Center. Query Tools: Current and Historical Data, Historical Data Selector. California Department of Water Resources. Queried monthly snow water content for stations Dynamite Meadow, Etna, Middle Boulder 1, Middle Boulder 3, Swampy John, and Wolford, July 7, 2021.

CDFW (2020). California Department of Fish and Wildlife. California Endangered Species Act Status Review for Upper Klamath and Trinity Rivers Spring Chinook Salmon (*Oncorhynchus tshawytscha*). State of California, Natural Resources Agency, Department of Fish and Wildlife, Sacramento, CA.

David AT, Asarian JE and Lake FK (2018). Wildfire smoke cools summer river and stream water temperatures. *Water Resources Research* **54**(10): 7273-7290.

Dugdale, SJ, Hannah, DM and Malcolm IA. (2017). River temperature modelling: A review of process-based approaches and future directions. *Earth-science Reviews* **175**: 97–113.

Elder D, Olson B, Olson A and Villeponteaux J (2002*). Salmon River Sub-basin Restoration Strategy: Steps to Recovery and Conservation of Aquatic Resources: Report for the Klamath River Basin Fisheries Restoration Task Force, Interagency Agreement 14-16-0001-90532*. USDA-Forest Service, Klamath National Forest, Yreka, Klamath National Forest and Salmon River Restoration Council, Sawyers Bar, CA. September 2002: 52 pp.

Garwood JM, Fountain AG, Lindke KT, van Hattem MG, and Basagic HJ (2020). 20th Century Retreat and Recent Drought Accelerated Extinction of Mountain Glaciers and Perennial Snowfields in the Trinity Alps, California. *Northwest Science* **94**(1): 44-61.

Karuk Tribe (2006). Water Quality Assessment Report 2006. Karuk Tribe Department of Natural Resources, Orleans, CA. 52 p.

Karuk Tribe (2007). Water Quality Assessment Report 2007. Karuk Tribe Department of Natural Resources, Orleans, CA. 64 pp.

Karuk Tribe (2016). *Karuk Tribe Climate Vulnerability Assessment: Assessing Vulnerabilities from the Increased Frequency of High Severity Fire*. Karuk Tribe Department of Natural Resources. Compiled by Dr. Kari Marie Norgaard with key input from Kirsten Vinyeta, Leaf Hillman, Bill Tripp and Dr. Frank Lake.

Karuk Tribe (2018). 2018 Quality Assurance Project Plan for Water Quality Sampling and Analysis, CWA 106 grant identification # BG-97991217. Karuk Tribe Department of Natural Resources, Orleans, CA. 64pp.

Karuk Tribe (2019). Karuk Climate Adaptation Plan. Karuk Tribe Department of Natural Resources. March 2019.

Karuk Tribe (2021). Press release: Karuk Tribe Petitions California Water Board to Regulate Scott Valley Water Users. *Tribe calls on agency to use emergency powers to prevent extinction* (July 1, 2021).

KNF (2011) Klamath National Forest. *Klamath National Forest, Water and Air Temperature Monitoring Protocol.* May 2011.

NCRWQCB (2005). North Coast Regional Water Quality Control Board. Salmon River, Siskiyou County, California Total Maximum Daily Load for Temperature and Implementation Plan Adopted June 22, 2005, NCRWQCB Resolution No. R1-2005-0058. Prepared by North Coast Regional Water Quality Control Board, Santa Rosa, California.

NMFS (2021). National Marine Fisheries Service. Endangered and Threatened Wildlife, 90-Day Finding on a Petition To List Southern Oregon and Northern California Coastal Spring-Run Chinook Salmon as Threatened or Endangered Under the Endangered Species Act. 86 FR 14407.

Onset Computer Corporation (1999). StowAway® XTI User's Manual. Onset Computer Corporation, Bourne, MA.

Skinner CN, Taylor AH, Agee JK, Briles CE and Whitlock CL (2018). Chapter Eleven. Klamath Mountains Bioregion. In Fire in California's Ecosystems (pp. 171–194). University of California Press.

SRRC (2020) Salmon River Restoration Council. Brochure supported by the California Department of Fish and Wildlife Fisheries Restoration Grant Program.

TFWTWG (1990). Timber Fish/Wildlife Temperature Work Group. Evaluation of prediction models and characterization of stream temperature regimes in Washington, TFW-WQ3-90-006. Prepared for the TFW/CMER Water Quality Steering Committee and Washington Department of Natural Resources Forest Regulation and Assistance, Olympia, Washington.

Van Kirk RW and Naman SW (2008). Relative Effects of Climate and Water Use on Base-Flow Trends in the Lower Klamath Basin. *Journal of the American Water Resources Association* **44**(4): 1035–1052.

COASTAL OCEAN TEMPERATURE

Measurements at California's shore stations show that nearshore coastal waters have warmed over the past century, particularly in Southern California. Similarly, satellite-based records over the past four decades show warming ocean waters off Southern California. An unprecedented marine heatwave affected the West Coast of the United States from 2014 to 2016.

Figure 1. Annual average sea surface temperatures (SST) at selected shore stations (1916-2020)

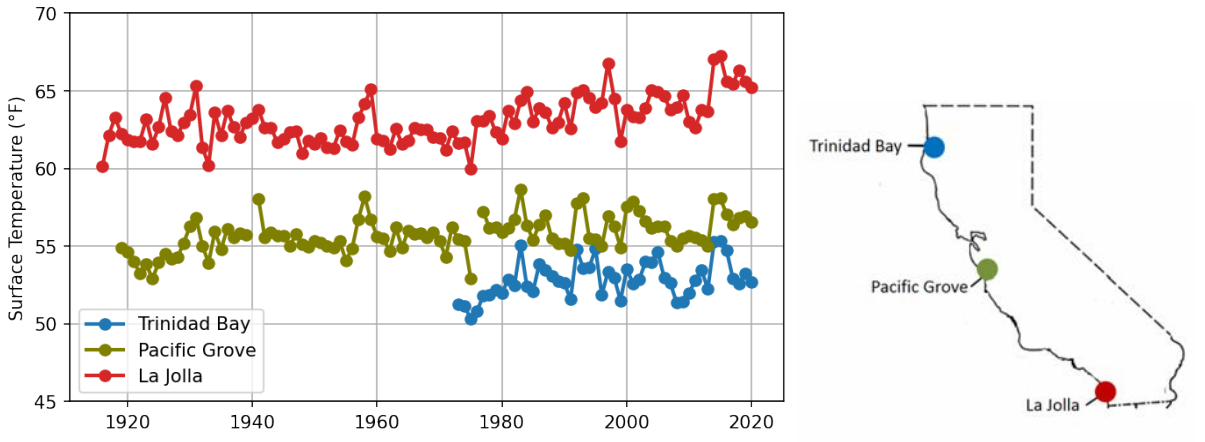

Source: SIO, 2021

Figure 2. Satellite-based sea surface temperature (SST) trends along the California Coast (1982-2021)

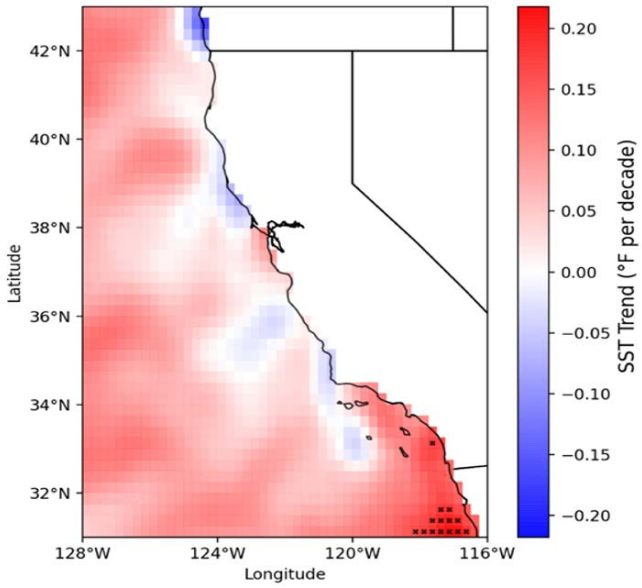

Source: NOAA, 2021a

The map shows SST trends off the California coast, in °F per decade, for the 40-year period (1982 to 2021). Black dots (one off San Diego County; the rest off Mexico) denote locations with statistically significant trends (p<0.05).

Figure 3. Marine heat waves off California (1982-2021)

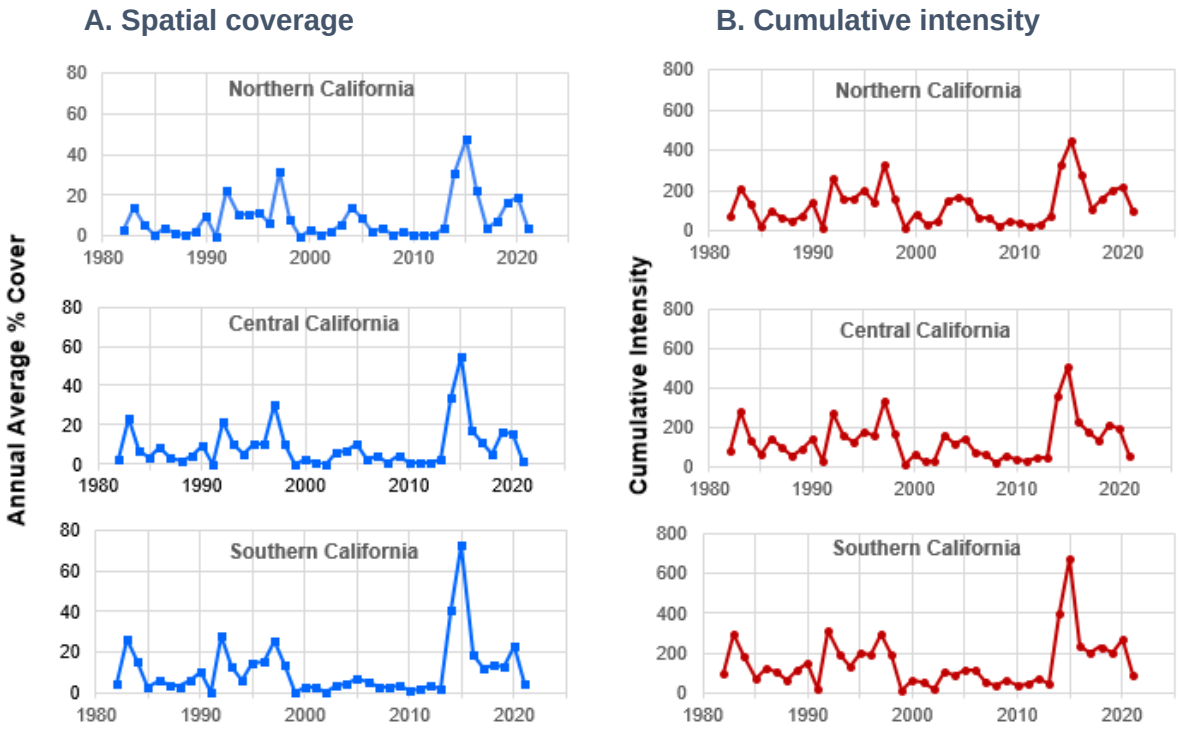

Source: Data provided by Leising, 2022; also available at NOAA, 2022

*A **marine heat wave** occurs over a region when the difference between the sea surface temperature (SST) and the long-term mean (1971-2000) is above the 90th percentile of all values for a given location on a given day of the year. **[A]**: **Spatial coverage** is the annual average percentage of the region in heat wave status; **[B]**: **Cumulative intensity** is the annual sum of daily average SST measurements above the long-term mean. See Figure 4 for a map of the regions.*

What does the indicator show?

California coastal ocean temperatures have warmed over the past century. Although sea surface temperature (SST) fluctuates naturally each year, warming SST trends of are clearly detected. The longest time series for SSTs are based on measurements at shore stations along the California coast. Figure 1 presents data for three of these stations. SST has increased at the rate of 0.2 degree Fahrenheit (°F) per decade at Pacific Grove between 1919 and 2020, and at a faster rate of 0.3°F per decade at La Jolla between 1916 and 2020. At Trinidad Bay, SSTs increased at the rate of 0.3°F per decade over a shorter time period (1973-2016). All three stations show statistically significant trends ($p<0.05$). SSTs have also increased at other shore stations along the coast (Table 1). Stations farthest south, La Jolla and San Clemente, are experiencing the most warming.

Table 1. Trends in sea surface temperature (°F per decade) at shore stations (p-values less than 0.05 indicate statistical significance.)

Station	Years	Decadal Trend	*p*-value
Trinidad	1973 - 2020	0.34	0.007
Farallon Island	1925 - 2020	0.09	0.061
Pacific Grove	1919 - 2020	0.18	< 0.001
Granite Canyon	1971 - 2020	0.33	0.001
Santa Barbara	1955 - 2020	0.23	0.009
Point Dume *	1956 - 2020	0.21	0.067
Newport Beach	1924 - 2020	0.08	0.194
San Clemente	1965 - 2020	0.39	< 0.001
La Jolla	1916 - 2020	0.27	< 0.001

**Uncertain values for Point Dume between 1995 and 2006 were not included in the analysis.*

Globally, average SSTs have increased by 0.88°C (~1.58°F) since the beginning of the 20th century (IPCC, 2021). The global surface temperature — over both land and oceans — has warmed at a rate of about 0.14°F per decade since 1880; the rate of warming from 1981 to 2020 was over twice that rate, at 0.32°F per decade, reflecting sharper increases in sea surface temperatures over the recent period (NOAA, 2021). The Southern California coastal trend over the last four decades is consistent with that sharp global increase.

Four decades of satellite-based data from the National Oceanic and Atmospheric Administration Optimal Interpolation SST reanalysis (NOAA OISST) allow the tracking of SST trends along the entire coast of California and offshore; this would not have been possible with shore station data alone (Huang et al., 2021; Reynolds et al., 2002). As shown in Figure 2, for the period 1982-2021, the waters over the state's continental shelf (within approximately 30 nautical miles offshore) have both warmed and cooled, although the trends are generally not statistically significant ($p>0.05$). However, offshore waters are largely warming. Both near-shore and offshore, Southern California is exhibiting a distinct warming trend compared to the rest of the state, with warming being more prominent near shore.

In recent years, prolonged periods of extremely high ocean temperatures, known as marine heatwaves (MHW), have occurred across the globe, focusing attention on their devastating effects on the marine ecosystem. Two metrics for tracking the size and intensity of MHWs are presented in Figure 3 for Northern, Central and Southern California; see Figure 4 for a map of the regions. A MHW is an extreme climate event in

which anomalously warm sea surface temperatures are observed in a region (Oliver et al., 2021). Specifically, a MHW over a region occurs when the difference between the SST and the long-term or "climatological" mean for the period 1971-2000 (the difference is also known as the "anomaly") for a given time and place is above the 90th percentile of the values for a baseline period (Hobday et al., 2016). See discussion in *Technical Considerations* for more information about the metrics. As shown in Figure 3, the largest and most intense MHW recorded in the three regions of California – known as "the Blob" – occurred in 2014 to 2016. While MHWs have occurred in the past, the magnitude and duration of the warming during this event was unprecedented for the west coast of North America (Di Lorenzo and Mantua, 2016; Gentemann et al., 2017). Other notable MHWs occurred in 1983, 1992, 1997 (all associated with El Niños), and more recently in 2019 and 2020 (which, unlike MWHs associated with El Niños, originated in the south, rather than from the Central North Pacific) (Leising et al., 2015).

Figure 4. Marine heatwave monitoring off the California coast

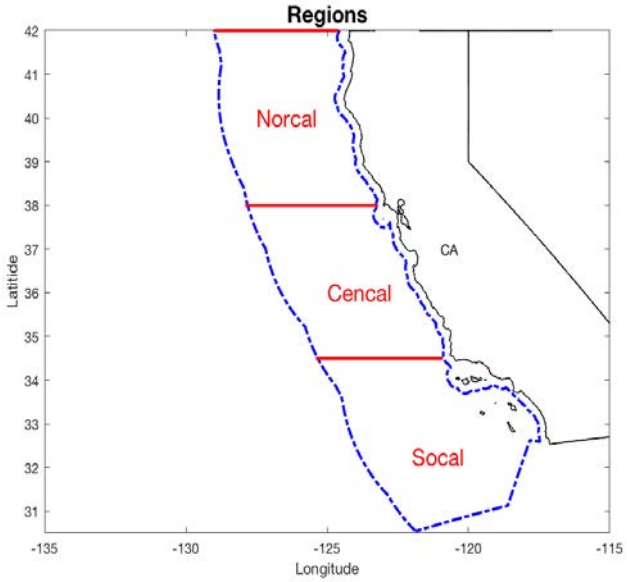

Source: NOAA, 2022

Marine heat waves are monitored along the California Current, including in three regions off the California coast designated as Northern, Central and Southern California regions.

In its latest assessment, the Intergovernmental Panel on Climate Change (IPCC) reports that MHWs have become more frequent over the 20th century, approximately doubling from 1982 to 2016; they have also become more intense and longer in duration since the 1980s (IPCC, 2021). Over the last two decades, MHWs have occurred in all of the world's ocean basins.

Why is this indicator important?

Temperature is one of the best-measured signals of climate change. As atmospheric concentrations of greenhouse gases increase, excess heat is absorbed and stored by the oceans and atmosphere. The ocean's large mass and high heat capacity allow it to store large amounts of heat. It is estimated that over 90 percent of the observed heat energy increase on the Earth over the past 50 years has occurred in the ocean (Jewett and Romanou, 2017; NOAA, 2021b; Rhein et al., 2013). In addition to absorbing excess heat, the ocean also absorbs about 30 percent of carbon emissions. As a result, the ocean acts as a buffer against global warming (IPCC, 2019).

Figure 5. Decadal changes in peak fish larvae abundance

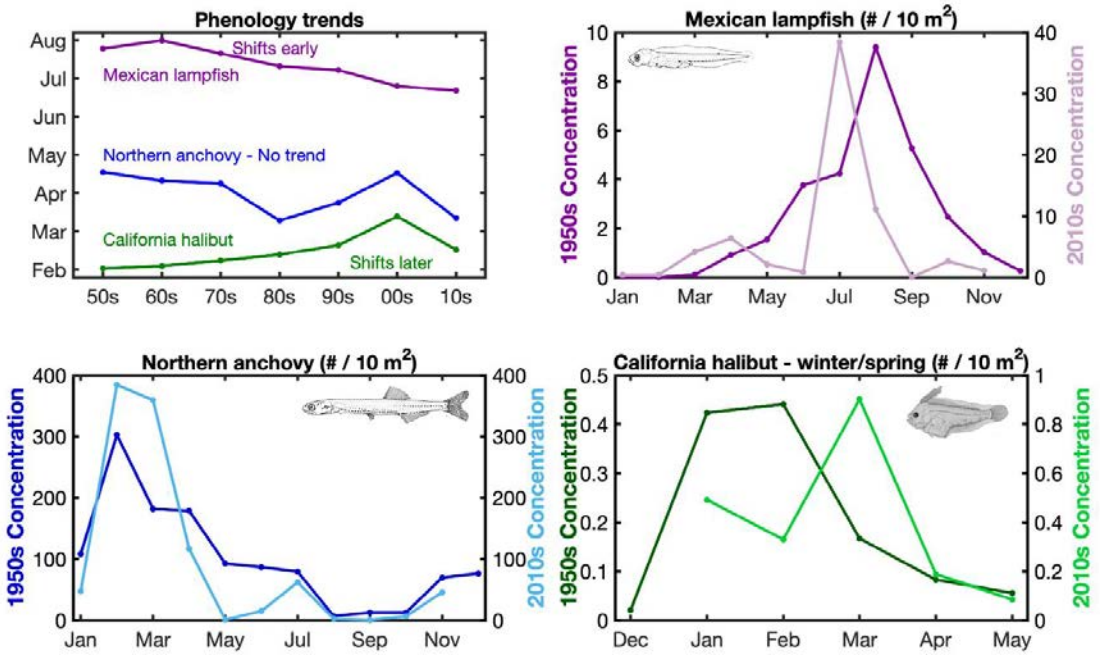

Source: Asch, 2015; updated 2021 using data from California Cooperative Oceanic Fisheries Investigations pers comm.

Graph, top left, shows shifts in the timing of peak larvae abundance (number of fish per 10 m^2) for the northern anchovy, California halibut and Mexican lampfish in Southern California waters. Separate graphs compare peak larvae abundance in the 1950s with the 2010s for three fish species. Peak timing shifts earlier in the year for Mexican lampfish and later for California halibut; northern anchovy showed no trend.

Changes in SST along the coast of California have been shown to alter the distribution, abundance, and recruitment of many marine organisms, including commercially important species. Fluctuations in the distribution and abundance of many California coastal marine populations have been related to temperature variability (e.g., Goericke et al., 2007; IPCC, 2019; Sagarin et al., 1999). The direct effects of temperature on the physiological performance of marine organisms and the timing of their key developmental stages (such as from egg to larva) are the likely mechanisms underlying these patterns. Several fish species have shifted their spawning phenology between the 1950's to the 2010's due to increased ocean temperature (Asch, 2015). Commercial species such as California Halibut shifted to reproduce earlier while prey fish Mexican Lampfish and Northern Anchovy shifted to later reproduction or had no change in spawning phenology, respectively (Figure 5). Water temperature can also influence species indirectly, by altering interactions between species and their competitors, predators, parasites, facilitators, and prey.

The California Current, which extends from British Columbia, Canada to Baja California, Mexico, is one of four major "Eastern Boundary Upwelling Systems" – biologically productive marine regions that cover less than one percent of the ocean area, but provide about 20 percent of the world's ocean fish catch (Mann, 2000). In these

systems, coastal upwelling creates a band of cool waters along the coast, supplying the food chain with nutrients, and providing habitat that supports high biological productivity. During the Blob, anomalously warm offshore waters in the California Current Ecosystem restricted the cool upwelling habitat to a narrow band along the coast, resulting in reduced upwelling habitat, or "habitat compression" (Santora et al., 2020). This compression was associated with changes in the composition and distribution of marine species, including whale prey. Alterations in prey abundance and distribution, in combination with a delayed Dungeness crab season and other factors, contributed to record increases in whale entanglements in fishing gear during this MHW. To support efforts to understand and mitigate the causes of whale entanglements, a recently developed "habitat compression index" (HCI) tracks patterns in the surface area of cool water over time. A low HCI value indicates that cool habitat is compressed onshore. The HCI is used to assess the likelihood of ecosystem shifts and shoreward distribution patterns of whales and other top predators. The HCI and other indicators of conditions associated with whale entanglements are presented in an online "Whale Entanglement Data Dashboard."

The extremely high temperatures during MHWs have had dramatic effects on the marine ecosystem. MHWs in the 1980's and 1990's, associated with El Niño events, led to negative consequences for the marine ecosystem through local processes (such as changes in physical and chemical properties, and food web changes) and advection, or poleward and/or onshore transport of organisms (Ohman et al., 2017). The 2014-2016 MHW was associated with mass strandings of some marine mammals and sea birds (Cavole et al., 2016; Piatt et al., 2020). High temperatures initiated toxic algal blooms that affected the commercial and recreational crab fishing season and poisoned marine mammals (Gentemann et al., 2017). The closure of the Dungeness crab fishery alone led to a loss of an estimated $48 million in revenue for crab fishermen statewide (Brown, 2016).

The MHW also contributed to the rapid and extensive loss of kelp forests in Northern and Southern California (Gleason et al. 2021, Cavanaugh et al., 2019). In Northern California this led to the closure of the recreational red abalone fishery and the commercial red sea urchin fishery (Gleason et al. 2021). Both kelp and abalone are culturally significant species to Native American Tribes, such as the Chumash and the Scotts Valley Band of Pomo Indians (Santa Ynez Band of Chumash Indians, 2022; Amah Mutsun Tribal Band, 2022; Big Valley Band of Pomo Indians and Middletown Rancheria of Pomo Indians, 2021). Since kelp provide a wide range of ecosystem services as primary producers and as essential habitat for marine organisms, among other things, the loss of kelp forests has larger scale consequences (Bell et al., 2020; Gleason et al, 2020; Teagle et al., 2017). For example, without kelp forests to act as buffers, the coast has become more vulnerable to coastal erosion from high energy storms and swell events; along with sea level rise, coastal erosion is threatening cultural

sites along the shoreline in the Amah Mutsun's ancestral territory (Amah Mutsun Tribal Band, 2022).

The 2014-2016 MHW was accompanied by northward shifts in the geographic distributions of a variety of marine animals including fish, sea turtles, pelagic red crabs, southern copepods and many other marine invertebrates (Leising et al., 2015; Cavole et al., 2016; Sanford et al., 2019). During the 2014-2016 and 2019-2020 MHWs, the increased abundance of lipid-poor southern copepods and the decreased abundance of lipid-rich, higher nutritional value northern copepod impacted the entire food web (Cavole et al., 2016, Weber et al., 2021).

Temporary shifts in other species distributions have also occurred during past warm-water anomalies, including major El Niño-Southern Oscillation (ENSO) events (Pearcy and Schoener, 1987), however, these recent North Pacific-originating MHWs differ from El Niños in that they tend to bring a somewhat different assemblage of organisms into the California Current (Leising et al., 2015; Cavole et al., 2016). While the impacts of coastal temperature change are increasingly being documented, offshore temperature variability is complex and may influence a suite of other biological processes, including migration patterns.

Changes in temperature can affect the chemical and physical properties of the ocean. Since warmer water is less dense than colder water, changes in SST can alter currents and transport patterns. Warming SSTs can cause more stable layers of seawater to form near the surface, thus increasing "stratification"; when this happens, upwelling and vertical mixing that transports nutrients, oxygen, carbon, plankton and other material across ocean layers is reduced (Roemmich and McGowan, 1995; Jacox and Edwards, 2011). Temperature also affects the solubility of gases in ocean waters. For example, warmer waters hold less oxygen, while also accelerating the rate of oxygen consumption by marine organisms (e.g., Somero et al., 2015; Breitburg et al, 2018).

Surface ocean water temperature affects weather, specifically the occurrence of coastal fog and the strength of winds, as well as the thickness of the marine atmospheric boundary layer. The latter is a primary factor controlling the inland intrusion of cool coastal air and therefore inland weather patterns. Warmer waters play a role in extreme weather events by increasing the energy and moisture of the atmosphere. Warmer ocean temperatures also contribute to global sea level rise because warming water not only expands but also accelerates the melting of land-based ice sheets (IPCC, 2021).

Global oceans are projected to continue to warm in the 21st century. MHWs are expected to further increase in frequency, duration, spatial extent, and intensity, although changes will not be globally uniform (IPCC, 2021). Given the severe impacts of MHW on the marine ecosystem and the coastal communities and economies it supports, oceanographers have developed the California Current MHW Tracker as a tool for forecasting future MHWs (NOAA, 2022).

What factors influence this indicator?

Global SSTs have increased due to a net heat flux from the atmosphere stemming from the greenhouse effect. Deeper regions of the oceans have also warmed, to depths of 3000 meters during the past several decades (first documented by Levitus et al., 2001; also Levitus et al., 2012). A combination of oceanic and atmospheric processes, including ocean currents, winds, and climate modes like El Niño can lead to the periods of extremely high ocean temperature, and their classification as MHWs depends on the magnitude of 'normal' warming events in a given location (Hobday et al., 2016).

Near-surface ocean water temperatures along the California coast are influenced by seasonal upwelling, already discussed above. Historically, upwelling was measured using only estimates of the amount of water transported. A new index called the Biologically Effective Upwelling Transport Index, or BEUTI (pronounced "beauty") incorporates estimates of the amount of nutrients (nitrate) in vertically transported waters, thus providing information relevant to biological responses (Jacox et al., 2018).

As shown in Figure 6A, annual mean values for BEUTI (in millimoles of nitrate per meter per second) are highest – indicating more effective upwelling – along Northern California, especially at 39°N (due to the enhancing effect of the promontories at Point Arena and Cape Mendocino on the winds). Considerably less effective upwelling occurs along the Southern California coast at 32°N (south of San Diego) and 34°N (off Los Angeles). This difference is due to a combination of strong upwelling-favorable winds in Northern California and cooler waters flowing from the north Pacific within the California Current; the small temperature difference between surface and deeper waters means weaker stratification, which facilitates upwelling. In contrast, Southern California experiences weak upwelling-favorable winds and greater stratification, as warmer waters from the equatorial Pacific dominate (Bograd et al., 2019). Figure 6B shows that over the past 33 years, upwelling trends have generally increased along a latitudinal gradient, with larger increases in Northern California.

Figure 6. Biologically Effective Upwelling Transport Index (BEUTI) along the California Coast

A. **Annual mean values at selected latitudes**

B. **Decadal trends, 1988-2021**

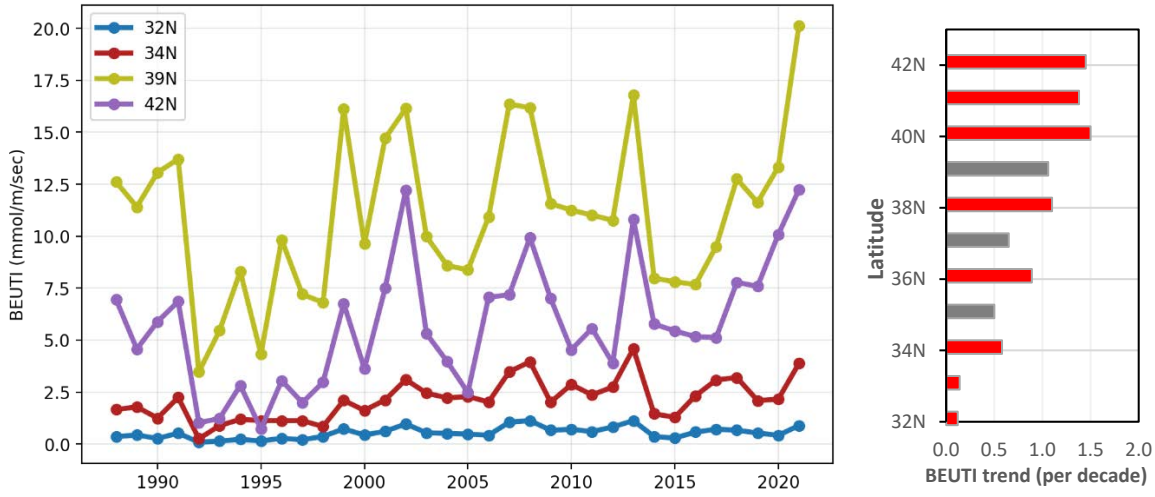

Source: NOAA, 2021

[A] Annual mean values of BEUTI at selected latitudes along the California Coast: 32°N, south of San Diego; 34°N, Los Angeles; 39°N near Point Arena, and 42°N near the California-Oregon border. [B] Linear trends in the magnitude of BEUTI per decade at different latitudes along the California Coast; red bars indicate statistically significant trends (p<0.05)

Trends in coastal temperatures are complex owing to the simultaneous interaction of surface warming and the cooling effect of upwelling. In general, it is expected that surface temperatures will increase offshore and in sheltered coastal waters, where upwelling does not occur or is weak, as observed in the warming trends of La Jolla. In contrast, cooler or non-changing SSTs are expected during the upwelling season in open shelf waters (Seabra et al., 2019), especially off Central and Northern California (García-Reyes and Largier, 2010; Largier et al., 2010). The lack of statistically significant warming trends in the Central and Northern California coast in the last four decades may be an indication of the cooling effect of upwelling in coastal waters. In certain upwelling regions, including the California Current, studies suggest that upwelling favorable winds may intensify with climate change (Bakun, 1990; García-Reyes et al., 2015; García-Reyes and Largier, 2010; Rykaczewski et al., 2015; Sydeman et al., 2014). In the last three decades, the influx of nutrients to the coastal area has increased (Figure 5), likely as a result of the concurrent increase in upwelling favorable winds.

Natural fluctuations in temperature, wind, and circulation patterns that occur in coastal waters can introduce significant interannual and interdecadal fluctuations in the long-term trend. The El Niño (or La Niña) events, positive (negative) phases of the El Niño-Southern Oscillation (ENSO), are responsible for anomalously warm (or cool) ocean temperatures along the California coast. El Niño is the warm or positive phase, with

major El Niño events occurring every 5-10 years (UCAR, 1994). La Niña is the cool or negative phase. Additionally, the West Coast is affected by multi-decadal variability in temperature, characterized by patterns such as the Pacific Decadal Oscillation, or PDO (Mantua et al., 1997), and the North Pacific Gyre Oscillation, or NPGO (Di Lorenzo et al., 2008). MHW occurrence involves two interwoven processes: a long-term increase in temperatures driven by anthropogenic climate change and large amplitude fluctuations that are enhanced because of that increase (Fumo et al., 2020). Recent work projects that future SSTs will continue to increase; globally, SSTs for the years 2070 to 2099 are projected in many regions to be warmer than the warmest year in the period from 1976 to 2005 (Alexander et al., 2018).

Technical considerations

Data characteristics

Coastal California is home to the longest continuous record of SST on the US West Coast and the Pacific Rim. Long-term time series from three sites — Trinidad Bay in Humboldt County, Pacific Grove in Monterey County, and La Jolla in San Diego — are presented in this report; these sites were chosen based upon their long operational duration (~40 to 100 years), public data availability, and regional/geographic coverage. Data for the three sites and other California coastal sites have been collected by the Shore Stations Program (SIO, 2021). The time series at Scripps Pier, La Jolla Shores, which extends back to 1916, is the longest running SST data set in the state.

Trinidad Bay temperature measurements are taken daily by staff from the Humboldt State University Marine Laboratory, located on the rocky headland between the ocean and Trinidad Bay. Bay temperature is measured from the fishing pier on the southeast side of the headland. Pacific Grove measurements are taken daily by staff from Stanford University's Hopkins Marine Station from a beach on the north side of Point Cabrillo. This location is representative of coastal conditions on the south side of Monterey Bay. La Jolla temperature measurements are taken daily at Scripps Pier by representatives from Scripps Birch Aquarium. The proximity of the pier to the deep waters at the head of La Jolla submarine canyon results in data representative of oceanic conditions.

The NOAA OISST reanalysis data (v2, Huang et al., 2021) merges satellite and in situ measurements from different platforms into a single gridded SST product, allowing a spatial resolution of roughly 13nm along California (here averaged longitudinally to ~30nmi), and daily temporal resolution, starting in September 1981.The dataset is interpolated to fill gaps on the grid and create a spatially complete map of sea surface temperature. Satellite and ship observations are referenced to buoys to compensate for platform differences and sensor biases (NOAA, 2021a). Data are provided by the NOAA/OAR/ESRL PSL, Boulder, Colorado, USA.

MHW cover and cumulative intensity are products reported in the California Current Marine Heatwave Tracker, an experimental tool for tracking marine heatwaves from

British Columbia to Baja, along the path of the California Current. The tool was designed to investigate the 2014-2016 MHW (NOAA, 2022). Indices are developed to help forecast or predict future MHWs expected to impact the coast. A MHW is based on the definition in Hobday, et al. (2016); however, no time constraint was used since values were summed over relatively large regions. The analysis presented here is based on a long-term baseline mean for the period 1971 to 2000, and the threshold was set at the 90th percentile of all values for the period 1982-2021. Further information about the tracker, including access to the data, is available at the Integrated Ecosystem Assessment webpage.

Five regions along the California Current are monitored, including three in California as shown in Figure 5. For each region, the "spatial coverage," is calculated as the annual mean of the daily percentage of the area in "heatwave status". This describes the size of the MHW each year. "Intensity" describes how hot the ocean waters are compared to a historical baseline. This index does not depend on whether it is in "heatwave status." The "cumulative intensity" presented in Figure 3B is the sum of daily intensity values in a year for a given region, specifically the sum of average daily SST measurements above the baseline temperature. These temperature measurements are standardized for the location and time of day to ensure that the data is comparable over time. The cumulative intensity is the sum of the daily intensity values.

Strengths and limitations of the data

A growing network of ocean monitoring along California is an important resource for separating natural and anthropogenic influences on increasing temperatures. The California Cooperative Oceanic Fisheries Investigations (CalCOFI) and National Oceanic and Atmospheric Administration (NOAA) National Data Buoy programs represent the largest coordinated efforts to collect SST data across broad spatial scales. In addition, the Central and Northern California Ocean Observing System and the Southern California Coastal Observing System provide coordinated long-term monitoring of environmental conditions to support ocean management decisions as part of an eleven-region US Integrated Ocean Observing System (IOOS, 2018).

The NOAA satellite-based product provides a shorter SST record than those of the shore stations, however its record has no spatial gaps and a larger cover offshore, allowing a better understanding of the different trends observed in this indicator along the California coast and over the continental shelf (NOAA, 2021a). It is important to note that the data points closest to shore cover waters over the continental shelf, and do not represent temperatures near shore (beaches and intertidal) values due to its coarser resolution. For nearshore values, the coastal values are more representative, although sparse in space.

Temperature and BEUTI were averaged annually before trends were calculated. This reduces the number of data points and therefore statistical significance.

OEHHA acknowledges the expert contribution of the following to this report:

Marisol García-Reyes, Ph.D.
Farallon Institute
marisolgr@faralloninstitute.org

Andrew Leising, Ph.D.
National Oceanic and Atmospheric Administration
Southwest Fisheries Science Center
Environmental Research Division
andrew.leising@noaa.gov

Fish larvae analysis provided by:
Rebecca Asch, Ph.D., East Carolina University

Additional input from:
Steven Bograd, Ph.D., NOAA
Tessa M. Hill, Ph.D., UC Davis Bodega Marine Laboratory

References:

Alexander AA, Scott JD, Friedland KD, Mills KE, Nye JA, et al. (2018). Projected sea surface temperatures over the 21st century: Changes in the mean, variability and extremes for large marine ecosystem regions of Northern Oceans. *Science of the Anthropocene* **6**(9).

Amah Mutsun Tribal Band (2022). Impacts of Climate Change on the Amah Mutsun Tribal Band. Prepared by Mike Grone, PhD, Amah Mutsun Land Trust. In: OEHHA 2022 Indicators of Climate Change in California.

Asch, R. G. (2015). Climate change and decadal shifts in the phenology of larval fishes in the California Current ecosystem. *Proceedings of the National Academy of Sciences of the United States of America* **112**(30): E4065–E4074.

Bakun A (1990). Global climate change and intensification of coastal ocean upwelling. *Science* **247**: 198-201.

Big Valley Band of Pomo Indians & Middletown Rancheria of Pomo Indians (2021). Summary of the Lake, Sonoma, and Mendocino County Tribal Listening Session (May 18-19, 2021), hosted by the Big Valley Band of Pomo Indians, the Middletown Rancheria of Pomo Indians, and the Office of Environmental Health Hazard Assessment.

Bindoff NL, Cheung WWL, Kairo JG, Arístegui J, Guinder VA et al. (2019): Changing Ocean, Marine Ecosystems, and Dependent Communities. In: *IPCC Special Report on the Ocean and Cryosphere in a Changing Climate* [Pörtner H-O, Roberts DC, Masson-Delmotte V, Zhai P, Tignor M, et al. (Eds.)].

Bograd SJ, Schroeder ID and Jacox, MG (2019). A water mass history of the southern California Current System. *Geophysical Research Letters* **46**: 6690-6698.

Breitburg D, Levin LA, Oschlies A, Gregoire M, Chavez FP, et al. (2018). Declining oxygen in the global ocean and coastal waters. *Science* **359** (6371).

Brown EG (2016). Governor Edmund G. Brown, Jr. Letter to Honorable Penny Pritzker, Secretary, U.S. Department of Commerce, dated February 9, 2016.

Cavanaugh KC, Reed DC, Bell TW, Castorani MCN and Beas-Luna R. (2019). Spatial variability in the resistance and resilience of giant kelp in southern and Baja California to a multiyear heatwave. *Frontiers in Marine Science* **6**: 413.

Cavole LM, Demko AM, Diner RE, Giddings A, Koester I, et al. (2016). Biological impacts of the 2013–2015 warm-water anomaly in the Northeast Pacific: Winners, losers, and the future. *Oceanography* **29**: 273–285.

CSIRO. 2021. Forecasting Marine Heatwaves, The Project: Marine heatwaves in the Indo-Pacific region, their predictability and social-economic impacts.

Di Lorenzo E and Mantua N (2016) Multi-year persistence of the 2014/15 North Pacific marine heatwave. *Nature Climate Change* **6**(11): 1042–1048.

Di Lorenzo E, Schneider N, Cobb KM, Franks PJS, Chhak K, Miller AJ, et al. (2008). North Pacific Gyre Oscillation links ocean climate and ecosystem change. *Geophysical Research Letters* **35**(8).

Fumo JT, Carter ML, Flick RE, Rasmussen LL, Rudnick DL and Iacobellis SF (2020). Contextualizing marine heatwaves in the Southern California bight under anthropogenic climate change. *Journal of Geophysical Research: Oceans* **125**: e2019JC015674.

García-Reyes M and Largier J (2010). Observations of increased wind-driven coastal upwelling off Central California. *Journal of Geophysical Research* **115**(C4).

García-Reyes M, Sydeman WJ., Schoeman DS, Rykaczewski RR, Black BA, et al. (2015). Under pressure: Climate change, upwelling, and eastern boundary upwelling ecosystems. *Frontiers in Marine Science* **2**: 109.

Gentemann C, Fewings M and García-Reyes M (2017). Satellite sea surface temperature along the West Coast of the United States during the 2014-2016 Northeast Pacific marine heat wave. *Geophysical Research Letters* **44**: 312-310.

Gleason MG., Caselle JE, Heady WN, Saccomanno VR, Zimmerman J, et al. (2021). *A Structured Approach for Kelp Restoration and Management Decisions in California.* The Nature Conservancy, Arlington, Virginia.

Goericke R, Venrick EL, Koslow TL, Sydeman WJ, Schwing FB, et al. (2007). The State of the California Current, 2006-2007: Regional and local processes dominate. *CalCOFI Reports* **48**: 33-66.

Henson SH, Beaulieu C and Lampitt R (2016). Observing climate change trends in ocean biogeochemistry: When and where. *Global Change Biology* **22**: 1561-1571.

Hobday, AJ, Alexander LV, Perkins SE, Smale DA, Straub SC, et al. (2016). A hierarchical approach to defining marine heatwaves. *Progress in Oceanography* **141**: 227–238.

Huang, B, Liu , Banzon V, Freeman E, Graham G, et al. (2021). Improvements of the Daily Optimum Interpolation Sea Surface Temperature (DOISST) Version 2.1. *Journal of Climate* **34**: 2923-2939.

IPCC (2019). Summary for policy makers. In: *IPCC Special Report on the Ocean and Cryosphere in a Changing Climate* [Pörtner HO, Roberts DC, Masson-Delmotte V, Zhai P, Tignor, M, et al. (Eds.)].

IPCC (2021). Summary for Policymakers. In: *Climate Change 2021: The Physical Science Basis. Contribution of Working Group I to the Sixth Assessment Report of the Intergovernmental Panel on Climate Change* [Masson-Delmotte VP, Zhai A, Pirani SL, Connors C, Péan S, et al. (Eds.)].

Jacox, MG and Edwards CA (2011). Effects of stratification and shelf slope on nutrient supply in coastal upwelling regions. *Journal of Geophysical Research: Oceans 116*(C3).

Jewett L and Romanou A (2017). Ocean acidification and other ocean changes. In: Climate Science Special Report: Fourth Natoinal Climate Assessment, Volume I [Wuebbles DJ, Fahey DF, Hibbard KA, Dokken DJ, Stewart BC et al. (Eds)]. U.S. Global Change Research Program, Washington, DC, pp. 364-392

Largier, JL, Cheng BS and Higgason KD (2010). Climate Change Impacts: Gulf of the Farallones and Cordell Bank National Marine Sanctuaries. Report of a Joint Working Group of the Gulf of the Farallones and Cordell Bank National Marine Sanctuaries Advisory Councils (Marine Sanctuaries Conservation Series ONMS-11-04). National Oceanic and Atmospheric Administration.

Leising AW, Schroeder ID, Bograd SJ, Abell J, Durazo R, et al. (2015). State of the California Current 2014-15: Impacts of the warm water “blob”. CalCOFI Report **56**: 31-68.

Levitus S, Antonov JI, Boyer O, Baranova HE, Garcia RA, et al. (2012), World ocean heat content and thermosteric sea level change (0–2000 m), 1955–2010, *Geophysical Research Lett*ers **39**: L10603.

Levitus S, Antonov JI, Wang J, Delworth TL Dixon KW and Broccoli AJ (2001). Anthropogenic warming of Earth's climate system. *Science* **292**(5515): 267-270.

Mann KH. 2000. Ecology of coastal waters, with implications for management. 2nd edn. Malden: Blackwell Science.

Mantua N, Hare S, Zhang Y, Wallace J and Francis R (1997). A Pacific interdecadal climate oscillation with impacts on salmon production. *Bulletin of the American Meteorological Society* **78**: 1069-1079.

NOAA (2021a). National Oceanic and Atmospheric Administration, National Centers for Environmental Information, Optimum Interpolation Sea Surface Temperature (OISST) v2.1. Retrieved June 13, 2021.

NOAA (2021b). National Centers for Environmental Information, State of the Climate: Global Climate Report for Annual 2020, published online January 2021. Retrieved May 20, 2021.

NOAA (2022). National Oceanic and Atmospheric Administration, Environmental Research Division, NOAA Fisheries—Southwest Fisheries Science Center. The California Current Marine Heatwave Tracker – An experimental tool for tracking marine heatwaves. California Current Project.

Ohman MD, Mantua N, Keister J, Garcia-Reyes M. and McClatchie S. (2017). ENSO impacts on ecosystem indicators in the California Current System. Variations. CLIVAR & OCB Newsletter **15**(1): 8-15.

Oliver EC, Benthuysen JA, Darmaraki S, Donat MG, Hobday AJ, et al. (2021). Marine heatwaves. *Annual Review of Marine Science* **13**: 313–342

Pearcy WG and Schoener A (1987). Changes in marine biota coincident with the 1982-83 El Niño in the northeastern subarctic Pacific Ocean. *Journal of Geophysical Research* 92: 14417–14428.

Piatt, JF, Parrish JK, Renner HM, Schoen SK, Jones TT, et al. (2020). Extreme mortality and reproductive failure of common murres resulting from the northeast Pacific marine heatwave of 2014-2016. *PloS one*, **15(1)**: e0226087.

Rhein M, Rintoul SR, Aoki S, Campos E, Chambers D, et al. (2013). Observations: Ocean. In: Climate Change 2013: The Physical Science Basis. Contribution of Working Group I to the Fifth Assessment Report of the Intergovernmental Panel on Climate Change. Stocker TF, Qin D, Plattner G-K, Tignor M, Allen SK, et al. (Eds.). Cambridge, United Kingdom and New York, NY, USA: Cambridge University Press.

Roemmich D and McGowan J (1995). Climatic warming and the decline of zooplankton in the California Current. *Science* **267**(5202): 1324-1326.

Rykaczewski, R. R., Dunne, J. P., Sydeman, W. J., García-Reyes, M., Black, B. A., & Bograd, S. J. (2015). Poleward displacement of coastal upwelling-favorable winds in the ocean's eastern boundary currents through the 21st century. *Geophysical Research Letters* ***42***(15): 6424-6431.

Sagarin RD, Barry JP, Gilman SE and Baxter CH (1999). Climate-related change in an intertidal community over short and long time scales. *Ecological Monographs* **69**(4): 465-490.

Sanford, E., Sones, J. L., García-Reyes, M., Goddard, J. H., & Largier, J. L. (2019). Widespread shifts in the coastal biota of northern California during the 2014–2016 marine heatwaves. *Scientific reports* **9**(1): 1-14.

Santa Ynez Band of Chumash Indians (2022). *Impacts of Climate Change on the Santa Ynez Band of Chumash Indians.* In: OEHHA 2022 Indicators of Climate Change in California.

Santora JA, Mantua NJ, Schroeder ID, Field JC, Hazen EL, et al. (2020) Habitat compression and ecosystem shifts as potential links between marine heatwave and record whale entanglements. *Nature Communications* **11**: 536.

Seabra R, Varela R, Santos AM, Gomez-Gesteira M., Meneghesso C, et al. (2019). Reduced nearshore warming associated with eastern boundary upwelling systems. *Frontiers in Marine Science* **6**: 104.

SIO (2021). Shore Stations Program. Trinidad temperature measurements and salinity samples collected by staff at Humboldt State University Marine Laboratory; Pacific Grove measurements collected by the Stanford University Hopkins Marine Station; Scripps Pier measurements collected by the Birch Aquarium at Scripps staff and volunteers. Data provided by the Shore Stations Program, sponsored at Scripps Institution of Oceanography by California State Parks and Recreation, Division of Boating and Waterways, Award C1670003. Retrieved June 13, 2021.

Somero GN, Beers JM, Chan F, Hill TM, Klinger T and Litvin SY (2015). What changes in the carbonate system, oxygen, and temperature portend for the northeastern Pacific Ocean: A physiological perspective. *BioScience* **66**(1): 14-26.

Sydeman WJ, García-Reyes M, Schoeman DS, Rykaczewski RR, Thompson SA, et al. (2014). Climate change and wind intensification in coastal upwelling ecosystems. *Science* **345**: 77-80.

Teagle H, Hawkins SJ, Moore PJ, Smale DA (2017). The role of kelp species as biogenic habitat formers in coastal marine ecosystems, *Journal of Experimental Marine Biology and Ecology* **492**: 81-98

UCAR (1994). El Niño and Climate Prediction, Reports to the Nation on our Changing Planet. University Corporation for Atmospheric Research, pursuant to National Oceanic and Atmospheric Administration (NOAA) Award No. NA27GP0232-01.

Weber ED, Auth TD, Baumann-Pickering S, Baumgartner TR, Bjorkstedt EP, et al. (2021). State of the California Current 2019–2020: Back to the Future with Marine Heatwaves? *Frontiers in Marine Science* **8**.

SEA LEVEL RISE

Sea levels along the California coast have risen over the past century, except along the far north coast where an uplift of the land surface has occurred due to the movement of the Earth's plates, resulting in a small relative fall in sea level.

Figure 1. Annual mean sea level trends

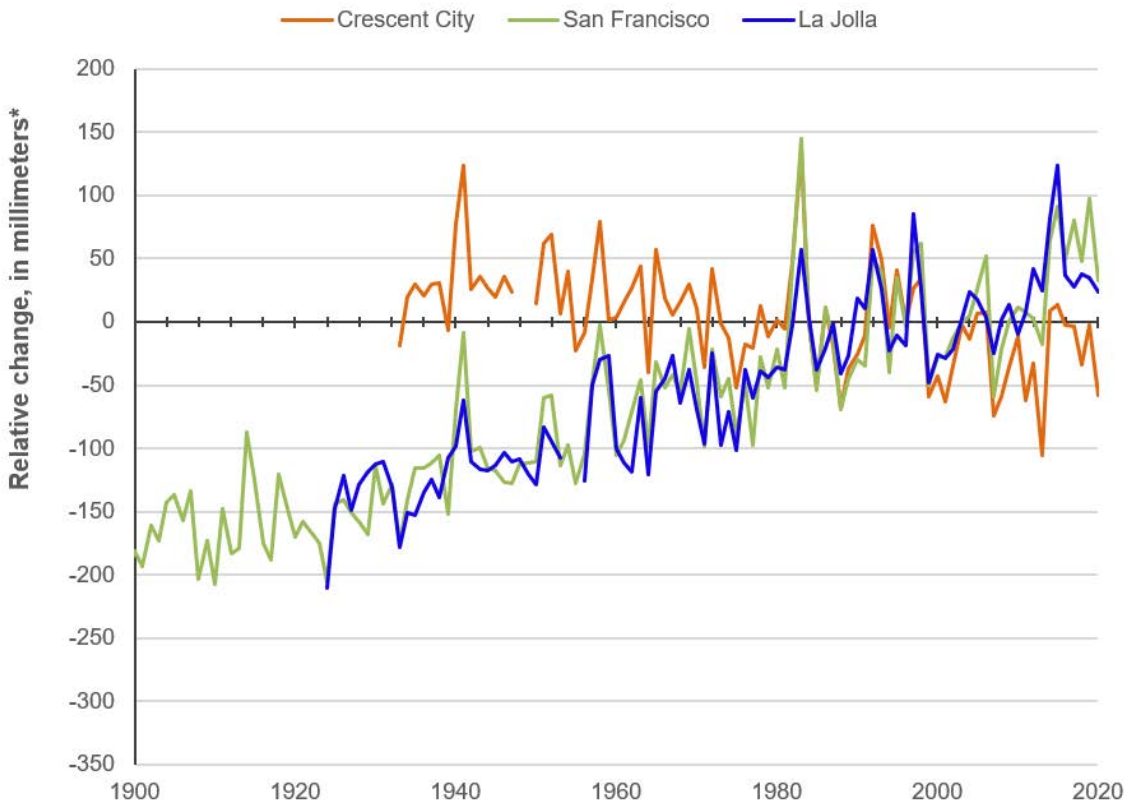

Source: NOAA, 2021a

*Relative to tidal datum (reference point set by NOAA)

What does the indicator show?

As shown in Figure 1, mean sea levels have increased over the past century by about 200 millimeters (mm) (8 inches (″)) in San Francisco and in La Jolla. This is consistent across the California coastline except for Crescent City where the sea level has declined by about 80 mm (3″) due to regional land uplift driven by the movement of the Earth's plates. Sea level values are the average height of the ocean relative to the tidal datum, a standard elevation established by the National Oceanic and Atmospheric Administration (NOAA) as a reference point (see *Technical Considerations* for details).

Mean sea levels show year-to-year (interannual) variability. They peak during El Niño years (when the waters of the eastern Pacific Ocean became warmer, temporarily raising coastal water levels from 10 to 40 centimeters (cm), or about 4 to 16″). Levels at

all three locations rose in 2014 and 2015, due to unusually warm sea surface temperatures in the Pacific Ocean during that period (Hu et al., 2017), further exacerbated by the large El Niño that peaked in late 2015 (Flick et al., 2016).

Trends at 17 tide stations in California (see map, Figure 2) are presented in Table 1, listed in order from north to south (NOAA, 2021a).

Figure 2. Trends at California tide stations

Source: NOAA, 2021a

Interactive map is online at NOAA's Tides and Currents webpage

Table 1. Sea Level Trends (stations listed from north to south)

Location	Period of record	Trend, mm/year (inches/year)
Crescent City	1933-2020	-0.79 (-0.03)
North Spit	1977-2020	+4.91 (+0.2)
Arena Cove	1978-2020	+0.89 (+0.04)
Port Chicago*	1976-2020	+2.03 (+0.08)
Point Reyes	1975-2020	+2.15 (+0.08)
Alameda*	1939-2020	+0.87 (+0.03)
San Francisco	1897-2020	+1.97 (+0.08)
Redwood City*	1974-2020	+2.54 (+0.1)
Monterey	1973-2020	+1.63 (+0.06)
Port San Luis	1945-2020	+0.96 (+0.04)
Santa Barbara	1973-2020	+1.08 (+0.04)
Rincon Island**	1962-1990	+3.22 (+0.1)
Santa Monica	1933-2020	+1.54 (+0.06)
Los Angeles	1923-2020	+1.03 (+0.04)
Newport Beach***	1955-1993	+2.22 (+0.09)
La Jolla	1924-2015	+2.13 (+0.08)
San Diego	1906-2020	+2.2 (+0.09)

** Gauge not along the outer coast*
*** Rincon Island is an artificial offshore island built for oil and gas production*
**** Inactive*

Source: NOAA, 2021a

The general trend towards higher sea levels in California is consistent with global observations (IPCC, 2021). Global sea-level rise is the most obvious manifestation of climate change in the ocean (Griggs et al., 2017). Global mean sea levels have been rising at increasing rates: by 1.3 mm/year between 1901 and 1971; 1.9 mm/year (about 0.07 inch/year) between 1971 and 2006; and 3.7 mm/ year (about 0.1 inch/year) between 2006 and 2018. Human influence on the climate was very likely the main driver of these increases since at least 1971 (IPCC, 2021).

Why is this indicator important?

As sea level rise continues to accelerate throughout this century and beyond, coastal flooding, beach erosion, bluff retreat, loss of ecosystems, salinization of soils, ground

and surface water, and impeded drainage will further increase along low-lying coasts worldwide without adequate adaptation efforts (IPCC, 2019).

Millions of residents, infrastructure, housing, natural resources, and economies in California's coastal counties face serious and costly threats from rising sea levels (LAO, 2020). The impacts of sea level rise will be amplified by storms, high tides, beach erosion and cliff retreat; flooding risks, in particular, will result from the combined effects of rising sea levels, heavy precipitation events, and shallower coastal groundwater (also due to sea level rise) (Barnard et al., 2019; Rahimi et al., 2020). Using a dynamic model (the Coastal Storm Modeling System or CoSMoS) that incorporates the effects of coastal storms in addition to estimates of sea level rise, projected areas of coastal flooding could impact over 600,000 people and $200 billion in property statewide over the next century (Figure 3; Barnard et al., 2019).

Critical infrastructure in many locations lies less than 4 feet above the high tide, including two international airports – Oakland and San Francisco – and about 172,000 homes (DWR, 2016). Rising sea levels place the airports, already vulnerable to storms and flooding, at greater risk (Griggs, 2020). Loss of service at either airport would result in major economic consequences regionally, nationally, and internationally (San Francisco Bay Conservation and Development Commission, 2012). Other critical infrastructure, such as ports, natural gas lines, and wastewater treatment plants, will also become more vulnerable to storms and flooding (Caldwell et al., 2013, CEC, 2017; Hummel et al., 2018). Notably, the areas projected to experience flooding events by 2100 contain at least 400 hazardous facilities including power plants, refineries, and industrial facilities. Sea level rise poses risks for such facilities experiencing flooding events that can potentially expose nearby residents to hazardous pollutants (UC Berkeley, 2021). Processes that result in significant short-term increases in water levels such as King tides (extremely high tides that typically occur a few times a year), seasonal cycles, winter storms, and patterns of climate variability (e.g., the Pacific Decadal Oscillation or the El Niño Southern Oscillation (ENSO)) cause the greatest impacts on infrastructure and coastal development due to the significantly higher water levels they produce compared to sea level rise alone (Griggs et al., 2017).

Low-income communities in California often are located in areas where infrastructure lack sufficient drainage capacity, making them particularly vulnerable to the impacts of flooding (Ramini et al., 2020). Climate-driven coastal hazards will amplify environmental justice-related inequities. Hazards in vulnerable areas disproportionately affect communities that are least able to adapt. For example, hazardous facilities at risk of flooding are disproportionately located in low-income communities and communities of color. Further, disadvantaged communities are over 5 times more likely to be located within 1 km of one or more hazardous facilities at risk of flooding in 2050, and over 6 times in 2100 (UC Berkeley, 2021).

Figure 3. Projected overland flood exposure over the next century in select locations across California based on results from the Coastal Storm Modeling System (CoSMoS)

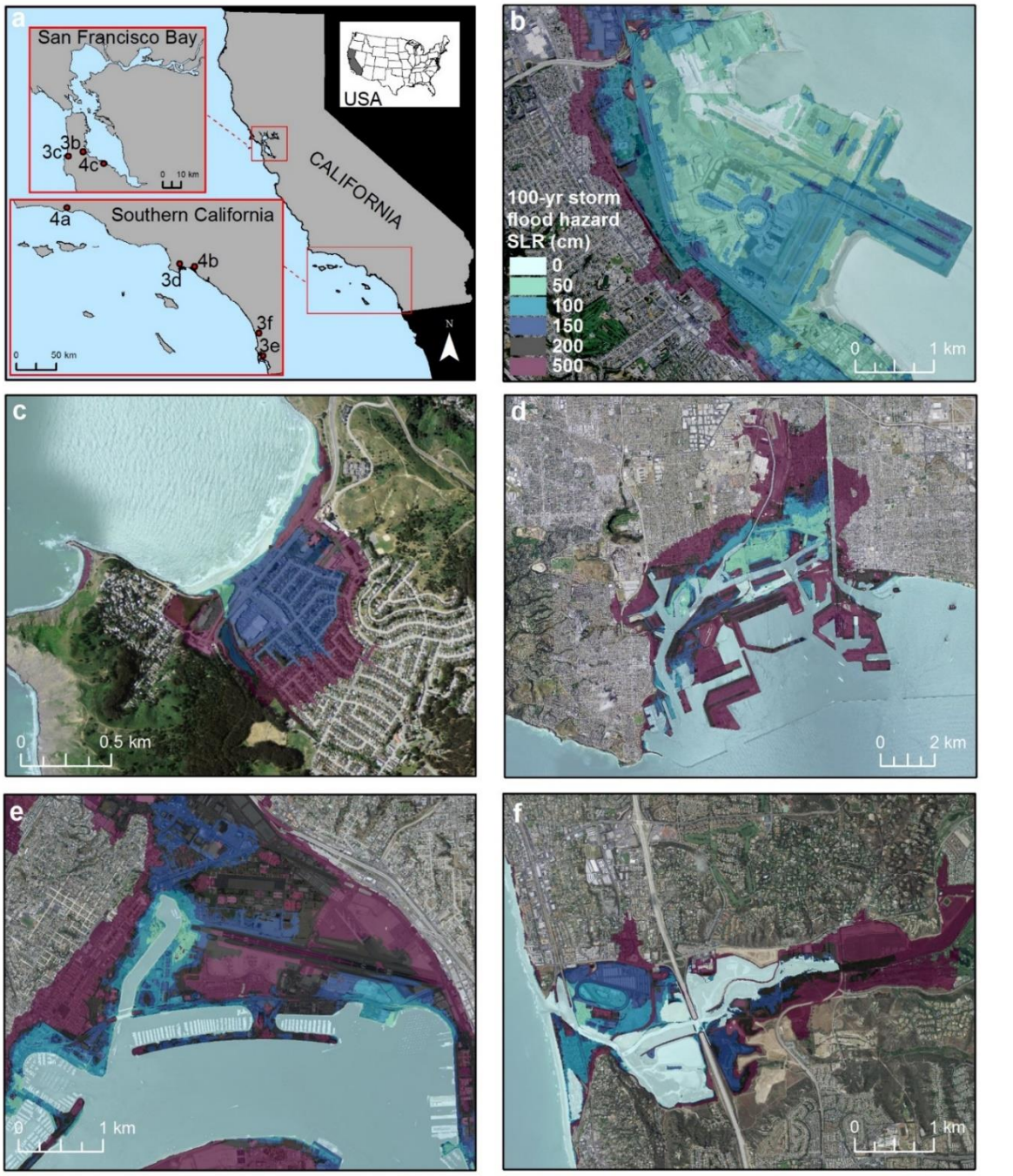

Source: Barnard et al., 2019

(a) Study area for CoSMoS with insets. Examples of modeled flood extents for the 100-year coastal storm in combination with 0, 0.50, 1.00, 1.50, 2.00, and 5.00 meters of SLR; (b) San Francisco International Airport, (c) City of Pacifica, (d) Port of Los Angeles and Port of Long Beach, (e) Port of San Diego and San Diego International Airport, and (f) City of Del Mar. (Figure generated using ArcGIS v. 10.4.2, by Esri. Local base maps from ArcGIS Online, World_Terrain_Base, and ESRI_Imagery_World_2D, accessed 2 Oct 2018.) Projections can be viewed interactively and translated into socioeconomic exposure.

Compared to higher-income communities and property owners, people with lower incomes and residents of rental units face disproportionately greater impacts from sea level rise (CCC, 2015; LAO, 2020). They are more likely to be displaced by flooding or related impacts because they are not able to rebuild or are less able to prepare their residences for floods. They may be unable to evacuate and thus have less control over their safety. They may have less resources and are likely to not have insurance to replace lost or damaged property or structures. The loss of local public beaches and recreational areas would disproportionately affect low-income communities that have few options for low-cost recreation (CCC, 2015).

Coastal erosion and cliff collapse (see Figure 4) threaten public safety, infrastructure, and property as they become more common with sea level rise (Vitousek et al., 2017; Limber et al., 2018; USGS, 2019). In Southern California, for instance, the projected sandy beach shoreline change indicates that 31 to 67 percent of Southern California beaches may become completely eroded by 2100 without human interventions (Vitousek et al., 2017). Further, sea cliffs could retreat at a rate nearly double that of the historical rate, causing an average total land loss of 19 to 41 meters (about 62 to 135 feet) by 2100 (Limber et al., 2018). As sea levels continue to rise, cliff collapses and the hazards they pose can also become increasingly common. In August 2019, three people were killed on a beach at Encinitas when the bluff above them collapsed, illustrating the damage a cliff collapse can cause.

Figure 4. Cliff collapse at Isla Vista, California (taken 2005)

Credit: Patrick Barnard, USGS

Coastal erosion and sea level rise, along with warming ocean temperatures and ocean acidification, collectively threaten cultural sites and resources along the shoreline for the Amah Mutsun and Chumash Tribes. Coastal erosion has damaged cultural sites, and as sea levels rise, sites previously used for gathering are no longer accessible (SCTLS, 2021; see Amah Mutsun and Santa Ynez Chumash Tribal reports). For example, traditional areas for the Chumash Tribe to gather Olivella shells (Figure 5), used in shell money, jewelry, and regalia, are often no longer

Figure 5. Olivella shells carved by the Chumash

Source: Science News, 2021

accessible. Without access to traditional sites, knowledge can be disrupted, and the weight of that loss is felt by generations of tribal members (PBMI and SYBCI, 2021).

Furthermore, rising seas will result in shallower coastal groundwater, leading to emergent groundwater (when groundwater rises to or above the surface of the ground) in some places (Befus et al., 2020; USGS, 2020). This elevated groundwater can flood communities, damage infrastructure, and release pollutants, all before seawater overtops the beach. (Grant et al., 2021 May, 2020; Plane et al., 2019; Figure 6). Areas with emergent groundwater may occur progressively inland, expanding the area affected by sea level rise beyond what is anticipated solely from flooding caused by water flowing overland (May, 2020). A 2-meter rise in sea levels could lead to significant hazards from shallow and emergent groundwater in communities along California's coast, potentially affecting 4 million residents and $1.1 trillion in property, 33,000 km of roads, and 3,000 critical facilities (such as schools, police stations, and hospitals), with 6 to 9 times greater population, property, and infrastructure exposure than overland flooding (Befus et al., 2020; Jones et al., 2017; USGS, 2021). Under a changing climate, surface flooding – resulting from sea level rise and episodic storm-driven waves, surge, precipitation, and river flows – and sea level rise-driven elevated groundwater levels can interact with each other and worsen the overall flood risk on coastal communities (Rahimi et al., 2020).

Figure 6. Emerging sources of inundations in coastal areas with climate change

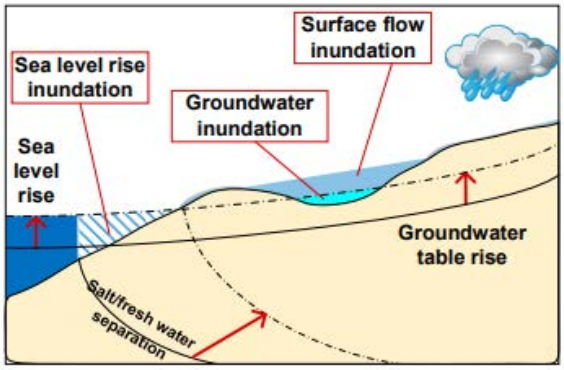

Source: Rahimi et al., 2020

Groundwater elevation can affect communities in other ways as well. As higher ocean water levels force up water levels underneath the ground, saltwater can intrude into fresh groundwater supplies, potentially affecting drinking water quality. Toxic contaminants can leak to the surface or flow through the subsurface to also compromise drinking water sources. Contaminated lands located along the coast and bay at risk of both surface and groundwater flooding include active and closed landfills, as well as "brownfields" which are undergoing or require cleanup. Moreover, raw sewage can seep into fresh groundwater aquifers or back up into streets and homes (LAO, 2020). Seawater intrusion into aquifers may require local communities to rely on other groundwater basins for their water supply (Coastal Resilience, 2020).

Coastal ecosystems in California are also threatened by sea level rise, including beaches, wetlands, estuaries, and fisheries. These wildlife areas provide flood protection, water treatment, carbon sequestration, biodiversity, wildlife habitat, and

recreation (CEC, 2009). The coastal environment also supports economically valuable commercial and recreational fishing activities (Caldwell et al., 2013).

The health of two such coastal ecosystems in California, sandy beach and tidal marshes, may plummet by 2050 without adequate adaptation and resilience strategies (Barnard et al., 2021; Myers et al., 2019). Predictions suggest that sea level rise will completely flood the mudflats at the San Pablo Bay estuary over the next 100 years, for instance (May 2020). This wildlife refuge protects the largest remaining contiguous patch of pickleweed-dominated tidal marsh in the northern San Francisco Bay, which provides critical habitat to the endangered salt marsh harvest mouse (Smith et al., 2018; US FWS, 2013). The combined effect of increased inundation and salinity projected under most climate change scenarios can significantly compromise pickleweeds and other plants important to the wetland habitats of the salt marsh harvest mouse (Smith et al., 2018).

Rising seas also present serious threats to the Sacramento-San Joaquin Delta. During storms and high-water flood events, higher sea levels increase the likelihood of Delta island levee failures, resulting in potentially catastrophic flooding to island communities and infrastructure. Sea level rise will increase the Delta's salinity, particularly during periods of reduced freshwater outflows from snowmelt. This puts the water supply for over half of California's population and much of the Central Valley's agriculture at risk. As previously mentioned, saltwater intrusion into groundwater may also increase with sea level rise, putting further pressure on limited drinking water supplies (DWR, 2013).

To assist with local adaptation strategies, online coastal flooding hazard maps using data produced by the scientific and research community in California may be accessed at: CalAdapt, Our Coast Our Future, Hazard Exposure and Reporting Analytics (HERA), and CoSMoS. These maps include predicted flooding for the San Francisco Bay, Sacramento-San Joaquin River Delta and California coast resulting from storm events at different sea level rise scenarios. Multiple efforts throughout California are underway to plan for, prepare, and adapt to rising seas and protect coastal ecosystems, infrastructure and communities (for examples, see CNRA, 2018 and 2021; OPC, 2021).

What factors influence this indicator?

As previously mentioned, human influence has very likely been the main driver of global sea level rise since at least 1971 (IPCC, 2021). Water from melting mountain glaciers and ice sheets is the main source of global mean sea level rise today (IPCC, 2019; Slater et al., 2020). The ice sheets in Greenland and Antarctica, while not expected to melt completely even on millennial time scales, contain enough ice to raise global mean sea level by 24 feet and 187 feet, respectively. In addition, the accelerating rate of ice loss from these ice sheets is of particular concern (Griggs et al., 2017).

Heat-driven expansion (also known as the steric effect) was the single greatest contributor to global mean sea level rise over the past century, accounting for about half

of the observed sea level rise (Griggs, et al., 2017). The ocean has absorbed more than 90 percent of the excess energy associated with anthropogenic greenhouse gas emissions, leading to ocean warming. As the ocean warms, water expands, and sea levels rise (IPCC, 2019).

Other sources of land-based water that contribute to sea level include anthropogenic activities. Groundwater that is pumped for agriculture, industry, and drinking ultimately drives more water to the ocean, thereby raising the sea level along the California coast (Griggs, et al., 2017). Conversely, dam building along rivers and associated reservoir impoundment can lower the sea level; however, estimates for the past few decades suggest that the effect of groundwater depletion and dam/reservoir contribution to sea level rise are secondary factors and largely cancel each other (Cazenave and Cozannet, 2014).

Global sea levels vary by region. Wind and water density gradients push sea levels higher in some places and lower in others. Climatic variability in different regions also affects local sea levels. ENSO in the eastern Pacific Ocean, for instance, produces alternating warm (El Niño) and cool phases (La Niña) that can bring sharp swings in sea level that are transient and typically last for only about a year. Additionally, ice sheets in Greenland and Antarctica, as well as mountain glaciers exert a gravitational pull on the ocean, resulting in a complicated distribution of sea level across the globe, called sea level fingerprints. When the ice melts, water that had once been pulled toward the ice mass due to gravitational attraction migrates away (NASA, 2017).

Understanding relative (local) sea level rise is important to understanding how low-lying coastal communities and ecosystems will be affected by flooding, wetland loss, and damage to infrastructure, and it can deviate from regional estimates of sea level rise, which typically don't resolve finer scale shifts in land movement. (Blackwell et al., 2020). Episodically, local sea level is modulated by processes that produce higher-than-normal coastal water levels, such as storm surge, wave effects, and spring and King tides. Over the long term, glacial isostatic adjustment (GIA) due to crustal loading/unloading and plate tectonics can play a significant role in regional and local sea levels. Additionally, fluid withdrawals from the subsurface (e.g., due to groundwater pumping and hydrocarbon withdrawal), as well as sediment compaction, can lead to high rates of local subsidence, as in the California Bay-Delta, and along the San Francisco Bay shoreline. Much of California's coast is subsiding due to regional changes in land levels.

A radar study of ~100 km wide swath of land along California's coast during the years 2007-2018 estimated that between 4.3 million and 8.7 million people in California's coastal communities live on areas of subsiding land (Figure 7; Blackwell et al., 2020). Many of the islands in the California Bay-Delta have dropped below sea level due to microbial oxidation and soil compaction caused by more than a century of farming (NASA, 2017). Conversely, plate tectonics can cause land uplift along the coast to outpace sea level rise, as is happening in Crescent City in northern California where

NOAA's records show a drop in sea level over time. The far north coast is the only area along California where sea level is dropping relative to land surface (Russell and Griggs, 2012).

Figure 7. Exposure to land subsidence along the coast of California

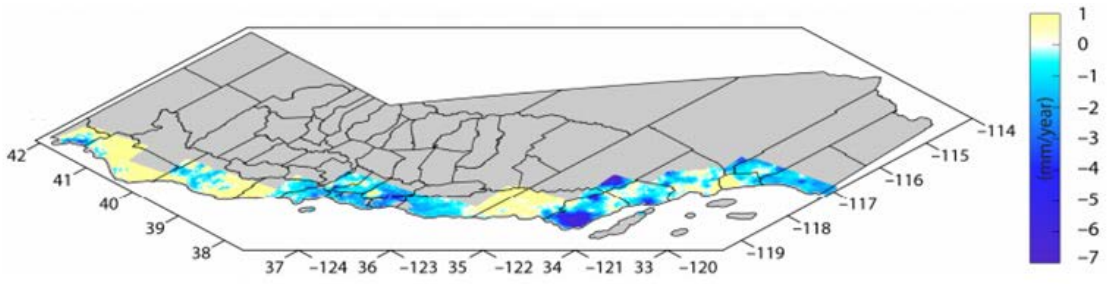

Map showing vertical land movement rates, in mm/year (2007-2018), along California's coast. Black lines identify California's counties.

Source: Blackwell et al., 2020

Technical considerations

Data characteristics

Sea level measurements came from federally operated tide gages located along the California coast which are managed by the National Water Level Observation Network, within NOAA, as well as from satellite altimetry operated by NASA. Data are available online at NOAA's Tides and Currents webpage and NASA's sea level webpage.

Tide stations measure sea level relative to specific locations on land. Short-term changes in sea level (e.g., monthly mean sea level or yearly mean sea level) are determined relative to a location's Mean Sea Level, the arithmetic mean of hourly heights observed over a specific 19-year period called the "National Tidal Datum Epoch" (NTDE) established by NOAA's National Ocean Service. The NTDE accounts for the effect of the 18.6-year lunar nodal cycle on variations in the tidal range. The current NTDE is 1983-2001 (previous NTDEs were for the periods 1924-1942, 1941-1959, and 1960-1978); NTDEs are updated roughly every 20 years (NOAA, 2000; Szabados, 2008).

The U.S. federal government first started collecting measurements of sea levels in the mid-19th century to assist with accurate navigation and marine boundary determinations. Data from these early observation efforts and continued monitoring are used to assess long-term changes in sea level in multiple locations in California. Monitoring efforts have expanded over the years to include more locations with tidal stations, allowing for analysis of sea level trends at more regions, although for shorter time scales (NOAA, 2006).

Strengths and limitations of the data

Monthly mean sea levels tend to be highest in the fall and lowest in the spring, with differences of about 6 inches. Local warming or cooling resulting from offshore shifts in water masses and changes in wind-driven coastal circulation patterns also seasonally alter the average sea level by 8.4 inches (21 cm) (Flick, 1998). For day-to-day activities, the tidal range and elevations of the high and low tides are often far more important than the elevation of mean sea level.

As noted above, geological forces such as subsidence, in which the land falls relative to sea level, and the influence of shifting tectonic plates and glacial isostatic adjustment (GIA) complicate regional estimates of sea level rise. Much of the California coast is experiencing elevation changes due to tectonic forces and GIA. Mean sea level is measured at tide gauges with respect to a tide gauge benchmark on land, which traditionally was assumed to be stable. This only allows local changes to be observed relative to that benchmark. Additional data from global positioning systems (GPS) are useful to record vertical land movement at the tide gauge benchmark sites to correct for seismic activity and the earth's crustal movements. Satellites have been used since the 1990s to track sea level rise at the global scale with uniform coverage and provide an additional check on sea level rise rates derived from tide gauges alone (Abdalla et al., 2021; NOAA, 2020).

OEHHA acknowledges the expert contribution of the following to this report:

Patrick Barnard, Ph.D.
Research Director, Climate Impacts and Coastal Processes Team
US Geological Survey
Pacific Coastal and Marine Science Center
(831) 460-7556
pbarnard@usgs.gov

Reviewer:
Ella McDougall, Ocean Protection Council

References:

Abdalla S, Kolahchi AA, Ablain M, Adusumilli S, Bhowmick SA, et al. (2021). Altimetry for the future: Building on 25 years of progress. *Advances in Space Research*.

Barnard PL, Dugan JE, Page HM, Wood NJ, Hart JA, et al. (2021). Multiple climate change-driven tipping points for coastal systems. *Scientific Reports* **11**(1): 1-3.

Barnard PL, Erikson LH, Foxgrover AC, Finzi Hart JA, Limber P, et al. (2019). Dynamic flood modeling essential to assess the coastal impacts of climate change. *Scientific Reports* **9**(4309).

Befus KM, Barnard PL, Hoover DJ, Hart JF and Voss CI (2020). Increasing threat of coastal groundwater hazards from sea-level rise in California. *Nature Climate Change* **10**(10): 946-952.

Blackwell E, Shirzaei M, Ojha C and Werth S (2020). Tracking California's sinking coast from space: Implications for relative sea level rise. *Science Advances* **6**: eaba4551.

Caldwell MR, Hartge EH, Ewing LC, Griggs G, Kelly RP, et al. (2013). Coastal Issues. *In: Assessment of Climate Change in the Southwest United States: A Report Prepared for the National Climate Assessment*. Garfin G, Jardine A, Merideth R, Black M, and LeRoy S (Eds.). Southwest Climate Alliance. Washington, DC: Island Press. pp. 168–196.

California Sea Grant (2021). King Tides: A Cosmic Phenomenon. Retrieved October 19, 2021.

Cazenave A and Cozannet GL (2014). Sea level rise and its coastal impacts. *Earth's Future* **2**(2): 15-34.

CCC (2015). *California Coastal Commission Sea Level Rise Policy Guidance: Interpretive Guidelines for Addressing Sea Level Rise in Local Coastal Programs and Coastal Development Permits.* California Coastal Commission. San Francisco, CA.

CEC (2009). *The Impacts of Sea-Level Rise on the California Coast* (CEC-500-2009-024-D). California Energy Commission.

CEC (2017). *Assessment of California's Natural Gas Pipeline Vulnerability to Climate Change (*CEC-500-2017- 008). California Energy Commission. University of California, Berkeley. Berkeley, CA.

CNRA (2018). *Safeguarding California Plan: 2018 Update. California's Climate Adaptation Strategy.* California Natural Resources Agency.

CNRA (2021). 2021 *Climate Adaptation Strategy*.

Coastal Resilience (2020). Santa Barbara County | Coastal Resilience.

DWR (2013). *California Water Plan Update 2013: Sacramento-San Joaquin Delta* (Regional Reports, Vol. 2). California Department of Water Resources. Sacramento, CA.

DWR (2016). *Quick Guide Coastal Appendix: Planning for Sea-Level Rise*. California Department of Water Resources. The National Flood Insurance Program in California. Sacramento, CA.

Elmilady HM, Van der Wegen M, Roelvink D and Jaffe BE (2019). Intertidal area disappears under sea level rise: 250 years of morphodynamic modeling in San Pablo Bay, California. *Journal of Geophysical Research: Earth Surface* **124**(1): 38-59.

Flick RE (1998). Comparison of California tides, storm surges, and mean sea level during the El Niño winters of 1982-1983 and 1997-1998. *Shore and Beach* **66**(3): 7-11.

Flick RE (2016). California tides, sea level, and waves — Winter 2015-2016. *Shore and Beach* **84**: 25-30

Grant AR, Wein AM, Befus KM, Hart JF, Frame MT, et al. (2021). Changes in liquefaction severity in the San Francisco Bay Area with sea-level rise. *InGeo-Extreme* 308-317.

Griggs G (2020). Coastal airports and rising sea levels. *Journal of Coastal Research* **36**(5): 1079-1092.

Griggs G, Arvai J, Cayan D, DeConto R, Fox R, et al. (2017). *Rising Seas in California: An Update on Sea-Level Rise Science*. California Ocean Science Trust.

Hu ZZ, Kumar A, Jha B, Zhu J and Huang B (2017). Persistence and predictions of the remarkable warm anomaly in the northeastern Pacific Ocean during 2014–16. *Journal of Climate* **30**(2): 689-702.

Hummel MA, Berry MS and Stacey MT (2018). Sea level rise impacts on wastewater treatment systems along the US coasts. *Earth's Future* **6**(4): 622-633.

IPCC (2014). *Climate Change 2014: Synthesis Report. Contribution of Working Groups I, II and III to the Fifth Assessment Report of the Intergovernmental Panel on Climate Change*. Core Writing Team, Pachauri RK, and Meyer LA (Eds.). Geneva, Switzerland: Intergovernmental Panel on Climate Change.

IPCC (2019). *Special Report on the Ocean and Cryosphere in a Changing Climate*. Pörtner HO, Roberts DC, Masson-Delmotte V, Zhai P, Tignor M, et al. (Eds.). Intergovernmental Panel on Climate Change. Geneva, Switzerland

IPCC (2021). *AR6 Climate Change 2021: The Physical Science Basis. Contribution of Working Group I to the Sixth Assessment Report of the Intergovernmental Panel on Climate Change*. Masson-Delmotte V, Zhai P,Pirani A, Connors SL, Péan C, et al. (Eds.). Intergovernmental Panel on Climate Change. Geneva, Switzerland.

Jones JM, Henry K, Wood N, Ng P and Jamieson M (2017). HERA: a dynamic web application for visualizing community exposure to flood hazards based on storm and sea level rise scenarios. *Computers and Geosciences* **109**: 124-133.

LAO (2020). *What Threat Does Sea Level Rise Pose to California?* California Legistlative Analyst's Office.

Limber PW, Barnard PL, Vitousek S and Erikson LH (2018). A model ensemble for projecting multidecadal coastal cliff retreat during the 21st century. *Journal of Geophysical Research: Earth Surface* **123**(7): 1566-1589.

May C (2020). Rising groundwater and sea-level rise. *Nature Climate Change* **10**(10): 889-890.

Myers MR, Barnard PL, Beighley E, Cayan DR, Dugan JE, et al. (2019). A multidisciplinary coastal vulnerability assessment for local government focused on ecosystems, Santa Barbara area, California. *Ocean and Coastal Management* **182**: 104921.

NASA (2017). National Aeronautics and Space Administration Sea Level Change: Observations from Space. Retrieved July 2017.

NOAA (2000). *Tidal Datums and their Applications* (NOAA Special Publication NOS CO-OPS 1). National Oceanic and Atmospheric Administration. Silver Spring, MD: Center for Operational Oceanographic Products and Services.

NOAA (2006). *Sea Level Variations of the United States 1854-2006* (NOS CO-OPS 053). National Oceanic and Atmospheric Administration. Silver Spring, MD: Center for Operational Oceanographic Products and Services.

NOAA (2020). National Oceanic and Atmospheric Administration. Climate Change: Global Sea Level. Retrieved Oct 27, 2021.

NOAA (2021a). National Oceanic and Atmospheric Administration, Center for Operational Oceanographic Products and Services: Tides and Currents. Retrieved February 2021.

NOAA (2021b). National Oceanic and Atmospheric Administration, National Ocean Service. What is glacial isostatic adjustment? Retrieved October 18, 2021.

OPC (2021). *Making California's Coast Resilient to Sea Level Rise: Principles for Aligned State Action*.

PBMI and SYBCI (2021). Pala Band of Mission Indians and Santa Ynez Band of Chumash Indians. Summary of the Southern California Tribal Listening Session hosted by the Pala Band of Mission Indians, Santa Ynez Band of Chumash Indians, and the Office of Environmental Health Hazard Assessment.

Plane E, Hill K and May C (2019). A rapid assessment method to identify potential groundwater flooding hotspots as sea levels rise in coastal cities. *Water* **11**(11): 2228.

Rahimi R, Tavakol-Davani H, Graves C, Gomez A and Fazel Valipour M (2020). Compound inundation impacts of coastal climate change: Sea-level rise, groundwater rise, and coastal watershed precipitation. *Water* **12**(10): 2776.

Russell N and Griggs G (2012). *Adapting to Sea Level Rise: A Guide for California's Coastal Communities*. California Energy Commission Public Interest Environmental Research Program.

San Francisco Bay Conservation and Development Commission (2012). Adapting to Rising Tides: Airports. Retrieved June, 2017.

Slater T, Hogg AE and Mottram R (2020). Ice-sheet losses track high-end sea-level rise projections. *Nature Climate Change* **10**(10): 879-881.

Smith KR, Riley MK, Barthman–Thompson L, Woo I, Statham MJ, et al. (2018). Toward salt marsh harvest mouse recovery: A review. *San Francisco Estuary and Watershed Science* **16**(2).

Sweet WW, Kopp R, Weaver CP, Obeysekera JT, Horton RM, et al. (2022). Global and regional sea level rise scenarios for the United States: updated mean projections and extreme water level probabilities along U.S. coastlines. NOAA Technical Report, SLR and Coastal Flood Hazard Scenarios and Tools: Interagency Task Force

Szabados M (2008). *Understanding Sea Level Change*. Reprint from ACSM Bulletin, 236: 10-14.

Thompson PR, Widlansky MJ, Hamlington BD, Merrifield MA, Marra JJ, et al. (2021). Rapid increases and extreme months in projections of United States high-tide flooding. *Nature Climate Change* **11**: 584-590.

UC Berkeley (2021). Toxic Tides. Retreived January 19, 2021.

USGS (2019). Coastal erosion researcher quoted in news coverage of fatal California cliff collapse. Retrieved October 20, 2021.

USGS (2020). New Model Shows Sea-level Rise Can Cause Increases in Groundwater Levels along California's Coasts. Retrieved April 13, 2021.

USGS (2021). Hazard Exposure Reporting and Analytics. Retrieved October 20, 2021.

Vitousek S, Barnard PL, Limber P, Erikson L and Cole B (2017). A model integrating longshore and cross-shore processes for predicting long-term shoreline response to climate change. *Journal of Geophysical Research: Earth Surface* **122**(4): 782-806.

DISSOLVED OXYGEN IN COASTAL WATERS

Dissolved oxygen concentrations are declining in ocean waters off southern California.

Figure 1. Dissolved oxygen concentrations across 66 monitoring stations in Southern California waters (1984-2020)

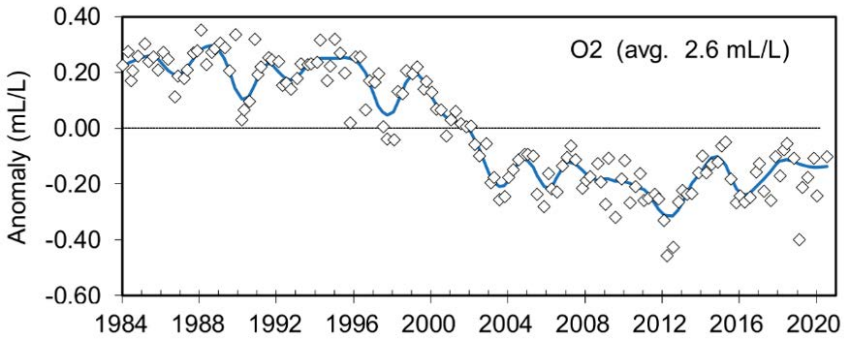

Source: Weber et al., 2021 Supplementary Figure 6

Each diamond on the graph represents the anomaly, or the difference between the average dissolved oxygen concentrations measured across 66 stations and the long-term average of 2.6 mL/L (based on values from a baseline period 1984 to 2013). The solid blue line connects annual averages. The stations are shown on the Figure 3 map; measurements were taken on the σ_θ=26.4 kg/m^3 isopycnal, the depth at which seawater is at a density of 1026.4 kg/m^3.

Figure 2. Dissolved oxygen concentrations at two monitoring stations on the Southern California Coast (1950-2019)

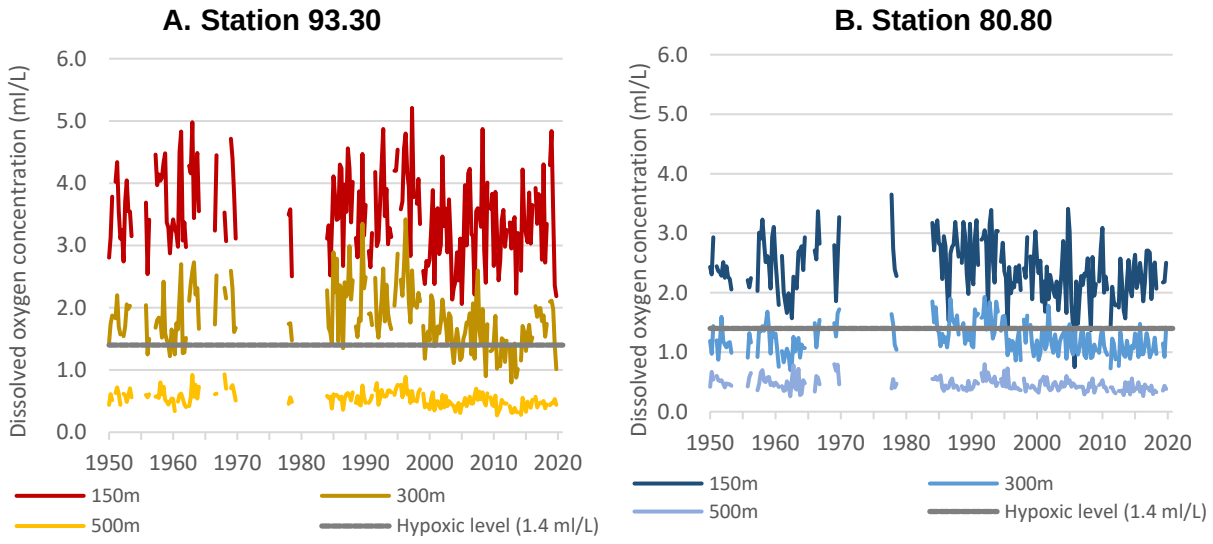

Source: CalCOFI, 2021a

Quarterly averages of dissolved oxygen concentrations in milliliters per liter (ml/L) measured at three depths (150, 300 and 500 meters) at Line 93, station 30 and Line 80, station 80 (see map, Figure 3).

What does this indicator show?

Instrumental measurements of dissolved oxygen (DO) concentrations point to increasing deoxygenation of coastal waters within the California Current in recent decades (Figures 1 and 2; also Bograd et al., 2019; Evans et al., 2020; Weber et al., 2021). The California Current extends from British Columbia, Canada to Baja California, Mexico. The California Cooperative Oceanic Fisheries Investigations (CalCOFI) has been taking measurements of DO periodically off southern California from San Diego to Point Conception since 1950, and consistently at a grid of stations four times per year since 1984 (see Figure 3 for locations). Figure 1 is based on measurements from the 66 core stations in the CalCOFI survey area. Figure 2 presents data collected from three depths at two stations: [A] Line 93, station 30 (93.30), and [B] Line 80, station 80 (80.80).

Throughout CalCOFI survey area, at depths corresponding to the "σ_θ-26.4 isopycnal" – the depth at which seawater is at a density of 1026.4 kg/m^3 – DO concentrations decreased significantly from about between the mid-1990s and the mid-2000s (Figure 1; also Bjorkstedt et al. 2012 as cited in Thompson et al., 2019). Following this decline, DO concentrations have been relatively constant, remaining below the long-term average since (Weber et al., 2021). Overall, DO concentrations in this region (to at least 500 m depth) have mostly declined to values lower than observed in the 1950's to 1960's (Bograd et al., 2008, 2015, 2019).

Figure 2A shows DO concentrations at three water depths at Station 93.30 offshore of San Diego. The data indicate overall mean decreases with minimal changes in the mean in the past 10 years. Since the mid-1990's, significant low-oxygen events have been observed: concentrations were below the hypoxic level (<1.4 ml/L), which can potentially cause physiological stress in marine organisms. This location is representative of the influence of the northward-flowing California Undercurrent, which is a major supplier of deeper source waters (200 to 500 meters (m)) to the region and has a large influence on oxygen content for much of the survey area. At 80.80 off Point Conception, within the core of the near-surface, southward-flowing California Current, DO concentrations have also declined sharply since the mid-1990's but have been generally increasing at 150-300 m in the past five years.

Figure 3. Sampling locations

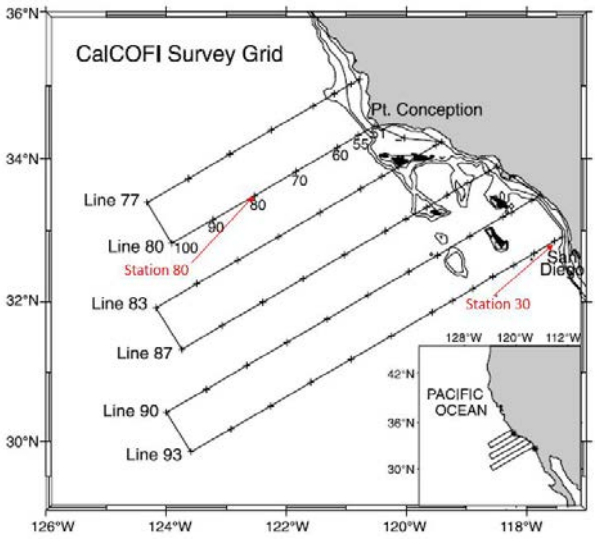

Modified from Bograd *et al.*, 2008

Why is this indicator important?

Declining DO concentrations in ocean waters and the associated changes in the depth and extent of low oxygen zones can lead to significant and complex ecological changes in marine ecosystems, including wide-ranging impacts on diversity, abundance, and trophic structure of communities (e.g., Levin et al., 2009; Somero et al., 2015; Stramma et al., 2010). Changing ocean chemistry, in concert with changes in temperature, may lead to even greater and more diverse impacts on coastal marine ecosystems (e.g., Somero et al., 2015).

Globally since 1950, more than 500 coastal sites have been reported to have experienced hypoxic conditions. Fewer than 10 percent of these were known to have hypoxia before then (Breitburg et al., 2018). Separate from these episodic hypoxic events, coastal California is characterized by the presence of a zone of depleted oxygen concentrations (Oxygen Minimum Zone, or OMZ) at depths from 600 to 1100 meters. The OMZ near California is expanding both vertically (moving upward towards the ocean surface (e.g., Bograd et al., 2008)) and horizontally (Somero et al., 2015). The declines in oxygenation observed off California are consistent with an observed expansion of the low oxygen zones elsewhere around the world (Breitburg et al., 2018; Stramma et al., 2008).

The expansion of oxygen-deficient zones can lead to a compression of favorable habitat for certain marine species and an expansion of favorable habitat for others. For example, following the 1997-98 El Niño event, the Humboldt squid (*Dosidicus gigas*) — which thrives in low-oxygen environments — expanded its range northward from Baja California to southeast Alaska, a shift that may have been affected by changes in the extent of oxygen-deficient zones (Gilly and Markaida, 2007). Studies have indicated that low-oxygen waters can reach nearshore coastal habitats via upwelling, with potential impacts on these habitats (Chan et al., 2019).

Oxygen plays a role in the cycling of nutrients such as nitrogen, phosphorus and iron. As a result, changes in oxygen levels can influence nutrient budgets, biological productivity and carbon fixation. In oxygen-depleted waters, anaerobic microbial processes can produce chemicals such as hydrogen sulfide, which is toxic to other organisms, and methane, a potent greenhouse gas (Breitburg et al., 2018).

What factors influence this indicator?

DO levels reflect a complex interplay between physical and biological drivers in the marine environment, including currents, upwelling, air-sea exchange, and biological productivity, respiration and decomposition. Warmer waters hold less oxygen, as the gas becomes less soluble, and surface warming produces stratification that reduces the overturning circulation essential in ocean ventilation processes. Warming also accelerates the rate of oxygen consumption by marine organisms (e.g., Breitburg et al, 2018; Somero et al., 2015). In addition to these processes, DO is influenced by high

surface productivity, regional circulation of the North Pacific Ocean, and anthropogenic nutrient inputs to the coastal ocean, as discussed below.

Upwelling is a wind-driven physical process wherein deep, nutrient rich waters move upward into the shallow surface ocean. There is evidence that upwelling has increased in some locations along the California coast due to anthropogenic impacts (García-Reyes and Largier, 2010; Wang et al., 2015). Upwelling brings nutrient rich waters to the surface, where it drives surface ocean productivity (photosynthesis). The amount of surface water productivity affects DO concentrations because as biological material sinks downward from the surface ocean and decays, oxygen is utilized in the decay and decomposition process. Thus, DO concentrations decrease in the subsurface below regions of high biological productivity.

DO concentrations are also controlled by regional and global oceanographic processes. For example, the Southern California Bight – the 400 miles of coastline from Point Conception in Santa Barbara County to Cabo Colnett, south of Ensenada, Mexico -- is impacted seasonally by the northward-flowing California Undercurrent. Much of the Bight is included in the CalCOFI survey region. Declining oxygen concentrations in this region imply a change in the properties of equatorial source waters (Bograd et al., 2015, 2019). A recent study estimated that equatorial waters transported via the California Undercurrent accounted for 81 percent of the deoxygenation trend in the CalCOFI region since 1993 (Evans et al., 2020).

Local nutrient inputs from human practices (e.g., agriculture, wastewater discharge) can also decrease oxygen concentrations in coastal waters. Fertilizers and nutrient enrichment from wastewater promote algal growth. As this material sinks and decays, it can create localized areas of low oxygen. Management of coastal pollution is an important aspect of minimizing changes in oxygen concentrations on a local scale.

Scientists estimate that about 15 percent of global oxygen decline between 1970 and 1990 can be explained by ocean warming and the remainder by increased stratification. In coastal areas, especially nutrient-enriched waters, warming is predicted to exacerbate oxygen depletion (Breitburg et al., 2018). In its Sixth Assessment, the Intergovernmental Panel on Climate Change concluded that oxygen levels have dropped in many upper ocean regions since the mid-20th century, and that deoxygenation will continue to increase in the 21st century (IPCC, 2021).

Technical considerations:

Data characteristics

This indicator is based on data from the CalCOFI program. Established in 1949, CalCOFI conducts quarterly cruises (18 to 28 days long) to measure the physical and chemical properties of the California Current System and census populations of organisms from phytoplankton to avifauna. Data collected at depths down to 500 meters include temperature, salinity, oxygen, phosphate, silicate, nitrate and nitrite, chlorophyll,

phytoplankton and zooplankton biodiversity, and zooplankton biomass (CalCOFI, 2021b).

DO measurements for CalCOFI Line 93.3, Station 30.0 (offshore of San Diego) and Line 80, Station 80 (within the offshore California Current core) were downloaded from the CalCOFI website. Quarterly averages were derived from oxygen concentrations reported for that calendar quarter. While sampling did occur between 1950 and1980, there are data gaps during this period.

Strengths and limitations of the data

Very few datasets describe DO conditions north of San Francisco and/or in coastal regions. One analysis suggests that 20-30 years of data are needed to robustly detect long-term declines in DO above natural variability (Henson et al., 2016). All of the CalCOFI datasets meet this criterion, thus CalCOFI currently represents the best resource for distinguishing long-term trends in DO from natural variability. CalCOFI has limited sampling availability in nearshore/coastal habitats, so establishing additional coastal monitoring sites may be critical for characterizing DO conditions in these areas.

These observations are limited by sites where oxygen concentration measurements are currently monitored along the coast and do not reflect oxygen declines that may be occurring across the entire California Current System. As described above, the observed DO concentrations could be influenced by both local thermodynamic or biological processes, as well as remote, large-scale changes. The oxygen concentrations can vary with the depth, temperature and time of year DO levels are measured.

OEHHA acknowledges the expert contribution of the following to this report:

Steven Bograd, Ph.D.
Environmental Research Division
Southwest Fisheries Science Center
National Oceanic and Atmospheric Administration
(831) 648-8314
Steven.Bograd@noaa.gov

Additional input from:

Marisol Garcia-Reyes, Farallon Institute;
Tessa Hill, UC Davis Bodega Marine Laboratory;
Andrew Leising, NOAA

References:

Bograd SJ, Buil MP, Di Lorenzo E, Castro CG, Schroeder ID, et al. (2015). Changes in source waters to the Southern California Bight. *Deep-Sea Research Part II: Topical Studies in Oceanography* **112**: 42-52.

Bograd SJ, Castro CG, Di Lorenzo E, Palacios DM, Bailey H, et al. (2008). Oxygen declines and the shoaling of the hypoxic boundary in the California current. *Geophysical Research Letters* **35**(12): L12607.

Bograd SJ, Schroeder ID and Jacox, MG (2019). A water mass history of the southern California Current System. *Geophysical Research Letters* **46**: 6690-6698.

Booth JAT, McPhee-Shaw EE, Chua P, Kingsley E, Denny M, et al. (2012). Natural intrusions of hypoxic, low pH water into nearshore marine environments on the Californian coast. *Continental Shelf Research* **45**:108-115.

Breitburg D, Levin LA, Oschlies A, Gregoire M, Chavez FP, *et al.* (2018). Declining oxygen in the global ocean and coastal waters. *Science* **359**: (6371).

CalCOFI (2021a): California Cooperative Oceanic Fisheries Investigations: CalCOFI Hydrographic Database – 1949 to Latest Update. Retrieved March 31, 2021.

CalCOFI (2021b): California Cooperative Oceanic Fisheries Investigations: About Us. Retrieved November 22, 2021.

Chan F, Barth JA, Kroeker KJ, Lubchenco,J and Menge BA (2019). The dynamics and impact of ocean acidification and hypoxia. *Oceanography* **32**(3):62-71.

Evans N, Schroeder ID, Pozo Buil M, Jacox MG and Bograd SJ (2020). Drivers of subsurface deoxygenation in the southern California Current system. *Geophysical Research Letters* **46**: e2020GL089274.

Frieder CA, Nam SH, Martz TR and Levin LA (2012). High temporal and spatial variability of dissolved oxygen and pH in a nearshore California kelp forest. *Biogeosciences* **9**: 3917-3930.

Gallo ND, Drenkard E, Thompson AR, Weber ED, Wilson-Vandenberg D, et al. (2019). Bridging from Monitoring to Solutions-Based Thinking: Lessons from CalCOFI for Understanding and Adapting to Marine Climate Change Impacts. *Frontiers in Marine Science* **6**: Article 695.

García-Reyes M and Largier J (2010). Observations of increased wind-driven coastal upwelling off Central California. *Journal of Geophysical Research* **115**(C4).

Gilly W and Markaida U (2007). Perspectives on Dosidicus gigas in a changing world. Olson R and Young J (Eds.). *The role of squid in open ocean ecosystems*. Report of a GLOBEC-CLIOTOP/PFRP workshop, 16-17 November 2006, Honolulu, Hawaii, USA. GLOBEC. Report 24: vi, 81-90.

Henson SH, Beaulieu C and Lampitt R (2016). Observing climate change trends in ocean biogeochemistry: when and where. *Global Change Biology* **22**:1561-1571.

IPCC (2021). Summary for Policymakers. In: *Climate Change 2021: The Physical Science Basis. Contribution of Working Group I to the Sixth Assessment Report of the Intergovernmental Panel on Climate Change* [Masson-Delmotte VP, Zhai A, Pirani SL, Connors C, Péan S, *et al.* (eds.)]. Cambridge University Press. In Press.

Levin LA, Ekau W, Gooday AJ, Jorissen F, Middelburg JJ, *et al.* (2009). Effects of natural and human-induced hypoxia on coastal benthos. *Biogeosciences* **6**(10): 2063-2098.

Rhein M, Rintoul SR, Aoki S, Campos E, Chambers D, *et al.* (2013): Observations: Ocean. *In: Climate Change 2013: The Physical Science Basis. Contribution of Working Group I to the Fifth Assessment Report of the Intergovernmental Panel on Climate Change*. Stocker TF, Qin D, Plattner G-K, Tignor M,

Allen SK, *et al.* (Eds.)]. Cambridge, United Kingdom and New York, NY, USA: Cambridge University Press.

Somero GN, Beers JM, Chan F, Hill TM, Klinger T et al. SY (2015). What changes in the carbonate system, oxygen, and temperature portend for the northeastern Pacific Ocean: A physiological perspective. *BioScience* **66**(1): 14-26.

Stramma L, Johnson GC, Sprintall J and Mohrholz V (2008). Expanding oxygen minimum zones in the tropical oceans. *Science* **320**(5876): 655-658.

Stramma L, Schmidtko S, Levin L and Johnson GC (2010). Ocean oxygen minima expansions and their biological impacts. *Deep Sea Research Part I: Oceanographic Research Papers* **57**(4): 587–595.

Thompson AR, Schroeder ID, Bograd SJ, Hazen EL, Jacox MG, et al. (2019). State of the California Current 2018–19: A novel anchovy regime and a new marine heat wave? *California Cooperative Oceanic Fisheries Investigations* **60**: 1–65

Wang D, Gouhier TC, Menge BA and Ganguly AR. (2015). Intensification and spatial homogenization of coastal upwelling under climate change. *Nature* **518**: 390-394.

Weber ED, Auth TD, Baumann-Pickering S, Baumgartner TR, Bjorkstedt EP, *et al.* (2021). State of the California Current 2019-2020: Back to the future with marine heatwaves? *Frontiers in Marine Science* **8**: 709454.